RESEARCH TRIANGLE INSTITUTE

RTI/3629/91-Annual

December 1991

SEMICONDUCTOR DIAMOND TECHNOLOGY

Annual Report
1 January 1991 - 31 December 1991

R. J. Markunas
R. A. Rudder
J. B. Posthill
R. E. Thomas

STRATEGIC DEFENSE INITIATIVE ORGANIZATION
Innovative Science and Technology Office

Office of Naval Research
Program No.
N00014-86-C-0460

POST OFFICE BOX 12194 RESEARCH TRIANGLE PARK, NORTH CAROLINA 27709 2194

REPORT DOCUMENTATION PAGE

Form Approved
OMB No 0704-0188

1. AGENCY USE ONLY (Leave blank)	2. REPORT DATE	3. REPORT TYPE AND DATES COVERED
		Annual Report, 1 January 1991 – 31 December 91

4. TITLE AND SUBTITLE

Semiconductor Diamond Technology

5. FUNDING NUMBERS

N00014-86-C-0460

6. AUTHOR(S)

R.J. Markunas, R.A. Rudder, J.B. Posthill, R.E. Thomas

7. PERFORMING ORGANIZATION NAME(S) AND ADDRESS(ES)

Research Triangle Institute
P.O. Box 12194
Research Triangle Park, NC 27709

8. PERFORMING ORGANIZATION REPORT NUMBER

83U-3629

9. SPONSORING/MONITORING AGENCY NAME(S) AND ADDRESS(ES)

Office of Naval Research
800 N. Quincy Street
Arlington, VA 22217-5000

10. SPONSORING/MONITORING AGENCY REPORT NUMBER

11. SUPPLEMENTARY NOTES

12a. DISTRIBUTION/AVAILABILITY STATEMENT

Approved for public release; unlimited distribution

12b. DISTRIBUTION CODE

13. ABSTRACT (Maximum 200 words)

The development of techniques to enhance diamond heteronucleation without abrasive ex situ surface treatment now permits researchers to study diamond heteronucleation (epitaxy) at growth temperatures far below the thermal desorptions of H and O. At these temperatures, surface chemistry on the nucleating surface will be controlled by chemical exchange and abstraction reactions. This final report highlights the important results achieved during 1991 in diamond production and in diamond surface chemistry. Of particular interest are O and H interactions on diamond (100) surfaces and the development of water-based processes exclusive of molecular hydrogen for high quality low temperature diamond growth. The role of oxygen or hydroxyl is becoming increasing illucidated as surface chemistry studies show the propensity for O to terminate and stabilize 1x1 surfaces and as water-based growth processes permit diamond stabilization and growth at lower and lower temperatures. For sake of completeness, publications for this year are included in the appendix to provide the reader with full details.

14. SUBJECT TERMS

15. NUMBER OF PAGES

109

16. PRICE CODE

17. SECURITY CLASSIFICATION OF REPORT	18. SECURITY CLASSIFICATION OF THIS PAGE	19. SECURITY CLASSIFICATION OF ABSTRACT	20. LIMITATION OF ABSTRACT
UNCLASSIFIED	UNCLASSIFIED	UNCLASSIFIED	

TABLE OF CONTENTS

1.0 SUMMARY OF PROGRESS

This is the final report for 1991 on the Semiconducting Diamond Technology program at Research Triangle Institute. The report highlights accomplishments in several areas critical to the development of semiconducting diamond. Research Triangle Institute during the course of the current program has developed a number of critical diamond technologies unique to the community. These developments now provide Research Triangle Institute a unique position to understand diamond surface chemistry as it relates to heteronucleation, growth, and epitaxy. Those developments include:

(1) Establishing an integrated processing system connecting CVD, MBE, substrate cleaning, and surface characterization equipment through ultrahigh vacuum transfer.

(2) Pioneering work in halogen-based diamond growth that has investigated thermal fluorine-assisted processes and plasma-assisted H_2/CF_4 processes.

(3) Establishing two alternative gas-phase-induced diamond nucleation techniques involving H_2/CF_4 with non-local carbon sources and involving H_2/CH_4 with local carbon sources.

(4) Demonstrating epitaxial lateral overgrowth on natural diamond substrates and limited diamond platelet growth on Ni(100).

(5) Identifying using temperature programmed thermal desorption important chemical pathways for the reactions of atomic hydrogen and atomic oxygen

with the diamond (100) surface.

(6) Finally, pioneering water-based processes for diamond CVD wherein no molecular hydrogen is required as a process gas for the growth of high quality material. In this technique, water vapor H_2O replaces molecular H_2 as the source for atomic hydrogen in diamond CVD.

Current work at Research Triangle Institute is establishing new science and new technology for diamond.

New Science: The surface chemistry facility using thermal mass desorption spectroscopy is exploring atomic H, F, Cl, and O interactions with the diamond (100) surface. Already in the study of atomic H interactions, new phenomena are being documented. Atomic hydrogen saturates the (100) 2x1 surface at near monolayer coverages. Post-saturation exposure of the surface to atomic hydrogen does <u>not</u> immediately open the surface dimer pair. Rather, it appears that the dimer unit back bonds are susceptible to atomic hydrogen attack and desorption. As these 2x1 surface units are desorbed, the surface converts toward at 1x1 surface. The 1x1 post-saturated surface shows a hydrogen doublet H_2 desorption around 950°C. Prior to the H_2 desorption, the post-saturated 1x1:H surface shows methyl desorptions at 700°C below the hydrogen desorption temperature. The methyl desorption is a considerable fraction of the H_2 desorption, thus, is an appreciable pathway for dehydrogenation of the diamond surface.

In contrast to this work, it appears that atomic O dosing of the diamond (100) surface readily converts the surface structure to a 1×1 bulk-like termination. We postulate that the atomic oxygen bridges the dimer rows so as to break the dimer bonds responsible for the 2×1 reconstructions. Upon annealing, oxygen desorbs from the surface as CO leaving the surface denuded and for temperatures less than 900°C unreconstructed. Close collaborations with Dr. Michael Frenklach at Pennsylvania State University are beginning to give insight into the chemical and physical processes at the diamond surface. A copy a joint paper recently submitted to the Journal of Chemical Vapor Deposition is included in this package.

New Science Experimentation with mixed hydrogen-fluorine chemistries for the CVD growth of diamond have lead to the discovery of two pathways for enhancing the nucleation of diamond. First, H_2/CF_4 plasmas have produced dense diamond nucleation on as-received Si substrates when the graphite surface of the susceptor was exposed to the plasma. Gasification of the graphite susceptor in the presence of the H_2/CF_4 plasma produced a precursor necessary for diamond nucleation. In contrast, H_2/CH_4 plasmas do not normally produce dense nucleation regardless of the status of the graphite susceptor. It was discovered that the nucleation density from the H_2/CH_4 plasma process could be greatly enhanced by placing graphite fibers in close proximity to the substrate. Dense diamond growth local to the region of contact between the fiber and the substrate was observed on Si, Ni, quartz, and spinel substrates. This suggests that a precursor species is formed from the dissolution of the graphite fiber in the H_2/CH_4 plasma that induces nucleation but is normally converted into a non-

nucleating species by the interactions with the gaseous boundary layer on the plasma.

Both experiments show that dissolution of graphite can produce species capable of inducing diamond nucleation. Previous experiments with non-nucleating species have been unsuccessful in producing 2-dimensional nucleation on non-diamond substrates. As a consequence, the preliminary problem to be addressed prior to heteroepitaxy is to develop CVD techniques which will deposit high quality diamond without nucleation barriers. Once the nucleation barrier is eliminated, then issues such as surface cleanliness, order, lattice match become critical as they are far all other heteroepitaxial systems. Determination of these species will be of paramount importance for the development of diamond heteroepitaxy.

New Technology: One impediment to the commercialization of diamond thin films is the costs and hazards of the molecular hydrogen required in almost all diamond CVD systems. In other systems such as the oxy-acetylene torch system which does not require molecular hydrogen, compressed, explosive gasses are used. Research Triangle Institute has discovered and is applying for a patent on a diamond growth process which does not rely on compressed, toxic, flammable, or explosive gasses. Diamond growth has been demonstrated using low-pressure rf-plasma assisted CVD at 1.0 Torr with gas mixtures of water vapor and alcohol. Gas vapors are pumped from a volumetric mix of 20% methanol or 20% ethanol or 20% isopropanol in water. No other gas sources are introduced. The system requires no pressure regulators, no mass flow controllers, no over-pressure sensors, no explosion containment. Both polycrystalline and homoepitaxial growths have been demonstrated. Given the economic advan-

tages of this mixture; this discovery should provide great impetus for commercialization of diamond films.

New Science and Technology: The water-based processes have been extended to even lower substrate temperatures through the addition of acetic acid to the water-alcohol solutions. The presence of acetic acid gives the plasma gas a readily ionizable molecule permitting magnetic field coupling to the plasma gas to be obtained at extremely low power input. The presence of the organic acid molecule also permits through plasma dissociation the presence of the carboxyl radical in the gas phase. The COO-H bond strength in the carboxyl radical is extremely low, only 15 kcal/mol. Thus, carboxyl radicals can easily donate H atoms to the growth surface. Reduction in power input permits low temperature diamond growth to proceed in the rf induction plasma as induction currents in the graphite susceptor are reduced. Currently, diamond growth at temperatures as low as 300°C has been demonstrated. By implementing a cooling stage to the growth reactor, lower temperature growth should be realized during the next quarter. The lower temperature technologically permits diamond application to materials which heretofore could not survive the temperature extremes. Scientifically, the growth at lower and lower temperatures will undoubtedly change the nucleation kinetics. In many lattice mismatched systems, growths at low temperatures initially is one means by which planar heteroepitaxial films can be obtained. At temperatures much lower than 200°C, water will not desorb from the growth surfaces. Under those conditions, the growth chemistries will undoubtedly undergo remarkable change. The study of growth nucleation and behavior in these temperature regimes

will yield profound insights into the water-based mechanisms.

Exciting scientific and technological discoveries were made at RTI during the course of the 1991 year. Exciting new growth chemistries and new knowledge of diamond surface chemistry permit current work to focus on heteroepitaxy with technological tools and intelligence not at ones disposal a year ago. These tools in some cases involve deposition technologies wherein the diamond nucleation density is high enough to permit in situ studies of nucleation, not in situ studies of diamond overgrowth from nucleation sites. These tools in some cases involve deposition technologies wherein the temperature can be significantly reduced below thermal desorption temperatures. The surface chemistry now will be controlled by chemical extraction and exchange. These tools in some cases involve knowledge that surface control and stabilization with hydrogen alone under low hydrogen flux conditions (likely to promote 3-dimensional nucleation) will have to be stabilized with a more reactive species such as O. These tools in some cases involve the knowledge that O stabilization is accompanied by etching through CO^{-} desorption at temperatures broadly centered about 600° C.

These important results have been summarized in this introduction. For the sake of completeness, publications on RTI work during this year are included in the following sections. Some of these publications appeared in earlier quarterly reports. The more recent publications appear in the first sections.

SUBMITTED TO JOURNAL OF CHEMICAL VAPOR DEPOSITION

Atomic Hydrogen Adsorption on the Reconstructed Diamond (100)-2x1 Surface.

R.E. Thomas, R.A. Rudder, and R.J. Markunas

Research Triangle Institute, Research Triangle Park. NC 27709

D. Huang, and M. Frenklach

Department of Materials Science and Engineering, Pennsylvania State University, University Park, PA 16802

ABSTRACT

A combination of theoretical and experimental techniques have been used to study atomic hydrogen adsorption on the diamond 2x1 surface. Low energy electron diffraction (LEED) has been used to study the effects of atomic and molecular species of hydrogen on the reconstructed 2x1 surface. Atomic hydrogen appears relatively inefficient at breaking C-C dimer bonds on the (100)-(2x1) surface. LEED patterns show only slight changes even after exposure of the surface to 40000L of H/H_2. Under similar conditions a silicon 2x1 surface converts to the 1x1 phase after an exposure of less than 600L. Calculations using modified neglect of diatomic overlap (MNDO) were done for two atomic hydrogen insertion reactions, direct attack of the dimer bond and attack of the back bond. Calculations indicate that there are substantial potential energy barriers to both reactions. The barrier to hydrogen addition on the dimer bond

was calculated as 48.7 kcal/mol as compared to 76.1 kcal/mol for addition to the dimer back bond. Based on experimental and theoretical results it appears that exposure of the C(100)-(2x1) surface to atomic hydrogen at 25°C does not readily convert the surface to the 1x1 state.

I. INTRODUCTION

Hydrogen is an integral constituent in many of the CVD diamond growth processes developed to date.[1] Hydrogen is thought to function in the growth process in a number of ways, including maintenance of sp^3 hybridization of carbon atoms at the growth surface. In spite of numerous growth studies, the details of the role of hydrogen in CVD growth environments are still unclear, as are fundamental questions concerning interactions of this gas with the diamond surface.

Although similar in structure to the silicon (100) surface, the diamond (100) surface has not been studied nearly as intensively, with only a handful of experimental studies[2,3,4,5,6] and theoretical studies[7,8,9,10,13] published to date. Important questions remain concerning the details of the reconstruction and the effect of adsorbates on surface structure. As with silicon (100), the diamond (100) surface reconstructs to a 2x1:1x2 dimer configuration upon heating.[2,4,6] Due to the higher bond strengths in the carbon system the reconstruction does not occur until the diamond is annealed to approximately 1000°C, as compared to 450°C for silicon. Hydrogen desorption has been found to occur at approximately 900°C for a heating rate of 20°C/s. Adsorption of atomic hydrogen has been reported to convert the surface back to the 1x1 configuration.[2] However, subsequent annealing to 1200°C did not convert the surface back to the 2x1 configuration.[2] Recently published theoretical calculations indicate a barrier of 34.1 kcal/mol for the insertion of hydrogen into the C-C dimer bond.[10] From these calculations it appears difficult to form the dihydride from the monohydride by the exposure of the surface to atomic hydrogen.

In the present paper we have used LEED and MNDO calculations to study the effects of atomic and molecular species of hydrogen on the reconstructed 2x1 surface. LEED combined with UHV dosing with atomic hydrogen was chosen in order to reduce extraneous surface interactions. Two atomic hydrogen insertion reactions were studied with MNDO calculations, direct attack of the dimer bond and attack of the dimer back bond. The attack of the dimer bond simulates the conversion of the surface from 2x1 to 1x1. Studies of hydrogen attack of the dimer back bond were stimulated by recent results of Boland wherein strained silicon back bonds on the reconstructed silicon (7x7) surface were found susceptible to attack by atomic hydrogen.[18]

II. METHODS

A. Experimental

Atomic hydrogen dosing and LEED observations were performed in a stainless steel UHV system. Turbomolecular pumps were used both on the main chamber and to differentially pump the chamber housing the quadrupole mass spectrometer. Base pressure was $5x10^{-10}$ Torr for the sample chamber and $1x10^{-10}$ Torr for the quadrupole chamber. LEED observations were performed with a Princeton Research Instruments reverse view system.

Sample heating was accomplished by clipping the crystals to a 0.25mm thick molybdenum resistive strip heater. All parts associated with the heater stage, including the clamps and current leads were manufactured from molybdenum. The sample temperature was measured by a 0.125mm diameter chromel/alumel thermocouple threaded

through a laser drilled hole in the diamond and held in tension against the crystal. Sample heating was controlled by feedback from the thermocouple which adjusted a SCR power supply. After an initial warm-up phase, temperature ramps are linear from approximately 150° C to over 1100° C.

Two type IIa (100). 5x5x0.25mm. diamond crystals were used in the course of the present study. Other than thermal cleaning, no technique is available in situ for removing surface contamination from the diamond crystals. Particular attention was therefore paid to preparing the diamond surface before entry into the vacuum system. The samples are initially hand polished for 5 minutes with 0.25μm diamond grit and deionized water on a nylon polishing pad. The samples are then ultrasonically degreased in a series of solvents, trichloroethylene, acetone, methanol, and deionized water. Following the deionized water rinse, the samples are swabbed under DI water to remove particles. The samples are rinsed again in the solvent series and then placed in CrO_3/H_2SO_4 (125° C) solution for 20 minutes to remove non-diamond carbon. The samples are rinsed in DI water and then boiled in a 3:1 solution of HCl/HNO_3 for 20 minutes to remove any metals contamination. Finally the samples are rinsed in deionized water and blow-dryed with compressed nitrogen. Samples subjected to this cleaning process typically show a good quality 1x1 LEED pattern with no annealing. For the initial thermal cleaning the sample was ramped up in temperature at approximately 10° C/sec until the pressure in the main chamber rose to $5x10^{-8}$ Torr at which point the power was shut off and the sample cooled. This cycle was repeated until a maximum temperature of 1150° C was reached.

In all cases atomic hydrogen was generated via a tungsten filament operating at a temperature of approximately 1500° C. The sample was positioned approximately 2 cm. from the filament during dosing. The sample was not actively cooled and at the lowest dosing pressures remained at room temperature. No attempt was made to quantify the percentage of atomic species generated by the filaments. All doses are given for the total H_2 exposure from uncorrected ion gauge tube readings. X-ray photoelectron spectroscopy was done ex-situ after extensive dosing with the tungsten filament and no evidence of metal contamination was seen.

B. Calculational

The energies were obtained, as in the previous studies,[11,12.13] using the MNDO all-valence electron parametrization of the NDDO SCF approximation.[14] Calculations were of restricted Hartree-Fock type with the half-electron method being used for single-radical species.[15] The computations were performed with the "AMPAC" computer program developed by Dewar and co-workers;[16] they were carried out on an IBM-3090/600S main-frame computer.

The "background" (100) surface element was represented in this study by a $C_{28}H_{46}$ cluster used in the previous study.[13] The cluster, shown in Fig. 1, consists of three layers of carbon atoms. All dangling bonds of these carbon atoms are saturated with hydrogen atoms. For identification purposes, the carbon sites of the first two layers are marked with letters *a, b, c,* and *d* in Fig. 1. The central C_a–C_a carbon site of the top layer, on which the reaction is taking place, is a carbon monohydride dimer.

It is a product of H_2 elimination from a 1x1 surface dihydride, $C_{28}H_{48}$. To simulate the rigidity of the real surface, the dihydride carbons of the top layer (C_b and C_e atoms) were fixed at the positions of an ideal diamond lattice (with distance between the dihydride carbons of 2.53 Å) and the positions of the rest of the carbon atoms were obtained by full minimization of the total potential energy.

III. RESULTS

A. Experimental Results

Upon annealing, more than 90% of the freshly polished surfaces used in the present study exhibited a transformation from the 1x1 configuration to the 2x1 configuration. During the initial annealing sequence the samples would typically show indications of the 2x1 structure at approximately 800°C, with the transformation completed by 1050°C on successive anneals. No correlations were observed between sample preparation conditions and failure of the surface to reconstruct.

Figures 2 and 3 show LEED patterns from two series of experiments where samples were annealed to convert the surface to the 2x1 state and then exposed to atomic hydrogen. The first of figures, Fig. 2, shows a sample as loaded (Fig. 2a) and then before (Fig. 2b) and after (Fig. 2c) exposure to H/H_2 at a pressure of $5x10^{-5}$ Torr for 30 min. There is perhaps a slight diminishment in the intensity of the second order spots but the 2x1 pattern is still quite evident. The dose used represents an equivalent exposure of 40000L where 1L is equivalent to $1x10^{-6}$ Torr-s. In contrast, a dose of 600L under identical conditions is sufficient to convert the silicon (100) surface from

the 2x1 state back to the 1x1 state. We note again that doses referred to here are for a total hydrogen dose of molecular plus atomic hydrogen. The dose is calculated from uncorrected ion gauge tube readings. Samples were also exposed to molecular hydrogen at equivalent doses and no evidence of reversion to the 1x1 structure was observed.

Figure 3 shows LEED results from a sample exposed to H/H_2 at much higher pressures, 0.95 Torr (Fig. 3b) and 6.5 Torr (Fig. 3c). These pressures are similar to what is currently used in plasma enhanced CVD diamond growth systems. Although the rate of atomic hydrogen generation by tungsten filaments decreases as the pressure is raised above 10^{-5} Torr, we see no evidence that the surface has been reconverted to the 1x1 state.

B. Calculational Results

The geometric results for the dimer of the background surface cluster is shown at the top of Fig. 1. The dimer bond length was calculated to be 1.64 Å. For addition of hydrogen to the surface, two reactions of H atom with the dimer were considered: first is the attack on the dimer carbon atom, C_a, and second is the attack on the second-layer carbon atom, C_d. In the former case, the results indicate the breaking of C_a-C_a dimer bond. The variational potential energy surface diagram and the corresponding change of C_a-C_a dimer bond length with the H atom approaching the dimer C_a atom are shown in Fig. 4. The potential energy barrier obtained for this reaction is 48.7 kcal/mol. The variational potential energy surface diagram and the corresponding change of C_a-C_d back bond length with the H atom approaching a C_d atom are shown

in Fig. 5. The results in this case indicate that the C_a-C_a dimer bond does not break but instead the C_a-C_d back bond is cleaved. However, the potential energy barrier obtained for this reaction, 76.1 kcal/mol, is substantially larger than that of the direct dimer attack.

IV. DISCUSSION

The dimer bond length of 1.64Å calculated here is in good agreement with Yang and D'Evelyn's[7] 1.63Å and Verwoed's[8] 1.67Å, but somewhat apart from the result of Mehandru and Anderson,[9] 1.73Å, and the result of Zheng and Smith, 1.56Å[10]. Although LEED observations have been made of the reconstructed surface[2,3,4,6], no quantitative experimental data has been published to date on the bond lengths.

Reconstruction of the diamond (100) surface to the 2x1 state is an experimentally well documented phenomena.[2,3,4,6] The resulting structure appears very similar to the 2x1 silicon reconstruction.[2,3] Although the process seems to be quite similar to that seen on silicon, researchers report that a varying percentage of the freshly polished surfaces studied do not reconstruct to the 2x1 structure upon annealing.[2,3,4,6] Hamza et al. have reported an association between residual oxygen on the surface detected by electron stimulated desorption and the ability of the surface to reconstruct.[2] Samples with the most oxygen detected were less likely to reconstruct. Given the surface preparation techniques available both in situ and ex situ for diamond it seems reasonable to assume that surface contamination may explain the failure of some samples to reconstruct. The effect of impurities on surface reconstruction has been noted in a number of other systems including silicon and platinum.[17]

Conversion of the surface back to the 1x1 state by exposure to atomic hydrogen has been studied experimentally by only one other group.[2] Results reported by Hamza et al. indicated that the surface converted to the 1x1 configuration upon dosing with atomic hydrogen at 180K coupled with annealing at 700K.[2] LEED patterns disappeared following the dosing and the 1x1 pattern was then seen after annealing.[2] We see no evidence of either obscuration of the LEED pattern following dosing or of a reversion to the 1x1 surface structure. The LEED patterns gradually deteriorated with repeated dosing and desorption cycles until only weak first order spots remained coupled with a very high background. One expects the dimer bond on the C(100)-(2x1) surface to be stronger than what is seen on the Si(100)-(2x1) surface given the greater C-C bond strength, 83 kcal/mol[19] versus 46 kcal/mol[19] for Si-Si, and the ability of carbon to form double bonds. Theoretical calculations in the present study indicate that it is difficult to break the C-C dimer bond with atomic hydrogen. A large potential energy barrier, 48.7 kcal/mol, was found for breaking of the dimer bond by hydrogen atom addition. The calculated energy barrier for hydrogen addition to the dimer bond is in fairly close agreement with the 39 kcal/mol reported in Fig. 5 of Verwoerd[8], and with the 34.1 kcal/mol estimated recently by Zheng and Smith[10]. The theoretical results obtained here support the LEED observations which indicate the 2x1 surface does not convert back to the 1x1 configuration even after substantial dosing with atomic hydrogen.

The results obtained for hydrogen attack of the dimer backbond reinforce the observation that the C(100)-(2x1) surface is resistant to restructuring by atomic hydro-

gen. The potential energy barrier obtained for addition to the backbond, 76.1 kcal/mol, is substantially larger than for direct attack of the dimer bond. Although the potential energy barrier for dimer attack is relatively lower than for backbond attack, neither reaction appears likely in light of the substantial absolute value of the potential energy barriers. Furthermore, Yang and D'Evelyn have argued that even if individual dihydride units form, steric constraints severely limit the ability of the surface to saturate in the dihydride phase and at most the surface assumes a disordered dihydride with random dihydride units scattered among monohydride pairs.[7]

It should be noted that all of the dosings used in the present study were with an atomic hydrogen flux considerably lower than found in a typical CVD growth environment and with a substrate temperature also much lower. Breaking of the dimer bond by atomic hydrogen was predicted to have a large potential energy barrier at low temperature. In a CVD environment, with much higher fluxes of atomic hydrogen, it may be that significant numbers of dimer bonds could be broken to form the dihydride. At higher substrate temperatures it is also likely that the reaction probability for dimer bond breaking and hydrogen atom insertion will increase. However, at room temperature and with nominal dosing fluxes, the conversion to the 1x1 structure appears to be very much slower than what is seen on silicon.

V. CONCLUSIONS

Atomic hydrogen appears relatively inefficient at breaking C-C dimer bonds on the C(100)-(2x1) surface compared to the Si(100)-(2x1) surface under identical conditions. LEED patterns show only slight changes even after exposure of the surface to

40000L of H/H_2. Under similar conditions a silicon-(2x1) surface converts to the 1x1 phase after an exposure of less than 600L. MNDO calculations were done for two atomic hydrogen insertion reactions, direct attack of the dimer bond and attack of the back bond. Calculations indicate that there are substantial potential energy barriers to both reactions. The barrier to the dimer addition was calculated as 48.7 kcal/mol and 76.1 kcal/mol for attack of the back bond. Based on experimental and theoretical results it does not appear that exposure of the C(100)-(2x1) surface to atomic hydrogen at 25 ° C readily converts the surface to the 1x1 state.

Acknowledgments.

RTI wishes to thank the Innovative Science and Technology Program of the Strategic Defence Initiative Organization for support of the LEED studies under Contract No. N00014-86-C-0460. The computations were performed using the facilities of the Pennsylvania State University Center for Academic Computing. The work at Penn-State was supported in part by Innovative Science and Technology Program of the Strategic Defence Initiative Organization (SDIO/IST) via the U.S. Office of Naval Research, under Contract No. N00014-86-K-0443.

REFERENCES

1. e.g.; "Proceedings of the Second International Conference on New Diamond Science and Technology", edited by R. Messier, J.T. Glass, J.E. Butler, and R. Roy (Materials Research Society, Pittsburgh, PA, 1991). and Conf. Proc. 179th meeting of The Electrochemical Society, Wash, DC, May 1991
2. A.V. Hamza, G.D. Kubiak, and R.H. Stulen, Surf. Sci. 237, 35 (1990).
3. B.B. Pate, Surf. Sci. 165, 83 (1986).
4. R.E. Thomas, R.A. Rudder, and R.J. Markunas, "Thermal Desorption From Hydrogenated Diamond (100) Surfaces", presented at 179th meeting of The Electrochemical Society, Wash, DC, May 1991i. To be published, Conf. Proc.
5. J.P.F. Sellschop, C.C.P. Madiba, and H.J. Annegarn, Nucl. Instrum. Meth. 168, 529 (1980).
6. P.G. Lurie, and J.M. Wilson, Surf. Sci. 65, 453 (1977).
7. Y.L. Yang, and M.P. D'Evelyn, J. Am. Chem. Soc., submitted.
8. W.S. Verwoerd, Surf. Sci. 108, 153 (1981).
9. S.P. Mehandru, and A.B. Anderson, Surf. Sci. 248, 369 (1991).
10. X.M. Zheng, and P.V. Smith, Surf. Sci. 256, 1 (1991).
11. D. Huang, M. Frenklach, and M. Maroncelli, J. Phys. Chem. 92, 6379 (1988).
12. D. Huang, and M. Frenklach, J. Phys. Chem. 95, 3692 (1991).

13. D. Huang, and M. Frenklach, J. Phys. Chem. 1992, in press.

14. M.J.S. Dewar, and W. Thiel, J. Am. Chem. Soc. 99, 4899 (1977).

15. See for example J. Sadlej, *Semi-Empirical Methods of Quantum Chemistry*, translated by I. L. Cooper, (Ellis Horwood: Chichester, 1985).

16. Available from the Quantum Chemistry Program Exchange (Chemistry Department, Indiana University) as QCPE Program #506 (1985).

17. A. Zangwill, *Physics at Surfaces*, (Cambridge University Press, Cambridge, England, 1988), pp. 96, 258.

18. J.J. Boland, Surf. Sci. 244, 1 (1991).

19. W.L. Jolly, *Modern Inorganic Chemistry*, (Mcgraw Hill, New York, USA, 1984), p. 60.

Figure Captions

Figure 1. The "background" (100) surface element. The filed circles designate carbon atoms and the open circles -- hydrogen atoms. Carbon atoms of different layers are shaded with different patterns. Letters *a*, *b*, c, and *d* identify distinct reaction sites at the top two layers. The bottom of the figure gives top view of the model compound, and the top of the figure -- side (left) and top (right) views of the reacting monohydride dimer.

Figure 2. LEED patterns at 157eV from diamond(100)-(2x1) surface as loaded (Fig. 2a), before (Fig. 2b), and after (Fig. 2c) exposure to atomic hydrogen for 30 min at a total hydrogen pressure of $5x10^{-5}$ Torr. There may be a slight diminishment of the second order spots in Fig. 2c but the 2x1 pattern is clearly evident.

Figure 3. This figure shows LEED patterns from a sample exposed to H/H_2 at much higher pressures than used for the sample shown is Fig. 2. Figure 3a shows the sample after thermal cleaning. The 2x1 pattern is evident. Figure 3b shows the sample after dosing at .95 Torr for 5 min at 25 °C. The 2x1 surface structure is still visible. Figure 3c shows the sample after annealing at 1150_{eC} and atomic hydrogen dosing at 6.5 Torr. The 2x1 pattern is still present.

Figure 4. Variational diagram for the addition of an H atom to a C_b atom of

the dimer: top -- potential energy, and bottom -- dimer C- C bond length.

Figure 5. Variational diagram for the addition of an H atom to a C_d atom: top -- potential energy, and bottom -- C-C back-bond length.

SUBMITTED TO FALL MRS PROCEEDINGS 1991

Chemical Vapor Deposition of Diamond Films Using Water:Alcohol:Organic-Acid Solutions

R.A. Rudder, J.B. Posthill, G.C. Hudson, D.P. Malta, R.E. Thomas, and R.J. Markunas, T.P. Humphreys[1] and R.J. Nemanich[1]

Research Triangle Institute, Research Triangle Park, NC 27709-2194

[1] Dept. of Physics, North Carolina State University, Raleigh, NC 276955-8202

ABSTRACT

A low pressure chemical vapor deposition technique using water-alcohol vapors has been developed for the deposition of polycrystalline diamond films and homoepitaxial diamond films. The technique uses a low pressure (0.50 - 1.00 Torr) rf-induction plasma to effectively dissociate the water vapor into atomic hydrogen and OH. Alcohol vapors admitted into the chamber with the water vapor provide the carbon balance to produce diamond growth. At 1.00 Torr, high quality diamond growth occurs with a gas phase concentration of water approximately equal to 47% for methanol, 66% for ethanol, and 83% for isopropanol. A reduction in the critical power necessary to magnetically couple to the plasma gas is achieved through the addition of acetic acid to the water:alcohol solution. The lower input power allows lower temperature diamond growth. Currently, diamond depositions using water:methanol:acetic-acid are occurring as low as 300 °C with only about 500 W power input to the 50 mm diameter plasma tube.

INTRODUCTION

To date, diamond films produced by chemical vapor deposition techniques have been grown principally using heavy dilution of organic gasses with molecular hydrogen.[1-12] The role of molecular hydrogen to the process is manifold, but the dissociation of molecular hydrogen into a high fraction of atomic hydrogen is critical to diamond stabilization and growth. A plethora of techniques have been applied to create concentrations of atomic hydrogen sufficient for high quality diamond growth. Typically, these techniques involve a high-temperature region (hot-filament, oxy-acetylene torch, microwave plasma, dc arc discharge, etc.) wherein high dissociations of molecular hydrogen is feasible. Some workers have avoided the use of molecular hydrogen by using source gasses rich in oxygen.[8-10] Other workers have augmented the molecular hydrogen with small percentages of water.[11-12] We report here on a low pressure rf-inductive plasma-assisted chemical vapor deposition technique for the growth of diamond which uses water not molecular hydrogen as a process gas stabilizing diamond growth. Atomic hydrogen necessary for diamond growth (in this process) is supplied from plasma-dissociation of water and alcohol vapors. Unlike previous work, addition of water to the alcohol is necessary to produce well-facetted diamond growth in this low pressure rf-plasma technique.[9] Furthermore, it has been observed that addition of acetic acid to this CVD process enables diamond growth to occur at reduced rf power levels and consequently at lower substrate temperatures.

EXPERIMENTAL APPARATUS AND APPROACH

A description of the chemical vapor deposition system used in this work has been previously reported.[13-14] The system produces diamond from both traditional H_2 - CH_4 mixtures as well as the water:alcohol:organic-acid solutions. The system consists of a 50 mm id plasma

tube appended to a standard six-way cross. A radio frequency (13.56 MHz) induction coil couples power from the rf power supply into the plasma discharge. Samples are located on a graphite carrier located immediately underneath the induction plasma. The rf excitation induces currents in the graphite susceptor which serve to heat the sample. Samples are introduced into the vacuum system via a vacuum load-lock which isolates the main chamber. The gasses (water, alcohol, acetic-acid) are introduced into the chamber through a leak valve on a storage tank which contains solutions of the water/alcohol or water/acetic-acid/alcohol Vapors above the liquid are pumped from the storage tank into the growth chamber. The vapor pressure of the constituents above the liquid should be a produce of their molar concentration and their respective vapor pressures. Water and alcohol solutions at room temperature have sufficient vapor pressures to supply a low pressure discharge (< 10 Torr). High pressure operations might require the liquid solutions to maintained at an elevated temperature. For the growths reported here, vapors from various volumetric mixtures have been evaluated for diamond growth. The leak rate into the growth chamber from the solutions results in a loss of ~ 0.2 cc/min from the liquid solutions. While there will be some depletion of the higher vapor pressure component, the practice of mixing allows a convenient method for evaluating different ratios of water-to-alcohol without the necessity of a gas manifold.

Samples are introduced to the growth system through a vacuum load lock. Prior to insertion, samples have been subjected to a diamond abrasive treatment with 1-μm diamond paste to enhance nucleation. Diamond growth proceeds by initiating a rf induction plasma with sufficient power to magnifically couple to the gas. J. Amorrim et al.[15] have shown that rf coils couple to the plasma gas at low power levels through E-field coupling. At higher power levels, the rf coil couples power to the plasma gas through B-field coupling. The B-field coupling is characterized by an intense plasma luminescence from a region of high density electrons, $\sim 10^{12}$ cm^{-3}. The E-field coupling at lower powers results only in a low density plasma, $\sim 10^{10}$ cm^{-3} with weak plasma luminescence. Introduction of water vapor alone to a low pressure (1.0 Torr) rf inductive discharge results in intense atomic H emission. The water plasma has a characteristic red color associated with atomic H emission at 656 nm. OH emission lines are clearly visible but not as dominant as the atomic H emission lines. One thus observes that water discharges are capable of generating ample atomic H along with OH from the water dissociation. Atomic O lines, if pesent in the emission spectrum, are minor and have not been identified at this time. Addition of alcohol to the water plasma changes the color of the plasma emission to a bluer spectrum as CH and CO emissions are observed along with the atomic hydrogen Balmer lines.

EXPERIMENTAL RESULTS

A. Water:alcohol results

We have previously reported the growth of polycrystalline diamond films using water/methanol, water/ethanol, or water/isopropanol mixtures.[16] In that work, the vapor mixture entered the deposition system and diffused from the main chamber into the plasma tube The vapors were not admitted into the system through the plasma gas feed For this work, the storage bottle containing the liquid solutions was located on the plasma gas feed Various water-alcohol mixtures were used to determine the effect of the C/O ratio on diamond growth Figure 1 shows SEM micrographs from samples deposited at 1.0 Torr from volumetric water-methanol mixtures ranging from 80% methanol to 33% methanol The results for 80% methanol produce poorly faceted diamond These results contrast remarkably from the work

by Buck et al. and Bachmann et al. in a microwave discharge at higher pressures using 100% methanol. In that work, high quality diamond was obtained from only methanol. In this work, water addition to the methanol is critical to the formation of well-faceted crystalline diamond. As observed in Figure 1, the quality of diamond growth increases as the methanol volumetric concentration is reduced. At 33% methanol in the water solution, well-faceted diamond growth is observed. From the respective vapor pressures of water and methanol at 20°C, we estimate the vapor pressures of water and methanol to be 11.7 and 31.5 Torr, respectively, above the 33% methanol mixture. Using these vapor pressures, one calculates the C/C+O, the O/O+H; and the H/C+H ratios to be 0.42, 0.22, and 0.83, respectively. According to the depositon phase diagram of Bachmann, the low C/C+O ratio of 0.42 should result in no diamond growth. Nonetheless, this oxygen rich ratio is necessary for diamond growth in this system. As noted in the Bachmann work, actual gas phase concentrations may vary due to interactions of the plasma with the carbonasceous walls of the reactor. In this case, the reactions of the water-vapor plasma with the graphite susceptor undoubtedly increase the carbon concentrations in the gas phase. The graphite susceptor has been observed to be etched by the water-alcohol discharges at a rate of 25/h.

B. Acetic-acid:water:methanol results

It was observed that diamond growth from the water-alcohol solutions required less rf power than diamond growth from more traditional H_2/CH_4. The lower rf power most likely was a consequence of the water-methanol have lower ionization potentials than the H_2 - CH_4. Water, for instance, has an ionization potential of 12.61 eV as compared to an ionization potential of 15.43 eV for H_2. Methanol, for instance, has an ionization potential of 10.84 eV as compared to an ionization potential of 12.64 eV for CH_4. The lower ionization potentials permit lower rf power levels to be applied for sufficient plasma ionization. Correspondingly, we have observed that the addition of organic acids to the water solutions substantially reduces the critical power necessary to magnetically couple to the plasma gas. It is suspected that these organic molecules have even lower ionization potentials than water.

As a consequence, diamond growth in the low-pressure rf-induction plasma can be evaluated at lower substrate temperatures (through reduction in the induced current in the graphite sample carrier). Figure 2 shows SEM micrographs of diamond films deposited at 0.50 Torr using a volumetric mixture of 2.2.1 acetic-acid.water.methanol. The sample temperature is reduced from one sample to the next by the reduction in rf applied power. The growths at all temperatures show well-faceted diamond polyhedra. There appears to be no severe degradation of the film properties despite the $\sim$ 300°C reduction in growth temperature. Indeed, Raman spectra from these samples seemed to indicate that higher quality growth was achieved between 300-400°C than at the higher temperatures. Raman spectra for the films grown at 300 and 400 °C are shown in Figure 3 All these films showed an amorphous carbon component at 1500 cm^{-1}. The reduction in applied power did reduce the deposition rate. The film deposited at 575°C grew at a linear rate of 6000 Å/hr while the film deposited at 300°C grew at a linear rate of 2000 Å/hr.

DISCUSSION

The growth of diamond is undoubtedly facilitated in the low-pressure rf-induction plasma by the high electron density achieved when at a critical power the coupling changes from *E*-field to *B*-field coupling In this work, we have replaced molecular hydrogen and methane with

various mixtures of water, alcohols, and organic acids. The vapor discharges from the water-based solutions are easily ionized in the rf plasma owing to lower ionization potentials for the water, alcohol, and acetic acid molecules. As a consequence, lower power levels are necessary for a *B*-field coupling.

Once the *B*-field coupling occurs, the high electron density and high electron temperature allows atomization of the parent molecules. Atoms and free radicals of both graphite etchant species such as H and OH and carbon-containing radicals are present at the diamond growth surface. Dissociation of those species will depend directly on the bond strengths. If one compares bond-strengths for the various molecules and radical species used in this work, a number of interesting observations are apparent. First, the H-OH bond (119 kcal/mol) is not significantly weaker than the H-H bond (104.2 kcal/mol). Thus, the high generation of atomic hydrogen from water discharges is probably a consequence of the lower ionization potential and a larger cross-section for electron-impact dissociation. Second, the bond strengths for H-liberation for a radical such as CH_2O-H (31 kcal/mol) from the methanol has a significantly lower dissociation energy than the parent CH_3O-H (112 kcal/mol) molecule. The CH_2O-H dissociation energy is also significantly lower than any of the energies for methane, methyl, or methylene dissociation. One would expect that electron energies in the plasma sufficient to dissociate on a hydrogen from the methyl group on the alcohol would be more than sufficient to dissociate the CH_2O-H bond. And third, the lowest dissociation energies for H- liberation are found for the carboxyl radical COO-H (12 kcal/mol). These radicals are contained on the organic acid and halogenated organic acid groups. It is the dissociation of this bond that gives the acidity to water solutions containing these organic molecules. One would expect then that, besides the lower ionization potential offered by the addition of the organic acid molecules to the plasma discharge, the organic acids would readily release H atoms to the plasma gas. The organic acid group behaves as graphite solvent in this process. To date, we have not been successful in depositing diamond from solutions of exclusively water and acetic acid. Concentrations of acetic acid in excess of 80% in water solution have not been evaluated. For the concentrations of acetic acid that we are using for the low temperature diamond growth 2 2 1 (acetic-acid:water:methanol), the primary roles of the organic acid group are (1) to promote ionization in the rf induction coil and (2) to contribute H atoms to the growth process.

We have previously been discussing mechanisms by which the water-based processes promote diamond growth in low-pressure rf-induction plasmas. These mechanisms have all been concerned with H atom generation. At low pressures, diffusion of H atoms to walls and recombination of H atoms on the walls limit the steady-state population of H atoms. The steady state population being the difference of the generation and loss rates. The water-based processed (besides producing higher generation rates per unit power than the molecular-hydrogen based processes) may also significantly reduce the loss rates at low pressure. Water passivation of tube walls in flowing afterglow hydrogen discharges has been used to reduce wall recombination. Water vapor (integral to the diamond growth in this work) would continuously passivate the reactor walls. Indeed, it might be possible to maintain the reactor walls at low a enough a temperature to condense multiple layers of water on the plasma tube walls The water condensate would serve to buffer the wall materials from the extremely aggressive plasma environment. In addition to wall passivation, the water-based process may also reduce loss rates by permitting H^+ complexing with neutral H_2O water molecules The hydronium ion H_3O^+ as in acidic-water solutions should remain highly reactive, yet complexed so as to retard rapid diffusion to the plasma walls. It, thus, seems plausible that the water-based processes for diamond growth can enhance diamond growth both by permitting higher generation rates of

active species and by reducing loss mechanisms.

CONCLUSION

A low pressure chemical vapor deposition technique using water-alcohol vapors has been developed for the deposition of polycrystalline diamond films and homoepitaxial diamond films. The technique uses a low pressure (0.50 - 1.00 Torr) rf-induction plasma to effectively dissociate the water vapor into atomic hydrogen and OH. Alcohol vapors admitted into the chamber with the water vapor provide the carbon balance to produce diamond growth. Unlike previous results obtained from microwave sources using only methanol or Ar/methanol mixtures, the rf-induction source grows poor quality diamond unless water vapor is admitted. At 1.00 Torr, high quality diamond growth occurs with a gas phase concentration of water approximately equal to 47% for methanol, 66% for ethanol, and 83% for isopropanol. In the operation of the rf induction plasma, there exists a critical power level at which the coupling to the plasma changes from *E*-field coupling to *B*-field coupling. The *B*-field coupling has been shown in Ar plasmas to produce about two orders of magnitude increase in the electron density. We have observed that the critical power to achieve *B*-field coupling is substantially lower for the water-based processes as compared to the traditional molecular hydrogen-based processes. Furthermore, reduction in the critical power necessary to *B*-field couple is achieved through the addition of acetic acid to the water.alcohol solution. The water-alcohol vapors permit diamond growth to occur at lower power levels as compared to the H_2/CH_4 discharges. The lower input power level required in turn reduces substrate-carrier inductive heating and allows lower temperature diamond growth. Currently, diamond depositions using water.methanol.acetic-acid are occurring as low as 300° C with only about 500 W power input to the 50 mm diameter plasma tube.

ACKNOWLEDGEMENTS

The authors would like to acknowledge the support of this work by SDIO/IST through the ONR Contact No. N0014-86-C0460. The authors would also like to thank R. Durkee, S. Ammons, and D. Brooks for their outstanding technical support of this work.

REFERENCES

1. B. Derjaguin and V. Fedoseev, Russ. Chem. Rev. 39, 783 (1970).
2. B.V. Spitsyn, L.L. Bouilov, and B.V. Derjaguin, J. Cryst. Growth 52, 219 (1981).
3. S. Matsumoto, Y. Sato, M. Kamo, and N. Setaka, Jpn. J. Appl. Phys. 21, 183 (1982).
4. Y. Hirose and Y. Teresawa, Jpn. J. Appl. Phys. 25, L51 (1986).
5. M. Kamo, Y. Sato, S. Matsumoto, and N. Setaka, J. Cryst. Growth 62, 642 (1983).
6. L.M. Hanssen, W.A. Carrington, J.E. Butler, and K.A. Snail, Mater. Letters 7, 289 (1988).
7. G. Janssen, W.J.P. Van Enckevort, J.J.D. Schaminee, W. Vollenberg, L J. Giling, M. Seal, J. Cryst. Growth 104, 752 (1990).
8. Peter K. Bachmann, Dieter Leers, and Hans Lydtin, Diamond and Related Materials 1, 1 (1991)
9. M. Buck, T.J. Chuang, J.H. Kaufman, and H. Seki, Mat. Res. Soc. Symp. Proc. 162, 97 (1990)
10. C.F. Chen, T. M. Hon and C.L. Lin, presented at 18th Int. Conf. on Metallurgical Coatings and Thin Films (ICMCTF), San Diego, CA, April 23, 1991.
11. Yukio Saito, Kouji Sato, Hideaki Tanaka, Kazunori Fujita, Shinpei Matuda, J. Mater Sci 23, 842 (1988).

12. Yukio Saito, Kouji Sato, Kenichi Gomi, Hiroshi Miyadera, J. Mater. Sci. 25, 1246 (1990).

13. R.A. Rudder, G.C. Hudson, R.C. Hendry, R.E. Thomas, J.B. Posthill, and R.J. Markunas, "Applications of Diamond Films and Related Materials", Materials Science Monograph 73, 395 (1991).

14. R.A. Rudder, G.C. Hudson, J.B. Posthill, R.E. Thomas, and R.J. Markunas, Appl. Phys. Lett 59, 791 (1991).

15. J. Amorim, H.S. Maciel, and J.P. Sudano, J. Vac. Sci, Technol. B9, 362 (1991).

16. R.A. Rudder, G.C. Hudson, J.B. Posthill, R.E Thomas, R.C. Hendry, D.P. Malta, and R.J. Markunas, to appear Jan 20, 1992 in Appl. Phys. Lett.

Water-Alcohol Growth From Various Methanol Tank Mixtures

33%

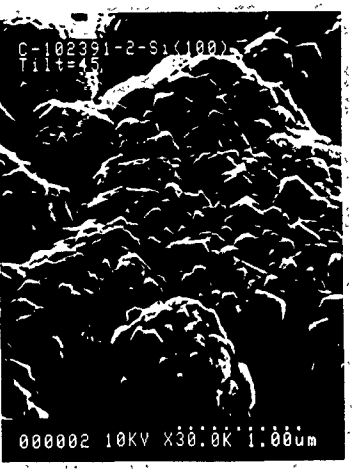

40%

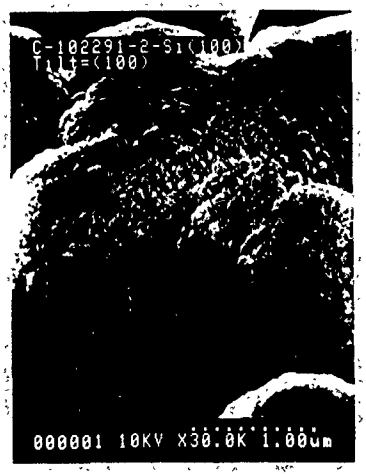

50%

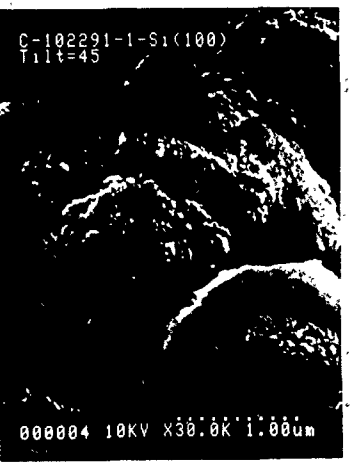

80%

RTI

Low Temperature Diamond Growth

550 °C

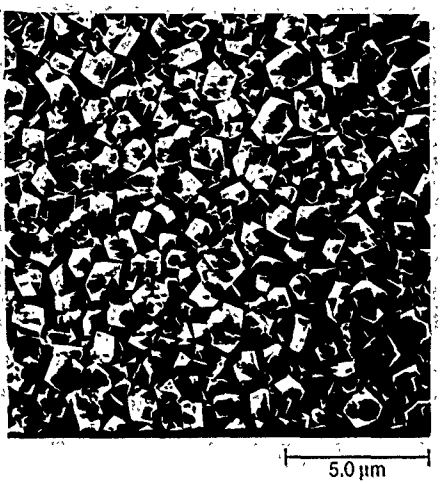

475 °C

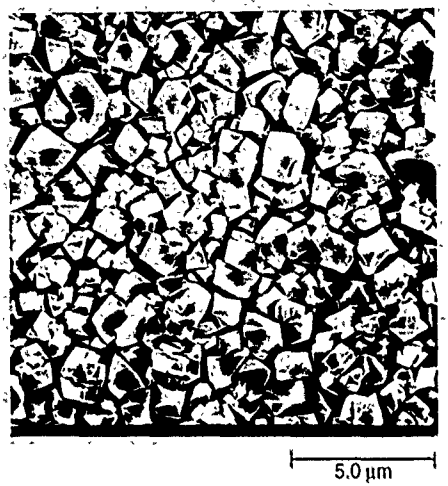

400 °C

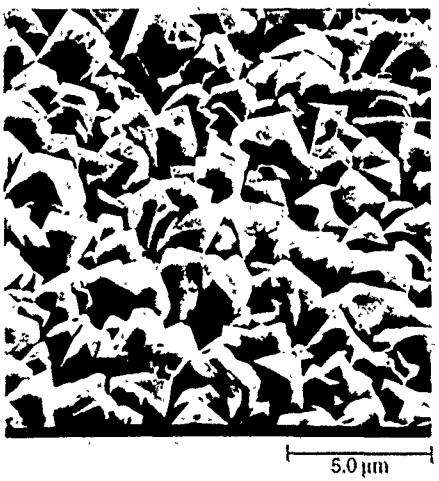

300 °C

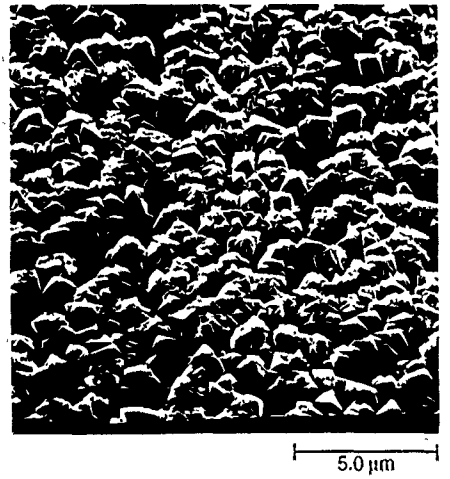

RTI

Low Temperature Diamond Growth

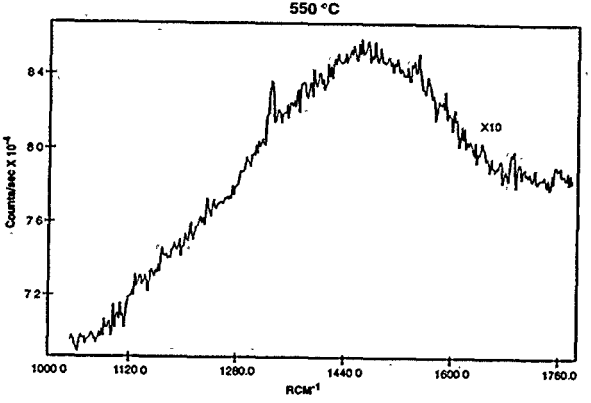

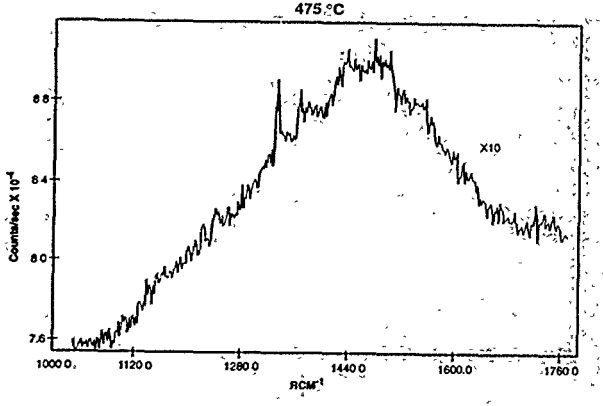

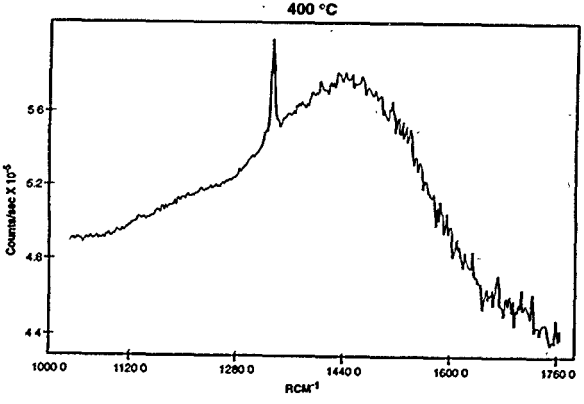

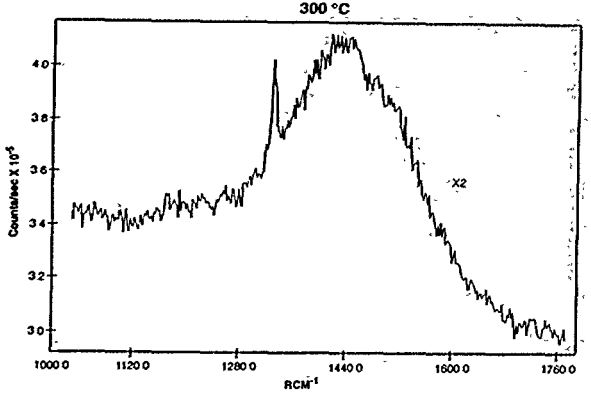

Cathodoluminescence from diamond films grown by plasma-enhanced chemical vapor deposition in dilute CO/H_2, CF_4/H_2, and CH_4/H_2 mixtures

R. J. Graham
Center for Solid State Science, Arizona State University, Tempe, Arizona 85287-1704

J. B. Posthill, R. A. Rudder, and R. J. Markunas
Research Triangle Institute, Research Triangle Park, North Carolina 27709-2194

(Received 19 June 1991; accepted for publication 30 August 1991)

Diamond films grown by rf plasma-enhanced chemical vapor deposition in dilute CO, CF_4, and CH_4 (diluent H_2) mixtures have been examined by cathodoluminescence (CL) in a transmission electron microscope to assess the incorporation of optically active impurities and defects. The details of the CL spectra are found to be dependent on the different gas mixtures and are correlated with the different film microstructures. Dislocation-related band *A* CL due to closely spaced donor-acceptor (*D-A*) pairs was observed from both the CO and CH_4-grown films, but was absent in the CF_4-grown material. Band *A* CL due to widely separated (*D-A*) pairs was seen in all samples but was especially dominant in the CF_4-grown film. Emission due to a di-Si interstitial impurity was observed in CO- and CF_4-grown films but was absent in the CH_4-grown material.

The chemical vapor deposition (CVD) of diamond films is currently receiving much attention.[1] At present, attempts at heteroepitaxial growth, usually on Si substrates, have resulted in heterogeneous polycrystalline films containing many defects and impurities. One of the goals of such growth methods must be the control of the formation of these inhomogeneities, especially if potential optical and electronic applications are to be realized. The aim of this study was to investigate how the use of dilute CO and CF_4, rather than the usual CH_4, in the CVD process might affect the incorporation of impurities or defects and the electronic states associated with them. The analytical technique used was spectrally resolved cathodoluminescence (CL) performed in a transmission electron microscope (TEM) which allows a simultaneous correlation of CL emission with specimen microstructure.

Three polycrystalline diamond films, 1–2 μm thick, were grown on Si(100) substrates by rf plasma-enhanced CVD (PECVD) using the following gas compositions and growth conditions: (1) 1% CH_4, 99% H_2, pressure = 5.0 Torr, temperature ~650 °C; (2) 2% CO, 98% H_2, pressure = 3.0 Torr, temperature ~630 °C; (3) 8% CF_4, 92% H_2, pressure = 5.0 Torr, temperature ~820 °C. Details of the growth of this last film are described in another publication.[2] An additional film was grown using 2% CO/98% H_2 at a temperature of ~725 °C on *R*-plane $(10\bar{1}2)$ sapphire to examine the effect of the substrate on the presence of impurities and defects. The substrates for the CO- and CH_4-grown films were scratched with diamond paste prior to deposition whereas the CF_4-grown film was grown on an unscratched and untreated Si substrate. Specimens were prepared for TEM by dimple polishing and milling with Ar^+ ions. Detection of CL was performed in TEM,[3] which also allowed the microstructure to be observed, using a 120 keV electron beam and liquid-nitrogen-cooled specimen stage.

Figure 1 shows CL spectra in the 300–900 nm range acquired from 15 μm-diam regions from all four films. The CH_4-grown film gave a spectrum which consists of a broad peak at 428±1 nm (2.90±0.01 eV) superimposed on an even broader band with a maximum around 470±1 nm (2.637±0.005 eV). The CF_4-grown film gave a broad band centered at 540±1 nm (2.295±0.004 eV), and a small peak at 737.8±0.5 nm (1.680±0.001 eV). Spectra from both CO-grown films exhibit a number of similar spectral features as summarized in Table I.

The CH_4-grown material consists of a perforated film containing 1–2 μm-sized grains, many with well-developed growth habits and microtwins. The grains often contain a high density of other small defects, possibly stacking faults or inclusions of nondiamond carbon, and associated static

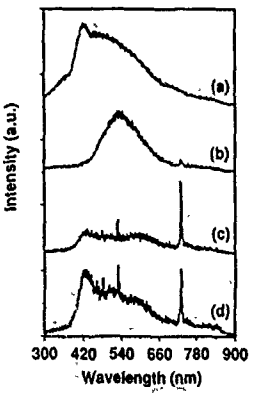

FIG. 1. CL spectra from polycrystalline diamond films: (a) 1% CH_4, 99% H_2, pressure = 5.0 Torr, temperature ~650 °C on Si(100), (b) 8% CF_4, 92% H_2, pressure = 5.0 Torr, temperature ~820 °C on Si(100); (c) 2% CO, 98% H_2, pressure = 3.0 Torr, temperature ~630 °C on Si(100), (d) 2% CO, 98% H_2, pressure = 3.0 Torr, temperature ~725 °C on *R*-plane $(10\bar{1}2)$ sapphire.

 0003-6951/91/442463-03$02.00

TABLE I. CL spectral features observed in dilute CO CVD-grown diamond on sapphire and Si substrates.

2% CO/98% H_2 sapphire substrate	2% CO/98% H_2 Si substrate
431 ± 1 nm (2.88 ± 0.01 eV) band	436 ± nm (2.84 ± 0.01 eV) band
464 ± 1 nm (2.671 ± 0.006 eV) peak	not obs.
484 ± 1 nm (2.561 ± 0.005 eV) peak	484 ± 1 nm (2.561 ± 0.005 eV) peak
503 ± 1 nm (2.464 ± 0.005 eV) peak	not obs.
534 ± 1 nm (2.321 ± 0.004 eV) peak	534 ± 1 nm (2.321 ± 0.004 eV) peak
586 ± 1 nm (2.115 ± 0.004 eV) shoulder	607 ± 1 nm (2.042 ± 0.003 eV) band
737.8 ± 0.5 nm (1.680 ± 0.001 eV) peak	737.8 ± 0.5 nm (1.680 ± 0.001 eV) peak

disorder, as also evidenced by significant diffuse scatter in convergent beam electron diffraction (CBED) patterns observed from individual crystals. The CF_4-grown film is continuous with a smaller grain size (0.1–0.3 μm). Although many grains are heavily microtwinned, inclusions are generally absent. Some grains are defect-free and CBED indicates a low degree of static disorder. The microstructure of the CO-grown films is very substrate dependent. On Si the film is continuous consisting of very defective 0.1–0.5 μm-sized grains whereas on sapphire highly defective connected nodules (1 μm diameter) form a perforated film. The weak CL intensity and small grain size in some of these films precluded a detailed correlation of microstructure with CL as has been demonstrated previously in CVD-grown diamond.[4] However, a general correlation with overall film structure is described below.

The emissions listed in Table I are identified as follows. The bands at 431 and 436 nm are known as band *A* and are due to closely spaced donor-acceptor (*D-A*) pairs. This emission is normally associated with natural, rather than synthetic, diamonds[5] but has often been observed from CVD-grown material[6–11] and has been correlated with dislocations.[4] The bands at 586 and 607 are probably also band *A* but are due to widely separated *D-A* pairs and are more typical of synthetic diamond, although the peak of the band at 607 nm is at the low-energy limit for band *A*. The intense peak at 737.8 nm is th same, within experimental error, as that observed previously in CVD-grown diamond and is due to di-Si interstitial impurities.[4,11–13] The origins of the emissions at 464, 484, and 503 nm are unknown although they have been observed previously in dilute CH_4 CVD-grown diamond.[8] The 534 nm peak has also been observed in CH_4-grown material and may be due to a nitrogen-vacancy-related complex.[8,9,12] For the CH_4-grown film, the 428 nm band is again due to closely spaced *D-A* pairs. The very broad band on which this is superimposed is probably also due to *D-A* pairs although it has an uncommonly large full width at half maximum (FWHM) of over 1100 meV and peaks at a higher energy than is usually encountered in *D-A* emission. For the CF_4-grown material, the band at 540 nm is typical of band *A* emission from widely separated *D-A* pairs in synthetic diamond. The small FWHM (7 meV) of the small peak at 737.8 nm confirms that this is again due to Si interstitials.

The *D-A* pair bands are due to nitrogen and boron impurities which presumably exist as contaminants of the source gases, vacuum system, and reactor components. Secondary-ion mass spectrometry (SIMS) of the films confirms the presence of these impurities. The interstitial Si impurity is believed to originate from the etching of either the Si substrate or silica reactor walls by the plasma. No new CL emissions from the CO- or CF_4-grown films were observed, suggesting that neither O or F are present as optically active impurities, although certainly F is incorporated in the CF_4-grown film during growth, as revealed by SIMS. In natural diamond, O has been found to exist at the 30–90 ppm level,[14] as elemental or mineralogical inclusions or possibly as a substitutional or interstitial impurity.[15] No optical activity has been documented which is consistent with our observations. No information about the presence of F in diamond was found in the literature.

The details of the CL emissions and film microstructure are, however, dependent on the growth gases and we now attempt to correlate the two. Dealing first with band *A* luminescence, all specimens, except the CF_4-grown films, show emission at around 430 nm due to closely spaced *D-A* pairs. Previous studies, which show that this emission is correlated with dislocations in CVD-grown diamond,[4] suggest that dislocations are present in these films. Potentially, other defects, e.g., stacking faults, nondiamond inclusions, may also allow *D-A* pairs to exist in the closer proximity normally associated with defect-free natural diamonds. This may account for the extremely broad band *A* observed in the CH_4-grown material where such defects in single crystals abound and to a lesser extent the CO-grown film on sapphire. However, if the density of other defects becomes too high resulting in poor crystallinity, increased nonradiative recombination reduces the overall CL intensity, as seen in the CO-grown films. Significantly, the CF_4-grown material was the least defective at a microscopic level, i.e., excluding microtwins, and showed no such band due to closely spaced *D-A* pairs. All films showed some degree of band *A* due to widely separated *D-A* pairs normally seen in synthetic diamond. In the CF_4-grown films this was the only peak of any significant intensity and the slightly higher peak energy, 2.3 eV compared with about 2.1 eV for the CO-grown films, suggests a smaller mean *D-A* pair separation. Faster growth rates have been observed when O is added to dilute CH_4,[14] which might result in *D-A* pairs being incorporated in even more random lattice sites resulting in larger mean *D-A* pair separation and a band *A* peak at lower energy.

The CO- and CF_4-grown films all showed some degree of interstitial di-Si impurity which is believed to originate from etching of Si-containing materials by the plasma in the growth zone. Although absent in the CH_4-grown film

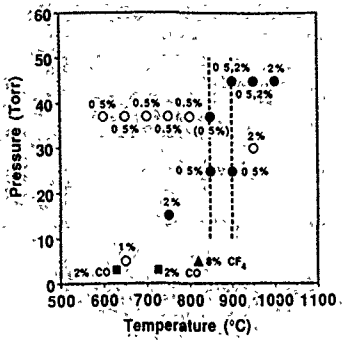

FIG. 2. Incidence of the di-Si interstitial defect, as observed by CL (1.681 eV peak), CVD-grown diamond on Si substrate as a function of growth temperature and pressure with the concentration of CH_4 used indicated: ● = peak observed, ○ = peak not observed, data from Refs. 4, 8–11, 13, and this work. For comparison, films grown using dilute CF_4 and CO (on Si and sapphire) which show the 1.681 eV peak are also represented (▲ = dilute CF_4, ■ = dilute CO). Broken vertical lines indicate range of pressures used for films shown as grown at 25 Torr, since exact pressures were not given. For the data point in parentheses, the peak in the CL spectrum was identified as GR1 due to neutral vacancy defect rather than di-Si (Ref. 9). Similarly, the peak in Ref. 10 was identified as GR1 but subsequently attributed to di-Si by the same workers (Ref. 13).

here, this has been observed in similar material by other workers.[4,11–13] The reason for this probably lies in the details of the growth conditions; previous observations by CL of the di-Si interstitial defect shown graphically in Fig. 2 suggest that it only occurs at higher growth temperatures and pressures and/or CH_4 concentration, although the limited number of data points, the different growth methods and other reactor-dependent variables make such a generalization only tentative. Intense peaks in the CO-grown films, grown under similar conditions to the CH_4-grown material, indicate that CO enhances the etching potency of the plasma resulting in higher levels of di-Si impurity. Conversely, the small size of this peak in the CF_4-grown film shows that little of this impurity has been incorporated as the optically active di-Si interstitial form during growth. This is surprising since CF_4-based plasmas are known to be very reactive; even visible etching of a glass viewport in the reactor occurred during previous runs. In addition, SIMS shows the Si content to be higher in this film than in the CO-grown films. This suggests that Si is also being incorporated as an optically inactive form and so implies that the nature of incorporation of Si depends on the gaseous species used and formed during the CVD growth process.

The source of the Si impurity has also been the subject of recent investigation. The spectra from the CO-grown material on the Si and sapphire substrates show the same basic emissions inspite of large differences in film microstructure. However, relative to band *A* and other emissions, the peak due to the di-Si interstitial defect was much more intense when the substrate was Si, indicating that much of this impurity originates from the substrate. The persistence of this peak when a sapphire substrate is used, indicates that at least some of the Si originates from the reactor which contrasts with recent studies by Ruan *et al.*[13] who found that this peak only when a Si substrate was used during growth with dilute CH_4. This could be explained by the apparently enhanced etching properties of the CO-containing plasma as previously discussed. The potential for reactor "memory" due to deposits on the reactor wall from earlier depositions on Si substrates also exists.

In conclusion, use of dilute CO and CF_4 does not introduce any optically active impurity or defect states not previously observed in dilute CH_4-grown CVD diamond. The different gases do, however, result in different film microstructures and concomitant CL spectra. Dislocation-related band *A* CL is observed from CO- and CH_4-grown films but only widely separated *D-A* pairs exist in the CF_4-grown material. The di-Si interstitial impurity was most readily incorporated in CO-grown films, with both the Si substrate and reactor walls believed to be the source. In comparison, the CF_4-grown film contained a higher concentration of Si, but only a small amount as the optically active di-Si form.

We are pleased to thank G. C. Hudson and D. P. Malta for their technical input and helpful discussions. This work was supported by the Facility for High Resolution Electron Microscopy at Arizona State University, supported by NSF Grant No. DMR-89-13384, JBP, RAR, and RJM gratefully acknowledge support of this work by the Strategic Defense Initiative Organization/Innovative Science and Technology through the Office of Naval Research (Contract No. N000014-86-C-0460).

[1] See, for example, "Diamond and Diamond-like Materials," special section of J. Mater. Res. 5, 2273 (1990).
[2] R. A. Rudder, G. C. Hudson, J. B. Posthill, R. E. Thomas, and R. J. Markunas, Appl. Phys. Lett. 59, 791 (1991).
[3] S. H. Roberts, Inst. Phys. Conf. Ser. 61, 51 (1981).
[4] R. J. Graham, T. D. Moustakas, and M. M. Disko, J. Appl. Phys. 69, 3212 (1991).
[5] P. J. Dean, Phys. Rev. 139, A588 (1965).
[6] H. Kawarada, K. Nishimura, T. Ito, J.-i. Suzuki, K.-S. Mar, Y. Yokota, and A. Hiraki, Jpn. J. Appl. Phys. 27, L683 (1988).
[7] A. T. Collins, M. Kamo, and Y. Sato, J. Phys. 1, 4029 (1989).
[8] A. T. Collins, M. Kamo, and Y. Sato, J. Phys. 22, 1402 (1989).
[9] L. H. Robins, L. P. Cook, E. N. Farabaugh, and A. Feldman, Phys. Rev. B 39, 13367 (1989).
[10] W. D. Partlow, J. Ruan, R. E. Witkowski, W. J. Choyke, and D. S. Knight, J. Appl. Phys. 67, 7019 (1990).
[11] A. T. Collins, M. Kamo, and Y. Sato, J. Mater. Res. 5, 2507 (1990).
[12] V. S. Vavilov, A. A. Gippius, A. M. Zaitsev, B. V. Deryagin, B. V. Spitsyn, and A. E. Alenksenko, Sov. Phys. Semicond. 14, 1078 (1980).
[13] J. Ruan, W. J. Choyke, and W. D. Partlow, Appl. Phys. Lett. 58, 295 (1991).
[14] H. W. Fesq, D. M. Biddy, C. S. Erasmus, E. J. D. Kable, and J. P. F. Sellschop, in *Physics and Chemistry of the Earth*, edited by L. H. Ahrens, J. B. Dawson, A. R. Duncan, and A. J. Erlank (Pergamon, Oxford, 1975), Vol. 9, p. 817.
[15] J. Walker, Rep. Prog. Phys. 42, 1605 (1979), and references therein.

Applications of Diamond Films and Related Materials
Y. Tzeng, M. Yoshikawa, M. Murakawa, A. Feldman (Editors)

Dense Nucleation of Polycrystalline Diamond Films Using CF_4-H_2 Low Pressure rf Discharges

R.A. Rudder, G.C. Hudson, D.P. Malta, J.B. Posthill,
R.E. Thomas, and R.J. Markunas

Research Triangle Institute, Research Triangle Park, North Carolina 27709-2194

Abstract

Dense nucleation of small-grain polycrystalline diamond films on Si(100) substrates has been accomplished without the use of any surface pretreatment such as abrasive diamond scratching, surface oil treatments, or diamond-like carbon predeposition. The depositions occurred in a low pressure rf plasma assisted chemical vapor deposition system using mixtures of CF_4 and H_2. Films deposited at 5 Torr and 850°C on as-received silicon wafers show dense nucleation, well-defined facets, and crystallites which ranged in size from 500 to 10,000 Å. X-ray photoelectron spectroscopy and electron energy loss show the films to be diamond with no major impurity and no detectable graphitic component. Raman spectroscopy shows a pronounced 1332 cm^{-1} line accompanied with a broad band centered about 1500 cm^{-1}. Preliminary data indicates that this process is applicable to substrates other than silicon. This process will have important applications in areas where surface pretreatments, such as diamond polishing, are not viable.

1. INTRODUCTION

Growth of polycrystalline diamond from the gas phase at pressures near and below atmospheric pressure has been well-documented and reported.[1-7] A variety of techniques have been developed for chemical vapor deposition of diamond. These techniques have involved microwave plasmas, rf plasmas, hot filaments, arc-jets, rf-plasma torches, and acetylene torches. Typically, the source gasses used for diamond deposition have been hydrogen with dilute concentrations of a variety of hydrocarbons. It has been observed that (1) diamond nucleates well on itself and cubic boron nitride, (2) scratching of non-diamond surfaces with diamond abrasive enhances the diamond nucleation, and (3) diamond deposition without surface pretreatments such as scratching, oiling, or diamond-like carbon deposition does occur but at a much reduced nucleation rate.

In this letter, we report on a technique for the deposition of diamond onto Si substrates without any pre-treatment of the wafer prior to its insertion into the growth reactor. Through the use of CF_4 as a carbon source gas, dense nucleation of

diamond crystals has been achieved. Prior to the work reported here deposition of thin continuous diamond films on substrates other than diamond has not been possible without subjecting the substrate to treatments designed to enhance or promote nucleation. For many applications the standard methods for promoting nucleation to achieve continuous films are not feasible. A process that avoids the need for surface pre-treatments extends the range of substrates and applications available for diamond thin films. Potential applications are seen in the deposition of diamond for heteroepitaxial growth, tool coatings, and optical coatings whereby dense nucleation is needed to promote epitaxial registration, chemical adherence, and optical transmission, respectively. In addition, studies of the chemical process differences between diamond deposition with traditional CH_4 in H_2 plasmas which do not promote nucleation and deposition with CF_4 in H_2 plasmas used in the present work which do promote diamond nucleation allows the fundamental mechanisms of diamond hetero-nucleation to be addressed.

2. EXPERIMENTAL

The diamond deposition was accomplished in a low-pressure rf-plasma assisted chemical vapor deposition system. The reactor consists of a inductively coupled plasma tube vacuum pumped by a 1000 l/s turbomolecular pump. The plasma tube is a water cooled quartz jacket of $\sim$ 50 mm on the inside diameter. The quartz tube walls have been thoroughly covered with carbon deposition from previous diamond depositions using 1% CH_4 in H_2 discharges. The plasma is maintained by a 1-3 kW rf generator at 13.56 MHz. The samples are located on a graphite susceptor just beneath the rf coils. The system is equipped with a quadrupole mass spectrometer for sampling of gas flux from the plasma tube.

During deposition, the pressure was maintained at 5.0 Torr using 25 sccm of H_2 and 2 sccm of CF_4 pumped through an automatic control butterfly valve. The samples were maintained at $\sim$ 850°C using both inductive heating of the graphite susceptor from the rf coils and radiative heating of the susceptor from a graphite resistive heater. The plasma is maintained for the duration of the growth via inductive coupling of approximately 2000 W from the rf generator. The deposition time was 3 hrs for the samples reported herein. Monitoring of the gas flux from the plasma tube during deposition shows that the parent gas mix of CF_4 and H_2 is converted into HF and C_2H_2. No fluoromethane groups were observed.

3. RESULTS AND DISCUSSION

Upon removal from the reactor, films showed dense nucleation of diamond over the unscratched Si surfaces. Scanning electron microscopy (SEM) micrographs from sample No. 1 are shown in Figure 1. At lower magnification, there is some thickness non-uniformity to the deposited layer. This may be a consequence of diamond nucleation having occurred locally at different times after initiation of the discharge.

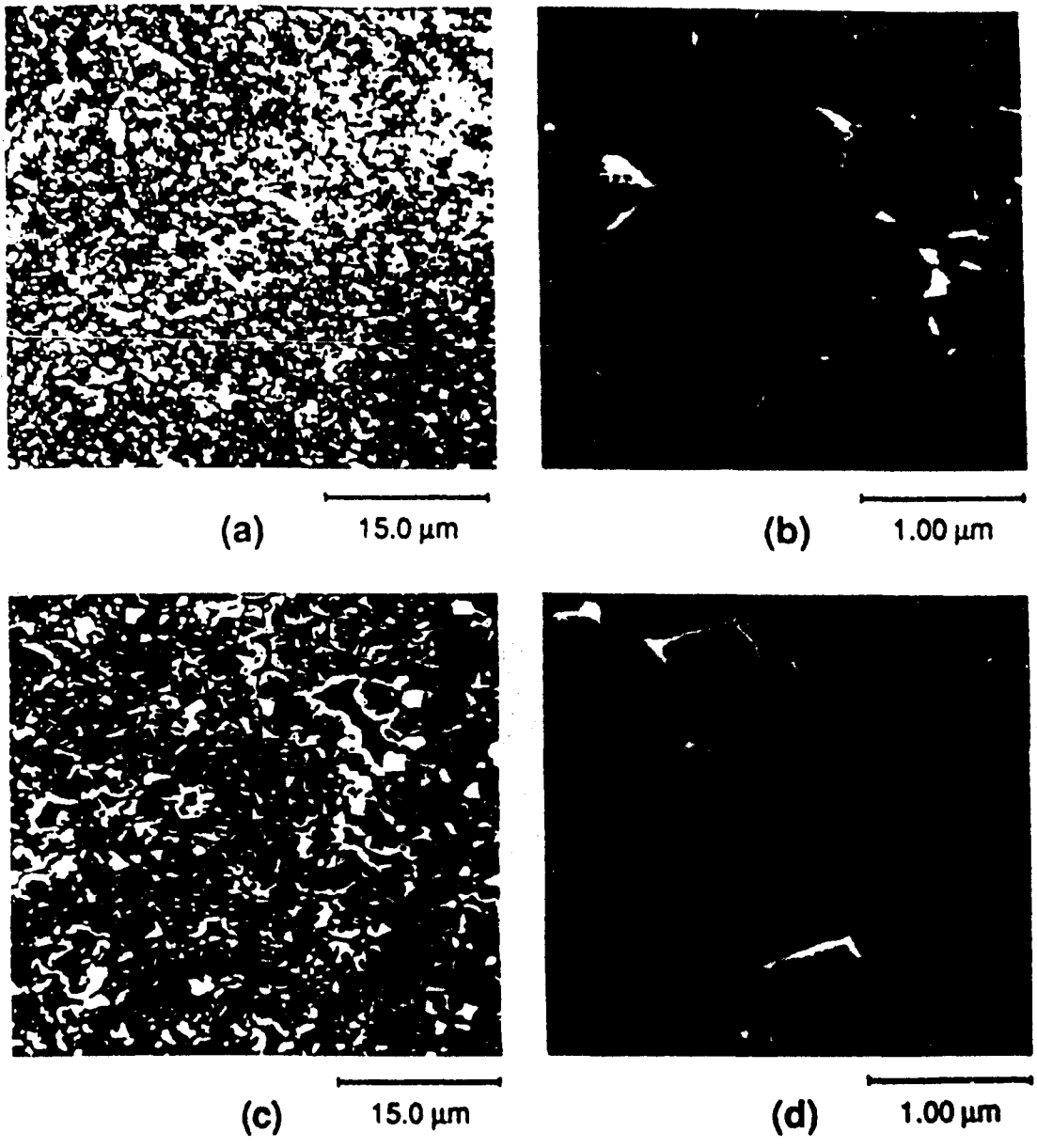

Figure 1. Scanning electron micrographs of sample No. 1: (a), (b), (c) are progressively higher magnification views of the polycrystalline diamond surface; (d) is a micrograph of a cleaved cross-section showing some interfacial roughness between the diamond layer and the silicon surface.

At higher magnification, all features show well-defined facets with a broad distribution in grain size. Figure 1(d) shows the cleaved cross-section micrograph of sample No. 1. The diamond film is ~ 1 μm in thickness. The cross sectional micrograph also shows that the silicon/diamond interface is non-planar; initially suggesting that the Si surface was chemically etched prior to diamond nucleation and growth. Initial cross-section TEM results show that the diamond film/substrate interface is in fact relatively planar, but an irregular thickness region in the substrate has developed between the bulk Si single crystal and the diamond film. The irregular region is also found to be amorphous. Further TEM studies of the diamond film/substrate interfacial material and the nucleation process are underway. SEM micrographs of sample No. 2 are shown in Figure 2. This sample was also deposited with a 8% CF_4 in H_2 gas mixture. The surface topography and crystallite size vary from sample to sample, but nearly the entire surface of the as-received silicon wafers show dense diamond nucleation.

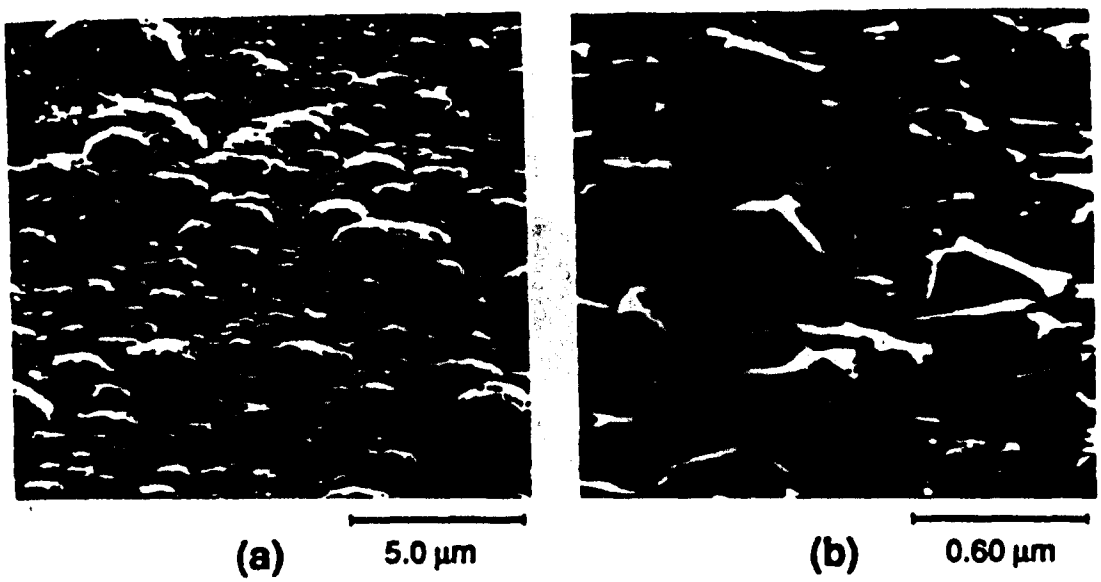

Figure 2. Scanning electron micrographs of sample No. 2 : (a) and (b) are different magnifications of the polycrystalline diamond surface.

Chemical determination of the films was accomplished with x-ray photoelectron spectroscopy (XPS). The XPS shows principally carbon present with some oxygen contamination probably from air transfer from the deposition system to the surface analysis unit. It is significant to note that no Si was observed in the films. It is

interesting to note that no fluorine was observed. One might expect that the deposition of diamond from a fluorocarbon source would result in fluorine termination of the growth surface. At the growth temperatures of 850°C employed in this work, work by Freedman and Steinspring[8] have shown that fluorine does not reside on a diamond (100) surface. Furthermore, in the atomic hydrogen environment produced by the high power rf discharge, any surface fluorine is energetically favored to be extracted from the surface via the formation of HF. Electron energy loss shows the surface of the film to be diamond. The bulk and surface plasmons of diamond are observed. The graphitic plasmon (6 eV from the primary beam) was not observed. Characteristic Raman spectra are shown in Figure 3 for the samples No. 1 and No. 3. The Raman spectrum from each of the samples shows a clear 1332 cm^{-1} diamond longitudinal optical (LO) phonon, and each spectrum shows a broad feature around 1500 cm^{-1}. The broad feature is associated with non-diamond material, perhaps residing between the grains.

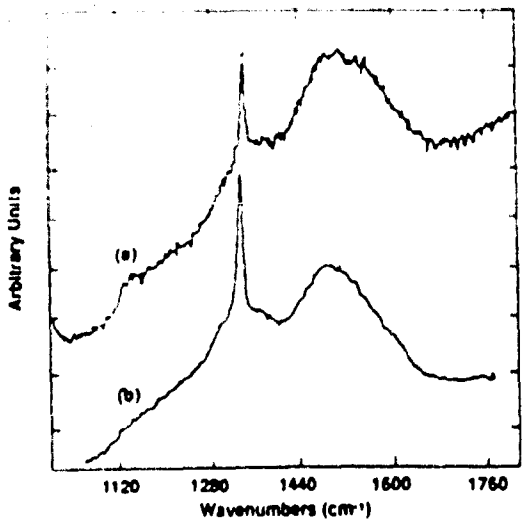

Figure 3. Raman spectra from polycrystalline diamond deposition on as-received silicon surfaces: (a) is the spectrum from sample 1, and (b) is the spectrum from sample No. 3.

4. CONCLUSIONS

In conclusion, a plasma based process involving H_2/CF_4 which promotes dense nucleation and growth of polycrystalline diamond films on as-received Si wafers has been demonstrated. Mass spectroscopy of the gasses downstream from the plasma tube show that the H_2/CF_4 mixture is converted to HF and C_2H_2 with no detection of any fluoromethanes. The layers were characterized and determined to be diamond by Raman spectroscopy, x-ray photoelectron spectroscopy, and electron energy loss. SEM observations show the grain size to vary from 500 to 10,000 Å. Without the necessity of surface pretreatments for the growth of diamond, it is anticipated that this technique will find broad application in heteroepitaxial studies, optical coatings, tool coatings, and other areas.

Acknowledgments: The authors wish to acknowledge the financial support of the Strategic Defense Initiative Organization / Innovative Science and Technology through the Office of Naval Research, Contract No. N-00014-86-C-0460. The authors also wish to thank Dr. T. P. Humphreys and Dr. R. J. Nemanich at North Carolina State University for Raman analysis.

5. REFERENCES

1. B. Derjaguin and V. Fedoseev, Russ. Chem. Rev. 39, 783 (1970).
2. S. Matsumoto, Y. Sato, M. Kamo, and N. Setaka, Jpn. J. Appl. Phys. 21, 183 (1982).
3. Y. Hirose and Y. Teresawa, Jpn. J. Appl. Phys. 25, L51 (1986).
4. M. Nakazawa, T. Nakashima, and S. Seikai, Appl. Phys. Lett. 45, 823 (1984).
5. M. Kamo, Y. Sato, S. Matsumoto, and N. Setaka, J. Cryst. Growth 62, 642 (1983).
6. S. Matsumoto, M. Hiro, and T. Kobayashi, Appl. Phys. Lett. 51, 737 (1987).
7. K. Kurihara, K. Sasaki, M. Kawarada, and N. Koshiro, Appl. Phys. Lett. 52, 437 (1988).
8. Andrew Freedman and Charles D. Steinspring, Appl. Phys. Lett. 57, 1194 (1990).

Direct deposition of polycrystalline diamond films on Si(100) without surface pretreatment

R. A. Rudder, G. C. Hudson, J. B. Posthill, R. E. Thomas, and R. J. Markunas
Research Triangle Institute, Research Triangle Park, North Carolina 27709-2194

(Received 18 February 1991; accepted for publication 3 June 1991)

Dense nucleation of small-grain polycrystalline diamond films on Si(100) substrates has been accomplished without the use of any surface pretreatment such as abrasive diamond scratching, surface oil treatments, or diamond-like carbon predeposition. Diamond depositions occurred in a low-pressure rf plasma-assisted chemical vapor deposition system using mixtures of CF_4 and H_2. Films deposited at 5 Torr and 850 °C on as-received silicon wafers show dense nucleation, well-defined facets, and crystallites which ranged in size from 500 to 10 000 Å. X-ray photoelectron spectroscopy and electron energy loss show the films to be diamond with no major impurity and no detectable graphitic component. Raman spectroscopy shows a pronounced 1332 cm^{-1} line accompanied with a broad band centered about 1500 cm^{-1}.

Growth of polycrystalline diamond from the gas phase at pressures near and below atmospheric pressure has been well documented and reported.[1-7] Techniques for diamond deposition have involved microwave plasmas, rf plasmas, hot filaments, arc jets, rf plasma torches, and acetylene torches. Typically, the source gases have been hydrogen with dilute concentrations of hydrocarbon. It has been observed that (1) diamond nucleates well on itself and cubic boron nitride, (2) scratching of nondiamond surfaces with diamond abrasive enhances the diamond nucleation, and (3) diamond deposition without surface pretreatments such as scratching, oiling, or diamond-like carbon deposition does occur but at a reduced nucleation rate. Without the surface pretreatments, deposition of thin, continuous diamond films is not possible.

In this letter, we report a technique for the deposition of diamond onto Si substrates without any pretreatment of the wafer prior to its insertion into the growth reactor. The process has potential application in the deposition of diamond for heteroepitaxial growth, tool coatings, and optical coatings, whereby dense nucleation is needed to promote epitaxial registration, chemical adherence, and optical transmission, respectively. More fundamentally, understanding the chemical process differences between traditional CH_4 in H_2 plasmas which do not promote nucleation and the CF_4 in H_2 plasmas used in the present work which do promote diamond nucleation may permit the mechanisms of diamond heteronucleation to be elucidated.

The dense nucleation of polycrystalline diamond was accomplished in a low-pressure rf plasma-assisted chemical vapor deposition system. A schematic of the system is shown in Fig. 1. The reactor consists of a inductively coupled plasma tube vacuum pumped by a 1000 *l*/s turbomolecular pump. The plasma tube is a water-cooled quartz jacket of ~50 mm inside diameter. The quartz tube walls were thoroughly covered with carbon deposition using 1% CH_4 in H_2 discharges prior to this work. The plasma is maintained by a 1–3 kW rf generator at 13.56 MHz. The samples are located on a graphite susceptor just beneath the rf coils. The system is equipped with a quadrupole mass spectrometer for sampling of gas flux from the plasma tube.

During deposition, a pressure of 5 0 Torr was maintained using 25 sccm of H_2 and 2 sccm of CF_4 pumped through an automatic control butterfly valve into a turbomolecular pump. The samples were maintained at ~850 °C using both inductive heating of the graphite susceptor from the rf coils and radiative heating of the susceptor from a graphite resistive heater. The plasma was maintained for 3 h via inductive coupling of approximately 2000 W from the rf generator. Monitoring of the gas flux from the plasma tube during the start of deposition shows that the parent gas mix of CF_4 and H_2 is converted into HF and C_2H_2. No fluoromethane groups were observed. It is important to note that these are equilibrium products after the CF_4-H_2 gas mixture has passed through the discharge. In the discharge region, there are undoubtedly atomic hydrogen, atomic fluorine, and a mix of fluorocarbon radicals.

The diamond films showed dense nucleation on the

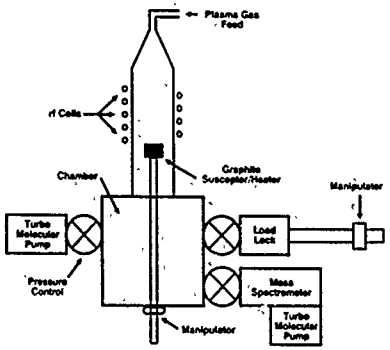

FIG. 1. Schematic of low-pressure rf plasma-assisted chemical vapor deposition system.

 0003-6951/91/320791-03$02.00

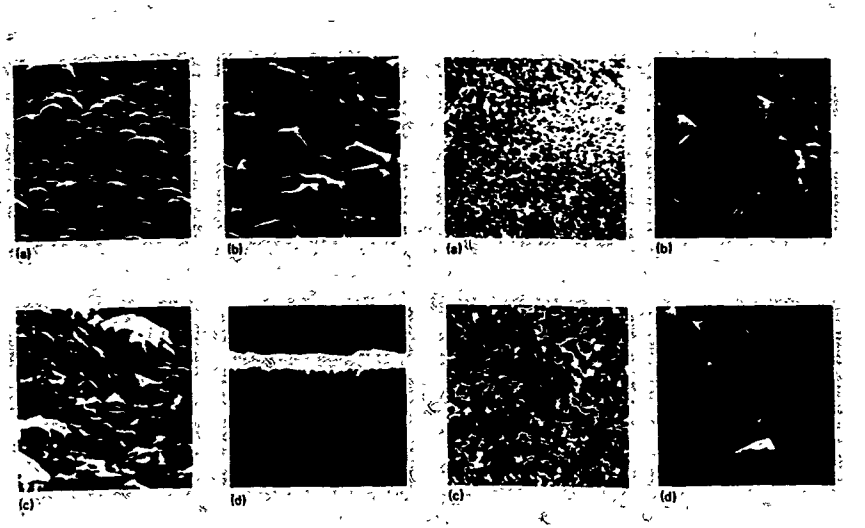

FIG. 2. Scanning electron micrographs of sample No. 1: (a), (b), (c) are progressively higher magnification views of the polycrystalline diamond surface; (d) is a micrograph of a cleaved cross section showing some interfacial roughness between the diamond layer and the silicon surface.

FIG. 3. Scanning electron micrographs of samples No. 2 and No. 3: (a) and (b) are different magnifications of the polycrystalline diamond surface for sample No. 2, (c) and (d) are different magnifications of the polycrystalline surface for sample No. 3.

Si(100) surfaces. Scanning electron microscopy (SEM) micrographs from sample No. 1 are shown in Fig. 2. At lower magnification, there is some thickness nonuniformity to the deposited layer. This may be a consequence of diamond nucleation having occurred locally at different times after initiation of the discharge. At higher magnification, all features show well-defined facets with a broad distribution in crystallite size. Figure 2(d) shows the cleaved cross-section micrograph of sample No. 1. The diamond film is $\sim 1\ \mu$m in thickness. The silicon/diamond interface is nonplanar suggesting that the Si surface was chemically etched prior to diamond nucleation and growth. Etching of the silicon surface probably occurred due to production of atomic fluorine from plasma dissociation of the CF_4. SEM micrographs of two other samples are shown in Fig. 3. These samples were also deposited with a 8% CF_4 in H_2 gas mixture. The surface topography and crystallite size vary from sample to sample, but all samples showed dense diamond nucleation.

Chemical analysis of the films with x-ray photoelectron spectroscopy (XPS) shows principally carbon present with some oxygen contamination probably from air transfer between the deposition system and the XPS unit. No Si was observed in the films. It is interesting to note that fluorine was observed bound to the surface carbon. Figure 4 shows a high-resolution XPS scan of the C 1s line. It shows both C—C bonding at 285 eV and C—F bonding at 288 eV. The fluorine bonding to the diamond may be present during growth, or it could possibly arises from residual contamination of the surface upon termination of the rf discharge. At the growth temperatures of 850 °C employed in this work, Freedman and Steinspring[8] have shown that fluorine does not reside on a diamond (100) surface. Furthermore, in the atomic hydrogen environment produced by the high-power rf discharge, any surface fluorine would likely be extracted from the surface via the formation of HF. Indeed, Simko *et al.* have observed that hydrogen discharges can remove fluorine from fluorocarbon residues on Si surfaces following reactive ion etching.[9] Electron energy loss shows the surface of the film to be diamond. The bulk and surface plasmons of diamond are observed. The graphitic plasmon (6 eV from the primary beam) was not observed. Characteristic Raman spectra are shown in Fig. 5 for samples Nos. 1 and 3. The Raman spectrum from each of the samples shows a clear 1332 cm^{-1} diamond longitudinal

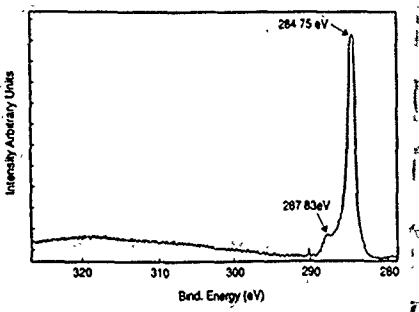

FIG. 4. High-resolution x-ray photoelectron spectrum from the carbon 1s region showing the presence of fluorine chemically bound to the diamond

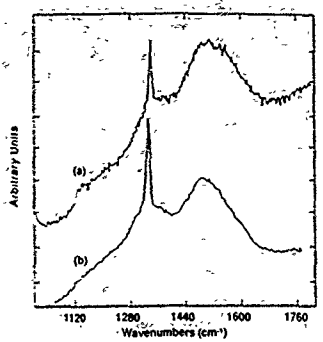

FIG. 5. Raman spectra from polycrystalline diamond deposition on as-received silicon surfaces: (a) is the spectrum from sample No. 1, and (b) is the spectrum from sample No. 3.

optical (LO) phonon, and each spectrum shows a broad feature centered at 1500 cm^{-1}. The broad feature is associated with nondiamond material that is perhaps residing between the grains. The full width at half maximum (FWHM) values of the 1332 cm^{-1} lines for the diamond films were around 7 cm^{-1}. It is not clear whether the large FWHM is due to the small crystallite size or due to defects or impurities in the diamond. It is quite probable that substantial impurities below the detection limit of the XPS could be incorporated from reactor fixtures.

In conclusion, a plasma-based process has been demonstrated which promotes dense nucleation and growth of polycrystalline diamond films on as-received Si wafers. The process has been demonstrated with 8% CF_4 in H_2 discharges. It is noted that, in reactive ion-etching processes, concentrations of H_2 exceeding 42% in CF_4 result in polymer deposition on silicon wafers.[10] The process reported here at higher hydrogen concentrations and at higher deposition temperatures results in diamond deposition. The layers were characterized and determined to be diamond by Raman spectroscopy, x-ray photoelectron spectroscopy, and electron energy loss. SEM observations show the grain size to vary from 500 to 10 000 Å. Mass spectroscopy of the gases downstream from the plasma tube shows that the H_2/CF_4 mixture is converted to HF and C_2H_2. No fluoromethane groups were detected in the gas stream downstream from the plasma. Undoubtedly, there are many reactive radical species in the plasma discharge region. These species are contributing to the stabilization of the diamond phase at CF_4 concentrations much higher than the CH_4 concentration that is commonly used for diamond growth in hot-filament, microwave plasma, or rf plasma techniques. Without the necessity of surface pretreatments for the growth of diamond, it is anticipated that this technique will find broad application in heteroepitaxial studies, optical coatings, tool coatings, and other areas.

The authors wish to acknowledge the financial support of the Strategic Defense Initiative/Innovative Science and Technology Office through the Office of Naval Research, contract No. N-00014-86-C-0460. The authors also wish to thank Dr. T. P. Humphreys and Dr. R. J. Nemanich at North Carolina State University for Raman analysis, and D. P. Malta for SEM analysis.

[1] B. Benaguin and V. Fedoseev, Russ. Chem. Rev. 39, 783 (1970).
[2] S. Matsumoto, Y. Sato, M. Kamo, and N. Setaka, Jpn. J. Appl. Phys. 21, 183 (1982).
[3] Y. Hirose and Y. Teresawa, Jpn. J. Appl. Phys. 25, L51 (1986).
[4] M. Nakazawa, T. Nakashima, and S. Seikai, Appl. Phys. Lett. 45, 823 (1984).
[5] M. Kamo, Y. Sato, S. Matsumoto, and N. Setaka, J. Cryst. Growth 62, 642 (1983).
[6] S. Matsumoto, M. Hiro, and T. Kobayashi, Appl. Phys. Lett. 51, 737 (1987).
[7] K. Kurihara, K. Sasaki, M. Kawarada, and N. Koshiro, Appl. Phys. Lett. 52, 437 (1988).
[8] Andrew Freedman and Charles D. Stinespring, Appl. Phys. Lett. 57, 1194 (1990).
[9] J. P. Simko, G. S. Oehrlein, and T. M. Mayer, J. Electrochem. Soc. 138, 277 (1991).
[10] L. M. Ephrath, J. Electrochem. Soc. 126, 1419 (1979).

Applications of Diamond Films and Related Materials
Y. Tzeng, M. Yoshikawa, M. Murakawa, A. Feldman (Editors)

Enhancement of diamond nucleation by graphite fibers local to substrate surfaces in H_2 - CH_4 rf discharges.

R.A. Rudder, G.C. Hudson, R.C. Hendry, R.E. Thomas, J.B. Posthill, and R.J. Markunas

Research Triangle Institute, Research Triangle Park, NC 27709-2194.

Abstract

A method has been discovered for enhancing diamond nucleation without using any mechanical treatment to the surface. We have observed that the presence of graphite fibers tangential to a substrate surface greatly enhances the nucleation of diamond crystals immediately underneath the fiber. Diamond growth has been observed along lines and in small clusters replicating the graphite fiber pattern following exposures of unscratched silicon, nickel, and fused quartz substrates to 2% CH_4 in H_2 rf-discharges.

1.0 INTRODUCTION

One of the foremost problems addressing the diamond community is the understanding of diamond nucleation on non-diamond substrates. Typically, workers depositing polycrystalline diamond enhance the diamond nucleation by abrading the surface with diamond polishing compound.[1-3] The exact role of the diamond polishing has not been resolved. Polishing with non-diamond abrasives also enhances nucleation, but the enhancement is not as pronounced as with the diamond paste. The polishing compound could either create defect sites upon which the nucleation can occur or leave small diamond particles on the surface upon which monolithic diamond growth can occur. Recent results indicate that the latter mechanism may predominate.[4] Indeed, Geis has purposely purposely attached diamond seed crystals to silicon surfaces for the growth of textured polycrystalline material. For applications of diamond thin films to many substrates, the abrasive polish is unacceptable. Such abrasive polish degrades the performance of the diamond/substrate device principally through damage to the substrate subsurface induced by the mechanical polish. We report here on a technique for enhancing diamond nucleation without the necessity of a mechanical treatment.

2.0 EXPERIMENTAL RESULTS

We have observed that the presence of graphite fibers tangential to a substrate surface greatly enhances the nucleation of diamond crystals immediately underneath the fiber. Note the fibers were merely placed on the surface; no abrasion was used. Silicon, nickel, fused silica, and crystalline quartz substrates thus "fiberized" show diamond growth along lines and in small clusters.

Depositions occurred in a low-pressure rf-plasma assisted chemical vapor deposition system that has been used previously to grow polycrystalline[5] and homoepitaxial[7] diamond films. In this work, various substrates were inserted into the reactor without any diamond polishing or surface treatments other than placing the graphite fibers on the substrates. The fibers used in this work were taken from a yarn of material composed of 3-5 μm diameter carbon-graphite fibers. The carbon fibers are not composed of highly oriented graphite. Growths on the substrates occurred at pressure of 5 Torr in a 2% CH_4 in H_2 atmosphere. The substrate temperature during growth was approximately 800°C. As shown in Figure 1, the deposition patterns on the substrates mimic the placement of graphite fibers on the substrates prior to diamond growth. Diamond deposition on the substrates underneath the fibers show clear facetting with lines of individual crystals. Each line consists of colinear, contiguous crystallites. Other areas show dense diamond nucleation and nearly a continuous diamond film with clearly-defined facets. These areas are 100–500 μm^2 in size. It is suspected that a cluster of fibers existed over that area during deposition. Cleaved sectional analysis of the colinear crystallites does not show the presence of an inner graphite core. The crystals on Si wafers strongly adhere to the substrate. The cleavage process frequently left pits on the Si surface where presumably a diamond crystallite had been removed by the fracture. Hence, the linear diamond growth on the substrates cannot be attributed to diamond deposition on a fiber resting on the surface of the substrate.

Many of the fibers following exposure to the H_2 - CH_4 discharge show dense clusters of fine grain polycrystalline diamond. Some fibers such as the one as shown in Figure 1 are completely enclosed with this fine grain diamond. Other fibers are void of diamond deposition. The fibers do not appear to have been seriously etched by the atomic hydrogen ambient present from the rf discharge. We do not currently understand why some fibers do nucleate diamond well and why other fibers do not. One possibility is that fibers in the yarn structure are masking each other or enhancing the growth on nearby fibers.

3.0 DISCUSSION

Dense diamond nucleation has been observed on as-received substrates in patterns mimicking the placement of the graphite fibers on the surface prior to diamond growth. Cleaved-sectional analysis of collinear crystals on the silicon surface does not show the presence of an inner graphite core (i.e. the fiber is not embedded). Some

On As-Received Si Wafers

On As-Received Si Wafers

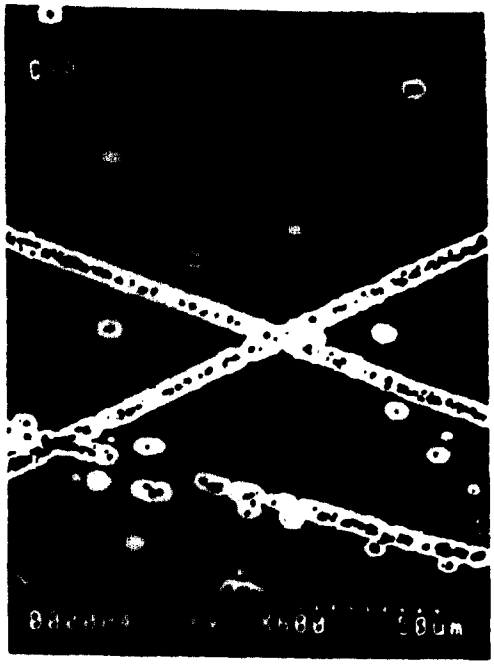

On As-Received Si Wafers

On Fiber

fibers, while contributing to the growth on the silicon, nickel, fused silica, and crystalline quartz substrates, also nucleate and grow diamond. Cleaved sectional analysis of those crystals show the presence of an embedded graphite fiber. Hence, the fiber has not been converted to diamond. Many fibers show no evidence of diamond growth.

The exact role of the graphite fiber in enhancing diamond nucleation has not been absolutely defined. One possibility is that the presence of the fiber is effecting the local gas phase chemistry nearby the fiber so as to enhance the nucleation. Another possibility is that the fibers are merely sources of local carbon contamination to the substrate surface, and therefore, the diamond growth on those surfaces comes from small graphite clusters transported to the growth surface by the deposition process. If this were the case, then one would expect the fibers rich in graphite would all show dense diamond nucleation. Furthermore, the morphology of the diamond grown on the substrate and the diamond grown on the fiber should be similar (both growing from a common seed). This is not the case. Thus, the graphite fiber's primary role would seem to be in altering the gas phase chemistry local to the substrate.

The authors wish to thank SDIO/IST for financial support of this program through ONR Contract No. N00014-86-C-0460. The authors wish to thank Daniel Neison at Fiber Materials Inc., Biddeford, Maine for supplying the fibers for this experimental work.

5.0 REFERENCES

1. M. Buck, T. J. Chuang, J. H., Kaufman, and H. Seki, Mat. Res. Soc. Symp. Proc. 162, 97 (1990).
2. Y. Liou, A. Inspektor, R. Weimer, D. Knight, and R. Messier, Mat. Res. Soc. Proc. 162, 109 (1990).
3. Jing Shen Ma, Hiroshi Kawarada, Takao Yonehara, Jun-ichi Suzuki, Jin Wei, Yoshihiro Yokota, Yosuke Mori, and Akio Hiraki, Mat. Res. Soc. EA-19, 67 (1989).
4. S. Tijima, NEC Corporation, private communication (1990).
5. M. Geis, Appl. Phys. Lett. 55, 550 (1989).
6. R.A. Rudder, G.C. Hudson, Y.M. LeGrice, M.J. Mantini, J.B. Posthill, R.J. Nemanich, and R.J. Markunas, Mat. Res. Soc. EA-19, 89 (1989).
7. R.A. Rudder, J.B. Posthill, G.C. Hudson, D.P. Malta, R.E. Thomas, R.J. Markunas, T.P. Humphreys, and R.J. Nemanich, to appear in ICDNST-2, Washington, DC, September 23-27, 1990.

SELECTED-AREA HOMOEPITAXIAL GROWTH AND OVERGROWTH ON Si PATTERNED DIAMOND SUBSTRATES

R.A. Rudder, J.B. Posthill, G.C. Hudson, D. Malta, R.E. Thomas and R.J. Markunas
Research Triangle Institute, Research Triangle Park, NC 27709-2194

J.P. Humphreys and R.J. Nemanich, Department of Physics
North Carolina State University, Raleigh, NC 27695-8202

ABSTRACT

Epitaxial diamond overgrowth on Si patterns on natural diamond substrates has been demonstrated using low pressure rf plasma-assisted chemical vapor deposition. The plasma-assisted technique uses a 13.56 MHz rf generator and inductive coupling to excite gas mixtures of H_2, CH_4 and CO at a reduced pressure of 5 Torr. The overgrowth was approximately isotropic, extending over the Si pattern by 0.45 μm and above the Si layer by 0.50 μm.

INTRODUCTION

The thermal and electrical properties of diamond make it an excellent candidate for high speed, high power transistors. A number of significant problems must be overcome before the potential of diamond can be realized. These problems include the unavailability of n-type dopants and the lack of a suitable substrate for heteroepitaxy. However, a number of useful devices can be fabricated with epitaxial p-type layers. Grot, *et al*[1] have reported the fabrication of an insulated gate field effect transistor (a depletion mode device). Others[2,3] have reported Schottky diodes and Schottky-gate field effect transistors. The development of any material to its full electronic potential depends critically on the support technologies such as metallization, etching, epitaxy, passivation, etc. In silicon microelectronics, selected-area growth is now allowing the fabrication of sophisticated three-dimensional devices[4,5]. In GaAs, selected-area growth is found to pin substrate defects to the area of epitaxial growth above the original seed window. Few defects are observed to propagate into the epitaxial overgrowth[6].

We report here on the successful epitaxial overgrowth by diamond of Si patterns that were lithographically defined on natural diamond (100) substrates. Given the difficulty of diamond nucleation on non-diamond materials, the selectivity for homoepitaxial growth on the exposed diamond seems assured. The challenge is then to have a mask material that 1) does not dissolve rapidly under the atomic hydrogen ambient, and 2) does not spontaneously nucleate diamond growth which would not be in registry with the advancing diamond growth front that is propagating across the mask. A polycrystalline Si mask was used for this study. Previous work in the low-pressure rf-plasma assisted chemical vapor deposition system had always used scratched Si substrates for polycrystalline diamond growth. Deposition on Si wafers which had not been diamond scratched produced only a few scattered particles of diamond. The nucleation density, thus, is very low in this deposition system for unscratched Si. While Si does dissolve under an atomic hydrogen environment, the reaction rate decreases with increasing temperature[7]. A slow dissolving of the mask material might be beneficial, allowing early stages of carbon nucleation on the Si

New Diamond Science and Technology © 1991 MRS Int. Conf. Proc.

surfaces to be undercut by an atomic hydrogen etch. In our study, we observed that a nominally 400 Å thick Si mask did dissolve preserving small areas of homoepitaxial growth. Consequently, a 2000 Å thick Si mask was employed. The thicker mask did not dissolve during the growth. Some spontaneous diamond nucleation was observed, but the density of nucleation was low.

EXPERIMENTAL RESULTS

Details of the low-pressure rf-plasma assisted chemical vapor deposition system have been described elsewhere[8]. Briefly, the system consists of a 13.56 MHz inductively-coupled plasma assisted chemical vapor deposition system. A gas mixture of 98.8% H_2, 0.6% CO and 0.6% CH_4 flowed through a 62.5 mm quartz tube at a rate of 30 sccm at 5.0 Torr. A rf power input of approximately 1000 W was used to excite the plasma. The characteristic color of the plasma was red owing to emissions from the Balmer series of atomic hydrogen. The substrate temperature was estimated to be 800 °C for this work. The diamond substrate was located on a graphite susceptor located below the rf coil. The susceptor was heated both by induction currents from the rf and by radiation from a graphite resistive heater located underneath the susceptor. The diamond substrates were subjected to a standard RCA clean followed by polycrystalline Si deposition in a MBE growth system. Standard lithography was used to open holes in the Si layer where homoepitaxial growth could nucleate. Following diamond deposition, the samples were characterized using secondary electron microscopy (SEM) and micro-Raman spectroscopy. SEM showed smooth epitaxial growth above the window areas. This growth extended beyond the lithographically defined area. Figure 1 shows plan-view SEM micrographs of the pattern used for the overgrowth experiments. The bright regions are regions of diamond growth. The dark regions are regions of Si. In the higher magnification, one sees that (1) the window areas are extremely smooth, (2) some spontaneous nucleation has occurred on the Si mask, and (3) the overgrowth areas show a roughened edge due to crystal faceting. Crystal faceting on overgrowth is a common occurrence in Si overgrowth of SiO_2 islands. Figure 1 also shows a cleaved cross-section of this structure. The diamond overgrowth is proceeding from the right to left-hand side. This picture shows clearly the faceting on the overgrowth front.

Micro-Raman has also been used to examine the epitaxial overgrowth. Figure 2 shows a micro-Raman spectrum taken from the region above the diamond window. The spectrum shows a 1332 cm^{-1} diamond line with a full-width-half-maximum (FWHM) of 3.4 cm^{-1}. The FWHM measured here is at the resolution limit of the instrument. The beam focus is approximately 1 μm in spot size. Figure 3 shows a micro-Raman spectrum taken with the beam centered on a region of overgrowth. This spectrum shows a 1332 cm^{-1} line with a FWHM of 3.5 cm^{-1}, very close to the 3.4 cm^{-1} taken from the homoepitaxial growth above the window. In contrast, a micro-Raman spectrum was taken from one of the diamond crystallites which spontaneously nucleated on the Si. It shows a 1332 cm^{-1} line with a broadened FWHM of 5 cm^{-1}. The FWHM of 5 cm^{-1} is what is typically seen on polycrystalline films. This contrast in FWHM illustrates the importance of the "seed" in the quality of the film growth. Under identical plasma and growth conditions, growth from a diamond seed produces better diamond than growth from a site on the Si that spontaneously nucleated Figure 4.

Finally, the overgrowth was elucidated by chemically etching the Si from the diamond. Figure 5 shows SEM of a cleaved cross-section showing diamond epitaxial

Figure 1. SEM photographs showing patterns defining selected growth. Bright regions are diamond while the dark regions are silicon.

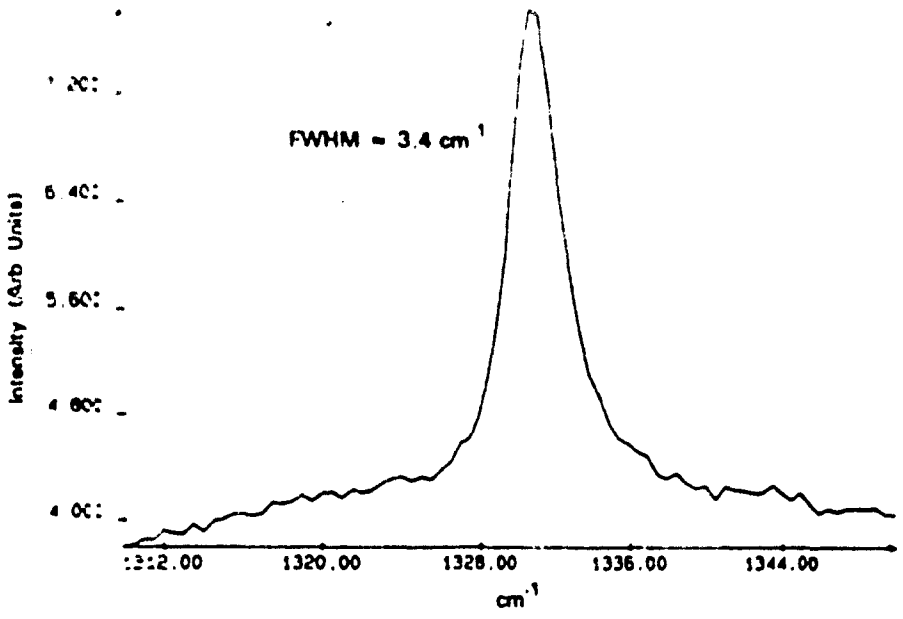

Figure 2. Micro-Raman spectrum from homoepitaxial growth above window.

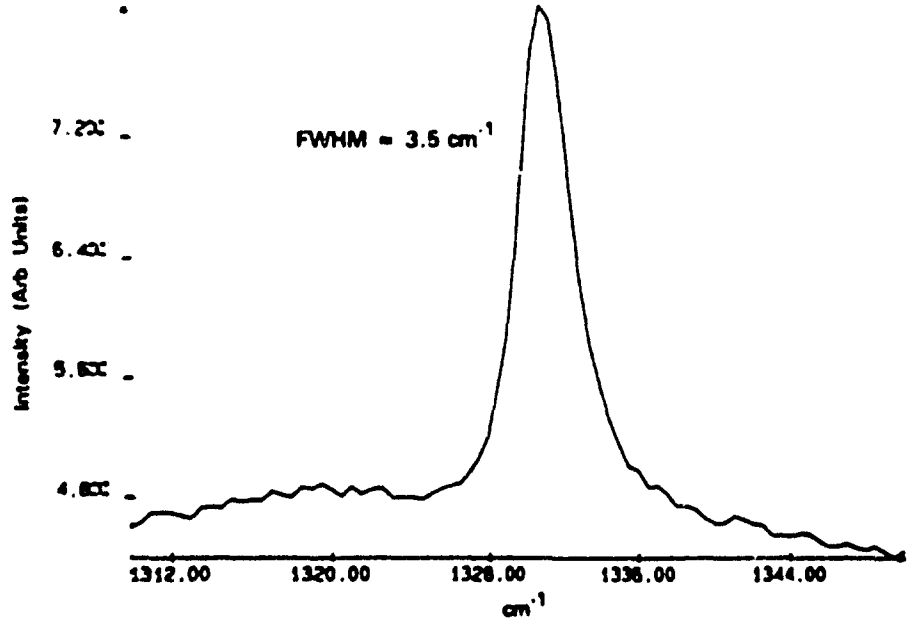

Figure 3. Micro-Raman spectrum centered on overgrowth region.

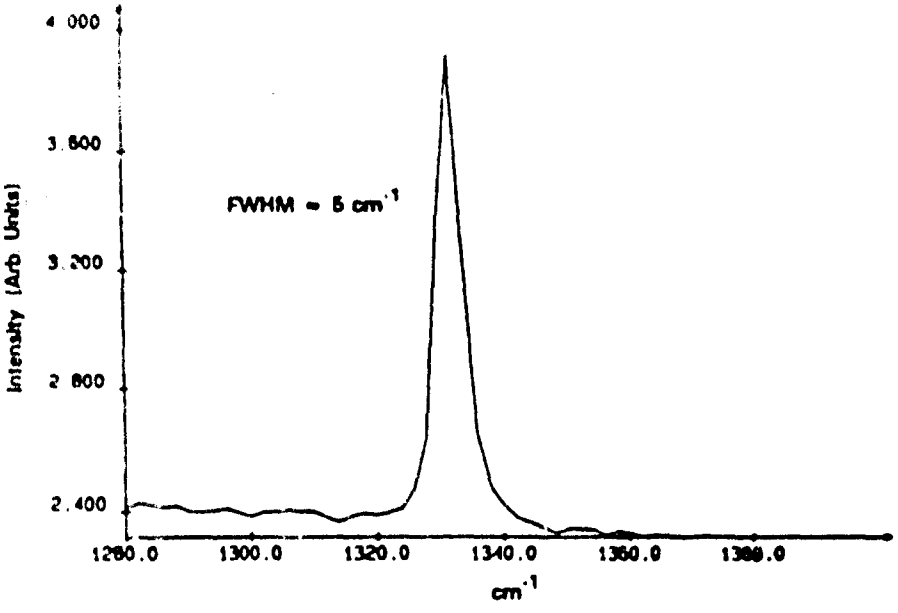

Figure 4. Micro-Raman spectrum from diamond that spontaneously nucleated on Si mask.

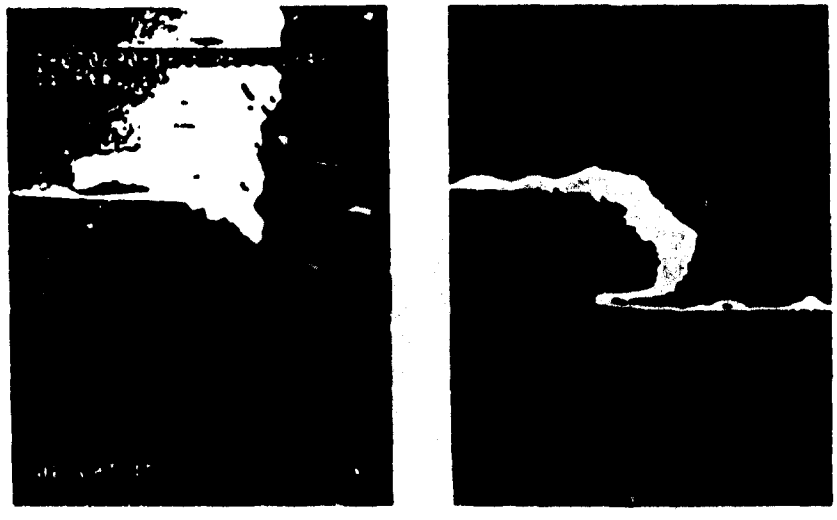

Figure 5. SEM micrograph of cleaved-cross section showing lateral overgrowth. The sample has been sputter coated with Pt to prevent charging.

lateral overgrowth. The sample has been sputter-coated with ~ 100 Å of Pt to prevent charging. The left photograph shows the smooth epitaxial growth and faceting on the overgrowth. Notice the scratches (remnants from polishing) that are on the diamond surface that had been covered by Si during the overgrowth experiments. The right photograph in Figure 5 gives a measure of the lateral overgrowth. The overgrowth appears to be isotropically advancing by 0.45 μm laterally and 0.50 μm vertically.

CONCLUSIONS

Epitaxial lateral overgrowth has been demonstrated using a low pressure rf-plasma assisted chemical vapor deposition technique. A 2000 Å thick Si mask has been used to define the diamond "seeds". The Si shows some spontaneous nucleation, but the density of nucleation is low. The overgrowth is isotropic, extending over the Si mask 0.45 μm and above the mask 0.50 μm. Some faceting is observed on the overgrowth areas. Micro-Raman analysis shows the overgrowth areas to have a FWHM comparable to the homoepitaxial layers deposited above the diamond windows. This was contrasted by a FWHM of 5 cm^{-1} from a polycrystalline diamond that nucleated spontaneously on the Si mask.

ACKNOWLEDGEMENTS

The authors gratefully acknowledge the support of this work by the Strategic Defense Initiative/Innovative Science and Technology Office through the Office of Naval Research, Contract N-00014-86-C-046. The authors wish to thank Max Yoder of the Office of Naval Research for discussions which stimulated this work.

REFERENCES

1. S.A. Grot, C.W. Hatfield, G. Sh. Gildenblat, A.R. Badzian, and T. Badzian, presented at this conference.
2. G. Sh. Gildenblat, S.A. Grot, C.W. Hatfield, A.R. Badzian, and T. Badzian, IEEE Electron Device Lett. 11, 371 (1990).
3. Hiromu Shiomi, Yushiki Nishibayashi, and Naoji Fujimori, Jpn. J. Appl. Phys. 28, L2153 (1989).
4. Rene P. Zingg, Joerg A. Friedrich, Gerold W. Neudeck, and Bernard Hofflinger, IEEE Trans. Electron Devices 37, 1452 (1990).
5. Peter J. Schubert and Gerold W. Neudeck, IEEE Electron Device Lett. 11, 181 (1990).
6. D. Pribat, M. Dupuy, P. Legagneux and C. Collet, Appl. Phys. Lett. 57, 375 (1990).
7. J. Abrefah and D.R. Olander, Surf. Sci. 209, 291 (1989).
8. R.A. Rudder, G.C. Hudson, Y.M. LeGrice, M.J. Mantini, J.B. Posthill, R.J. Nemanich, and R.J. Markunas, Mat. Res. Soc. EA-19, 89 (1989).

THERMAL DESORPTION FROM HYDROGENATED DIAMOND (100) SURFACES

R.E. Thomas, R.A. Rudder, R.J. Markunas
Research Triangle Institute, Research Triangle Park, NC 27709

ABSTRACT

Thermal desorption spectroscopy and low energy electron diffraction (LEED) have been used to study the interaction of atomic hydrogen with the diamond (100) surface. Heating a diamond crystal in-vacua readily reconstructs the surface from a (1x1) configuration to a (2x1) structure. Unlike the case for silicon, exposure to atomic hydrogen does not easily convert the surface back to the (1x1) structure. Hydrogen thermal desorption peaks from the (2x1) surface exposed to atomic hydrogen at $1x10^{-6}$ Torr are seen at approximately 950°C for heating rates of 20°C/sec. After exposure of the surface to atomic hydrogen in amounts in excess of that required to terminate the surface, 10^{-2} Torr, thermal desorption peaks associated with methyl radicals and acetylene are observed in addition to hydrogen. Upon further exposure at 10 Torr the surface appears to be partially converted to a (1x1) structure and acetylene desorption features are no longer observed.

Introduction

Hydrogen plays a key role in most diamond growth processes developed to date. However, the details of the behavior of hydrogen on the diamond surface are not well understood. It is thought to both etch non-sp^3 bonded carbon, which may be deposited during the growth process, and to stabilize the cubic structure on the growing diamond surface by terminating dangling bonds. Previous studies of hydrogen interactions on diamond indicate that hydrogen desorbs from the surface at approximately 900°C (1,2). Typically, researchers find that heating the diamond to approximately 1000°C results in the (1x1) surface structure converting to the (2x1) surface structure (2,3). One might expect, as in the case of silicon, the surface would convert back to the (1x1) state upon exposure to atomic hydrogen. Hamza et al. have observed the transition back to a (1x1) configuration on exposure to atomic hydrogen but find that on subsequent annealing the (2x1) surface is not recovered (2).

In the present work thermal desorption spectroscopy and LEED were used to study interactions of atomic hydrogen with the diamond (100) surface. Transitions from the (1x1) phase to (2x1) phase upon annealing and from the (2x1) phase to the (1x1) phase upon exposure to atomic hydrogen were studied with LEED. Thermal desorption spectroscopy was used to determine desorption kinetics and products from hydrogen terminated surfaces.

Experimental

Thermal desorption spectroscopy and LEED observations were performed in a stainless steel UHV system. Base pressure was $5x10^{-10}$ Torr for the sample chamber and $1x10^{-10}$ Torr for the quadrupole chamber. The sample chamber was separated from the quadrupole chamber by a 2mm diameter aperture. Sample heating was accomplished by clipping the crystals to a 0.25mm thick molybdenum resistive strip heater. All parts associated with the heater stage, including the clamps and current leads were manufactured from molybdenum. The sample temperature was measured by a 0.125mm diameter chromel/alumel thermocouple in intimate contact with the crystal. The thermocouple was threaded through a hole in one corner of the crystal, and the thermocouple bead then held in tension against the crystal. Two (100), 5mmx5mmx0.25mm, diamond crystals were used in the course of the present study. One of the crystals had approximately .5 microns of homoepitaxial diamond deposited prior to insertion into the system. Diamond polishing of the substrates leaves fine scratch marks on the surface, which previous work has shown can be covered by deposition of a homoepitaxial film (4). The homoepitaxial diamond was grown with an rf discharge plasma CVD process using CH_4 in H_2 as feedstock. The uncoated samples were cleaned by hand-polishing with 0.25 micron diamond grit and water. Following the polishing, the samples were ultrasonically cleaned in two series of baths of TCE, acetone, and methanol. Between solvent bath series the samples were vigorously swabbed to remove particulates. Once the samples were introduced to the chamber, no additional cleaning was performed aside from thermal desorption of adsorbed species. Several pressure regimes were used in dosing with atomic hydrogen, which necessitated slightly different procedures. For samples dosed at pressures from $1x10^{-7}$ Torr to $1x10^{-5}$ Torr, the hydrogen was flowing through the system. Samples were also dosed at pressures of 10^{-3} Torr-10^{-2} Torr and 1-10 Torr. For these samples the main chamber was sealed and hydrogen was admitted to the desired pressure. In all cases atomic hydrogen was generated via a tungsten filament operating at a temperature of approximately 1500 °C. The sample was positioned approximately 2 cm. from the filament during dosing. The sample was not actively cooled and at the lowest dosing pressures remained at room temperature. At dosing pressures in the 1-10 Torr range the sample temperature rose to approximately 125 °C. All thermal desorption spectra were taken with a heating rate of 20 °C/sec.

Results

The surface structure of the samples was monitored with LEED immediately after introduction to the chamber, after dosing, and after thermal desorptions. All samples exhibited a LEED pattern without annealing. For most samples this was a (1x1) configuration. The one exception was the homoepitaxial sample which gave a (2x1) pattern. Since this sample remained at the growth temperature, 800-900 °C, while the plasma and the gasses were shut off, it is likely that surface hydrogen simply desorbed and consequently the surface reconstructed before the sample was removed from the growth chamber. Upon annealing to 800 °C-1000 °C and for times ranging from 5 seconds to 120 seconds, all samples exhibited some degree of reconstruction to the (2x1) configuration. Annealing at temperatures greater than approximately 1100 °C usually resulted in a degradation of the LEED pattern. Typically, the second order spot intensity was

reduced, and the background intensity increased. In these cases first order spot intensity usually remained strong. The quality of the (2x1) LEED patterns obtained upon annealing samples varied considerably, and no consistent trends were observed to account for the variability.

Samples exhibiting good reconstructions were then exposed to atomic hydrogen in an attempt to convert the surface back to a (1x1) configuration. Three pressure regimes were investigated: 10^{-6}-10^{-5} Torr, 10^{-3}-10^{-2} Torr and 1-10 Torr. Only at the highest pressures studied were we able to partially convert the surface back to a (1x1) state. Samples exposed to atomic hydrogen at the maximum pressure showed only very faint second order spots. Annealing of these samples to 1000°C restored the (2x1) configuration. At the two lower pressure regimes studied little if any change was seen in the (2x1) LEED patterns upon addition of atomic hydrogen.

Given the difficulty in converting the surface back to a (1x1) configuration, all thermal desorption spectra were, perforce, from surfaces that had an indefinite degree of surface reconstruction. The three dosing regimes used in the LEED study were also used in the thermal desorption studies. Of the masses monitored during the course of the study, (2,13,14,15,16,18,26,27,28, and 44), desorption peaks were seen only for masses 2,15, and 26.

Figure 1 shows a series of hydrogen desorption spectra taken from a hydrogen dosed natural diamond surface. The sample was subjected to atomic hydrogen doses at fixed pressures and for a series of increasing times. A single desorption peak is evident at 900°C. Figure 2 shows a similar series of hydrogen thermal desorption traces for the CVD homoepitaxial sample dosed at a pressure of $3x10^{-6}$ Torr. In this case two closely spaced hydrogen desorption peaks can be seen at 900°C and at 1000°C. It is apparent from both figures that extending the dosing time does not result in dramatically increased amounts of hydrogen desorbing from the surface. We also do not see any evidence for a shift in the desorption temperature as the coverage increases. The next series of figures shows thermal desorption spectra from the CVD diamond film after exposure to atomic hydrogen at the three pressure regimes used in the LEED study. Figure 3 shows that after exposure to atomic hydrogen at $1x10^{-5}$ Torr, hydrogen desorbs at 900°C and perhaps a small amount of CH_3, but little evidence of C_2H_2. Figure 4 shows the sample after dosing at $2x10^{-3}$ Torr, a dosing pressure far higher than what is required to terminate the (2x1) surface. At this dosing pressure we now see clear evidence of desorbing methyl radicals (700°C) and acetylene (600°C). Although the sample has received an atomic hydrogen dose far in excess of what is required to saturate the (2x1) surface, LEED indicates the sample is in fact still in a (2x1) configuration. These two species are desorbing in significant quantities compared to the hydrogen desorption. The hydrogen desorption peak has broadened considerably after dosing at this pressure but the peak desorption temperature has not shifted. Figure 5 shows the sample after dosing at 3 Torr for 2700 seconds. In this case the sample has lost much of the (2x1) structure as seen in LEED but has not fully regained the (1x1) surface structure. The hydrogen desorption peak has remained at 950°C. The methyl peak has shifted to approximately 800°C and the acetylene peak has virtually disappeared.

Discussion

Surface reconstruction on the diamond (100) face has been reported previously (2,3). As noted by these authors, the reconstruction process was not always reproducible. For all of the newly polished surfaces used in the present study, some reconstruction was noted upon annealing. However, as indicated in the results, section not all surfaces fully reconstructed. Field emission SEM indicates the starting morphology for all the hand-polished surfaces was quite similar. If surface morphology is influencing the reconstruction, it is at a scale of less than 1000Å. Hamza et al. have suggested that adsorbed oxygen can affect the ability of the surface to reconstruct (3). Ex-situ measurements of samples show the presence of oxygen on the surface, some or all of which may have been added to the surface during the air transfer to the XPS system. No clear trend connecting the quantity of adsorbed oxygen and the quality of the reconstruction was observed. Other contaminants below the detection limit of XPS remain a possibility. Annealing at temperatures higher than required to establish the (2x1) structure appears to degrade the surface. The (1x1) pattern is still apparent but, as an increase in the background is observed, it is likely that the surface is becoming disordered and the (1x1) pattern is from the bulk.

Conversion of the (2x1) surface structure back to the original (1x1) structure appears very difficult. Extended dosing at high pressures is only partially successful at restoring the surface. In contrast, silicon (100) samples in the same chamber and under identical dosing conditions readily convert from the (2x1) state to the (1x1) state at dosing pressures of $1x10^{-6}$ Torr and at dosing times on the order of 1000 sec. For diamond samples in this pressure regime, we do not see conversion even after 2000 seconds at $5x10^{-6}$ Torr; a dose 10 times at great as used on silicon. This is not too surprising as the C-C bond strength at 83 kcal/mole is much greater than the Si-Si bond of 46 kcal/mole. Cluster calculations by Verwoerd indicate the diamond surface dimer bond is very resistant to attack by atomic hydrogen (5). The apparent stability of the dimer bond may also help explain results of the thermal desorption experiments described next, particularly the appearance of acetylene.

It appears difficult to maintain a well characterized surface during the course of thermal desorption experiments. The surface structure is evidently a function of sample history and it is difficult to return to a standard starting point. In the case of the thermal desorption experiments there may be several sites which are contributing to the hydrogen observed. LEED in this case is a very rough measure of surface characteristics. On a nominally (2x1) surface we find the hydrogen uptake saturates. By comparing this with data obtained from silicon samples under identical conditions, we find the quantity of hydrogen desorbed is consistent with monohydride coverage, or 1 hydrogen per carbon atom. Extended dosing does not significantly increase the hydrogen yield from the surface. The substrate which had received the homoepitaxial film showed two hydrogen desorption peaks only after film deposition. Before the film was deposited, a single peak is observed at 900° C. The desorption temperature does not appear to be coverage dependent. This indicates a first order reaction with fixed activation energy. A simple calculation using a standard frequency factor of 10^{13} gives an activation energy of 74 kcal/mole, which is considerably smaller than the C-H dissociation energy of 104 kcal/mole. First order kinetics are also found by Sinniah et al. for hydrogen desorption

from the monohydride phase on the silicon (100) surface (6). Along with first order kinetics, an activation energy was found which was much less than the dissociation energy for the Si-H bond.

As additional hydrogen is added to the saturated (2x1) surface we see the appearance of new desorption products, methyl radicals and acetylene. Since the dimer bonds resist attack by atomic hydrogen it may be possible for the dimer back bonds to be hydrogenated. If one or two of the back bonds were broken on the dimer unit, it would then be possible for the two carbon atoms to desorb as a unit, perhaps resulting in the acetylene production seen. Methyl radicals are also seen desorbing from the surface, but at a higher temperature. Since the two species desorb at different temperatures, one expects evolution from different sites. Mass 15 could be a fragmentation product of either ethylene or ethane. Mass 28 was monitored for ethylene species but given the large background seen at this mass it is difficult to discern a peak. No significant desorption products were seen at mass 27 either, which one would expect if large quantities of ethylene or ethane were desorbing. Given the size of the hydrocarbon desorption peaks relative to the hydrogen peak, it is clear that an appreciable fraction of a monolayer of carbon is desorbing from the (2x1) surface after extended dosing. It is not clear what sites the methyl radicals may be desorbing from. It seems likely that the methyl radicals are desorbing from dihydride sites.

If breaking of back bonds is occurring during hydrogen dosing, it seems likely that etching of the dimer units is also occurring on a continuous basis. If completed, we should see a reduction in amount of acetylene desorbed from the surface. At the highest hydrogen doses studied, the acetylene does in fact diminish dramatically. Methyl radicals, however, are still seen. Although the sample has moved closer to the (1x1) configuration as a result of the hydrogen dosing, the hydrogen desorption peak remains at 950°C. If desorption is occurring by processes similar to that on silicon, one would expect a peak to appear at a lower temperature corresponding to the desorption from the dihydride phase. Hamza et al. have results which indicate that both on the (100) and the (111) face of diamond, the surface reconstructs after the hydrogen desorbs (2,7). If there was little energy to be gained by formation of the dimer bonds on the surface, one would expect the desorption from the dihydride and the monohydride to occur near the same temperature.

Conclusions

The clean surface appears to saturate quite readily in the (2x1) configuration and hydrogen desorption from this phase follows first order kinetics. Conversion of a diamond (2x1) surface back to the (1x1) configuration by the addition of atomic hydrogen is difficult. It appears this is accomplished by hydrogenation of dimer back bonds and subsequent desorption of acetylene from the surface rather than by breaking of dimer bonds. Surfaces which show substantial reduction in the (2x1) surface phase after hydrogenation also show considerably reduced desorption of acetylene

Acknowledgements

The authors wish to thank the Strategic Defense Initiative Organization/Innovative Science and Technology Office through the Office of Naval Research (N-00014-86-C-0460) for the financial support of this work.

REFERENCES

1. S. Matsumoto, Y. Sato, and N. Setaka, Carbon 19, 232 (1981).
2. A.V. Hamza, G.D. Kubiak, and R H. Stulen, Surf. Sci. 237 35 (1990).
3. P.G. Lurie, and J.M. Wilson, Surf. Sci. 65, 453 (1977).
4. J.B. Posthill, R.A. Rudder, G.C. Hudson, D.P. Malta G.G. Fountain, R.E. Thomas, R.J. Markunas, T.P. Humphries, R.J. Nemanich, and D.R. Black, this proceedings.
5. W S. Verwoerd, Surf. Sci. 108 153 (1981).
6. K. Sinniah, M.G. Sherman, L.B. Lewis, W.H. Weinberg, J.T. Yates, and K C. Janda, Phys. Rev. Lett. 62 567 (1989)
7. A.V. Hamza, G D. Kubiak, and R.H. Stulen, Surf. Sci. 206 L833 (1988).

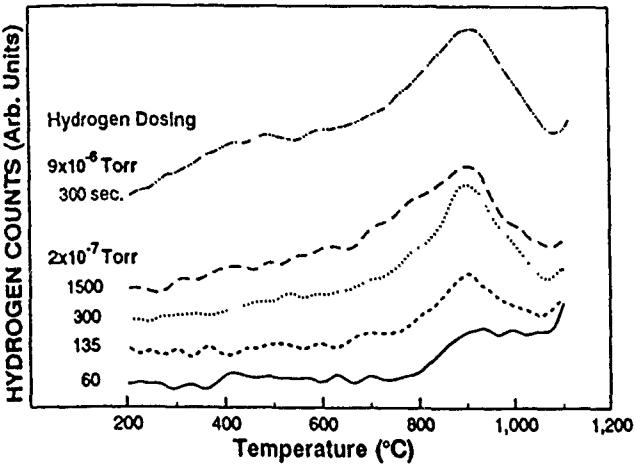

Figure 1. Thermal desorption spectra from natural diamond surfaces. An additional spectra was taken after dosing the sample at $9x10^{-6}$ torr with atomic hydrogen. The higher pressure is comparable to the dosing pressure used on the samples in Figure 2. Note that although the dose has increased by a factor of 3.5 between the sample exposed at $9x10^{-6}$ and the sample exposed for 1500 seconds at $2x10^{-7}$ torr, the magnitude of the desorption peaks is very close.

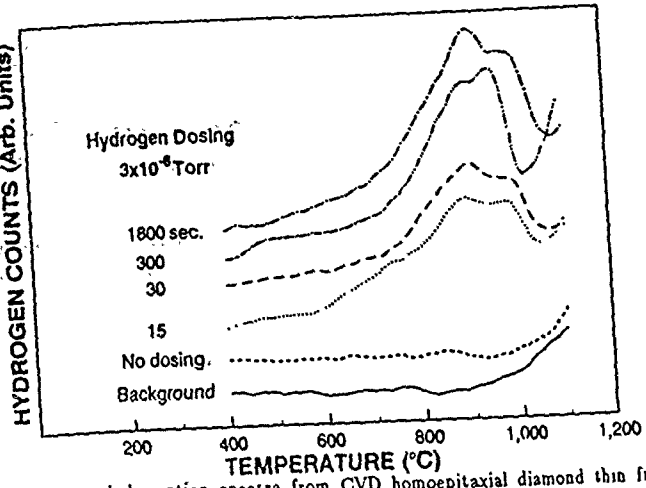

Figure 2. Thermal desorption spectra from CVD homoepitaxial diamond thin films deposited on natural diamond substrates. In addition to the hydrogen desorption spectra after dosing, a background spectrum is included where the sample was dosed but not placed adjacent to the aperture.

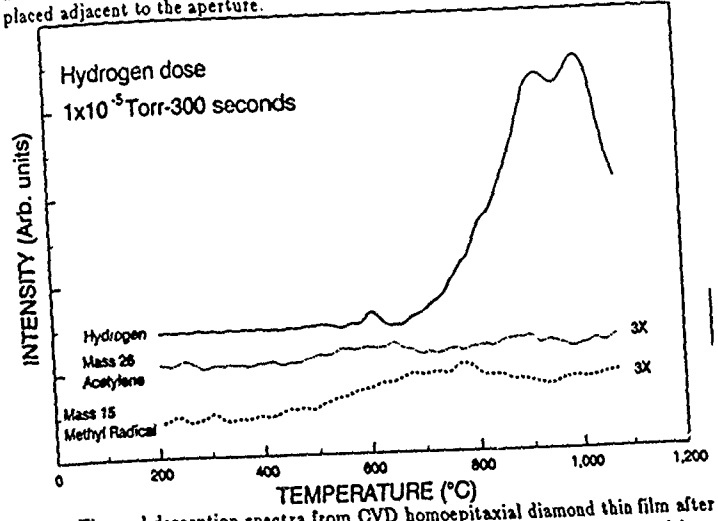

Figure 3. Thermal desorption spectra from CVD homoepitaxial diamond thin film after dosing at $1x10^{-5}$ torr. The vertical scale on masses 15 and 26 has been magnified by a factor of 3 to show detail.

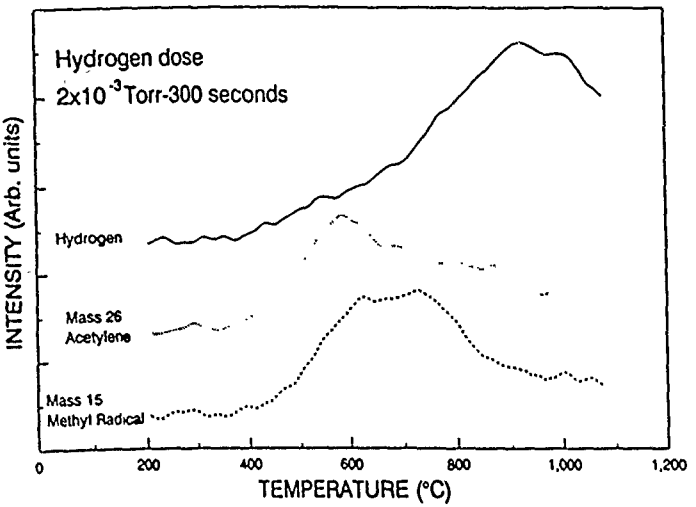

Figure 4. Thermal desorption spectra from CVD diamond film after hydrogen dosing at $2x10^{-3}$ torr. Note the large increase in methyl and acetylene production compared to Figure 3.

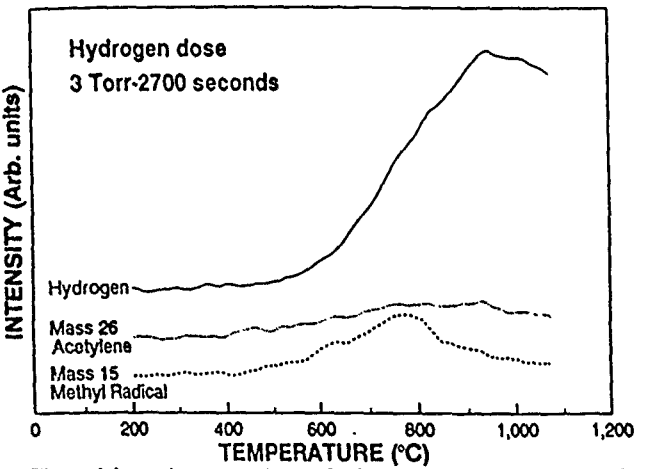

Figure 5. Thermal desorption spectra from CVD diamond film after hydrogen dosing at 3 torr. In this case the acetylene production is considerably reduced.

415

$F_2 - CH_4$ AND $H_2 - CF_4$ GAS INTERACTIONS ACROSS A HEATED GRAPHITE ELEMENT

R.A. Rudder, R.E. Thomas, G.C. Hudson, M.J. Mantini, and R.J Markunas
Research Triangle Institute, P.O.Box 12194, Research Triangle Park, NC 27709

ABSTRACT

We have investigated diamond film formation using mixed hydrogen-halogen chemistries at sub-atmospheric pressures. This work has been implemented in two reduced pressure cells. One cell contained a heated graphite element upon which reactant gasses were passed. Only thermal activation was used in this reduced pressure cell. Quadrupole mass spectroscopy was used to identify reaction products in the cell. The other cell was a low pressure rf-plasma assisted chemical vapor deposition system. Gasses were admitted to this cell which showed no thermal activation in the thermal cell. It was found that F_2 is activated in the thermal cell and can participate in reactions both in the gas phase and at the graphite surface. HF and $C_2F_2H_x$ were observed as by-products of $F_2 - CH_4$ gas interactions near the graphite oven. Carbon films that were deposited on nearby substrates proved not be diamond. Activation of $H_2 - CF_4$ in the thermal cell was not observed even at temperatures as high as 1000 °C. Plasma activation, on the other hand, does show evidence for HF and C_2H_2 formation from the H_2 - CF_4 gas system. With plasma activation of $H_2 - CF_4$ gas system, diamond deposition on as-received Si wafers without any ex situ treatment of the surface to enhance diamond nucleation is possible.

Introduction

Recent work by Patterson et al.(1) and previous work by Rudder et al.(2) has shown that diamond deposition from a fluorine-based environment is possible. Patterson exploited the use of mixed fluorine-hydrogen chemistries (i.e., F_2 and CH_4) to form solid carbon through a proposed reaction of:

$$CH_4 + 2F_2 \rightarrow C_{(s)} + 4HF \quad (1)$$

This reaction would be more exothermic than a corresponding hydrogen-based reaction involving CH_4 and H_2. The hot zone of the Patterson-type

reactor operated between 700 and 950 °C, and diamond growth occurred only in regions of the reactor where the temperature was between 250 and 750 °C. Mixtures of either H_2 and CF_4 or F_2 and CH_4 were reported to deposit diamond.

Experimental Apparatus and Approach

To gain insight into the fluorine-based process, we have performed a quadrupole mass spectroscopy of F_2/CH_4 and H_2/CF_4 gas interactions as a function of temperature of the graphite surface. This work has been implemented in two reduced pressure cells. One cell contained a heated graphite element upon which reactant gasses were passed. Only thermal activation was available in this reduced pressure cell. The other cell was a low pressure rf-plasma assisted chemical vapor deposition system. Gasses were admitted to this cell which showed no activation in the thermal cell.

The thermal work was performed in an UHV compatible chamber that is evacuated by a corrosive series, 1000 l/s turbomolecular pump. Gases are admitted into the chamber using mass flow controllers. The pressure in the chamber is maintained at 0.500 Torr for $F_2 - CH_4$ or $H_2 - CF_4$ gas work described here. A graphite resistive heater is enclosed in the chamber as well as a sample heater stage whereby growth attempts, independent of the graphite resistive heater, can be assessed. The graphite heater is machined from a dense, fine-grain graphite and is not highly oriented pyrolytic graphite. A mass quadrupole operating at low emission (0.25 mA) is used to sample the gases exiting the reactor. Changes in the gas composition as a function of substrate temperature or the graphite heater temperature are monitored.

The plasma activated cell was a low pressure rf-plasma assisted chemical vapor deposition system which has been used for the growth of diamond from H_2 - CH_4 mixtures(3). The reactor cell consists of a stainless steel, 150 mm conflat flange, 6-way cross to which the reactor tube, pumps, control orifice valve, vacuum gauges, mass spectrometer, and load lock are appended. The vacuum system is evacuated by a Balzers 500 l/s corrosive series turbomolecular pump. The base pressure of the reactor is 1.0×10^{-7} Torr. The heater stage is comprised of alumina standoffs separating the graphite susceptor from a graphite serpentine resistive heater. The reaction tube consists of a double-walled 50 mm inside diameter quartz tube sealed to the stainless chamber by compression viton o-ring seals. The reactor tube is water cooled to maintain the water temperature at 15 °C. An 8 mm water-cooled copper tube formed into a 3-turn helix 100 mm long provides the inductive coupling from the rf generator to the discharge. Wall deposits, for a limited time, can protect the quartz tube from erosion by fluorine based processes.

Experimental Results in Thermal Cell

The interactions of F atoms with both solid carbon such as graphite and with gaseous carbon such as CH_4, a graphite strip heater were studied in the thermal cell. By adjusting the current through the graphite element, the reactions of F_2 and/or F with the densified graphite were monitored as a function of temperature. One advantage in using a graphite heater to study the F_2/CH_4 gas interactions is that reactions of fluorine with graphite have been previously studied(4) so there exists comparative information. A second advantage to the graphite heater is that it avoids questions of metal catalysis reactions. Two difficulties with the graphite heater are memory effects from gasses absorbing in the porous graphite and delocalization of the hot zone across the machined graphite. This results in some areas of the heater operating about 100°C colder than the heater center. To minimize the memory effects, the heater was degassed at high temperatures before setting the temperature for each data point.

Fluorine reactions with the heated graphite were monitored by admitting the F_2 without CH_4 into the thermal cell. At elevated temperatures, fluorine reacted with the graphite to form CF_4. The CF_4 formation was monitored in the mass quadrupole through the mass peak at 69 arising from CF_3. CF_3 is the dominant fragment in the ionizer when CF_4 is introduced. Figure 1 shows the observed CF_3 mass counts in the reactor as a function of the graphite cell temperature. The CF_4 production is maximum at 600°C and is observed to decrease for temperatures in excess of 950°C. The decrease in CF_4 production below 600°C is probably a consequence of the formation of solid graphite fluoride. The temperature dependence is convoluted by the fact that there is a substantial temperature variation ± 100°C across the graphite heater element.

After observing the CF_4 production from the hot cell with only F_2 (admitted as 1% F_2 in He), CH_4 was introduced into the hot cell. Upon introduction of CH_4 into the hot fluorine, the CF_4 production decreased. Fluorine interactions with the CH_4 in the gas phase apparently depleted the gas phase of fluorine, resulting in a lower incident flux of F atoms to the graphite surface and, consequently, a lower production rate of CF_4. This is the first evidence for $F_2 - CH_4$ gas phase interactions. Besides the reduction in CF_4 production, the introduction of CH_4 into the hot fluorine resulted in production of HF and $C_2F_2H_x$ molecules. Figure 2 shows the production of those molecules as a function of the graphite temperature. Both exhibit a maximum in production around 900°C. The temperature dependence for the HF production is more pronounced than the temperature dependence for the $C_2F_2H_x$ production.

This work suggests that the proposed reaction of Patterson et al. for solid carbon production via equation (1) is basically correct. Our observations of graphite gasification and the formation of HF and $C_2F_2H_x$ suggests that the reaction in equation (1) should be extended.

$$2F_2 + CH_4 \rightarrow C_{solid} + 4HF \qquad (700^\circ C)$$

$$4F_2 + 2CH_4 \rightarrow C_2H_2F_2 + 6HF \qquad (700^\circ C)$$

$$2F_2 + C_{graphite} \rightarrow CF_4 \qquad (500 - 700^\circ C)$$

In a similar manner, the H_2 - CF_4 system was evaluated in the thermal cell. At the pressure of 0.50 Torr, no evidence of by-product formation was observed for temperatures below 1000°C. Temperatures higher than 1000°C and pressures higher than 0.50 Torr were not evaluated. We assumed that temperatures under 1000°C are not sufficient to produce H atoms from the H_2 or F atoms from the CF_4. Consequently, the H_2 - CF_4 gas system in this pressure and temperature range does not react with the graphite to produce gasification products, nor do they react with each other to form HF molecules.

Experimental Results in Plasma Cell

As a consequence of the inactivity of the H_2 - CF_4 in the thermal cell, gas mixtures of H_2 and CF_4 were admitted into the low pressure rf plasma assisted chemical vapor deposition system. Details of that work are being submitted elsewhere(5). Briefly, dense nucleation of polycrystalline diamond films on Si(100) substrates has been accomplished without the use of any surface pre-treatments such as diamond scratching, oil-coating, or diamond-like carbon predeposition. Films deposited at 5 Torr at 850°C, using an 8% CF_4 in H_2 mixture, show dense nucleation, well-defined facets, and crystallite sizes ranging from 500 - 10,000 Å. Figure 3 shows scanning electron micrographs of the diamond surface and a cleaved cross-section. Some roughening of the Si substrate is observed from the cleaved section suggesting that the Si surface underwent some chemical modification prior to or during diamond nucleation. X-ray photoelectron spectroscopy show the films to be diamond with no major chemical impurity and no detectable graphitic bonding. Besides carbon, fluorine is detected in the x-ray photoelectron spectrum. A high resolution spectrum of the C 1s line shows that some carbon is bound to fluorine on the surface as exhibited by a distinct feature at 288 eV, removed from the C-C bonding at 283 eV. A high resolution spectrum of the C 1s region is shown in Figure 4. The graphite $\pi - \pi^*$ plasmon is not present in the spectrum. The 34 eV bulk diamond plasmon is clearly present, but not shown in the high-resolution spectrum. A pronounced 1332 cm^{-1} Raman line was observed from the polycrystalline films along with a broad

band at 1500 cm^{-1}.

Quadrupole mass spectroscopy of the gases downstream from the plasma discharge reveals that the CF_4 - H_2 plasma converts the carbon tetrafluoride into HF and C_2H_2. No fluoromethane groups were observed. Given that, after 15 min into the plasma process, no fluorocarbon groups were detectable in the mass spectrum. the generation rate of HF and C_2H_2 must have been equal to the gas flow of CF_4 into the reactor, 3.2 sccm.

Preliminary data indicates that this process is applicable to substrates other than silicon. This process will have important applications in areas where surface pretreatments, such as diamond polishing, are not viable. In particular, this process may prove invaluable to those workers developing heteroepitaxy. With conventional methane-based processes, nucleation is inhibited on substrates other than diamond and c-BN. This process may allow heteroepitaxial studies to be undertaken on substrates whereby previously there has been little diamond nucleation.

Acknowledgements The authors wish to thank the Strategic Defense Initiative Organization/Innovative Science and Technology Office through the Office of Naval Research (N-00014-86-C-0460) for the financial support of this work.

REFERENCES

(1) Donald E. Paterson, Benjamin J. Bai, C. Judith Chu, Robert H. Hauge, and John L. Margrave, "Halogen-Assisted Chemical Vapor Deposition", presented at the second International Conference on the New Diamond Science and Technology, Washington, DC(USA), September 23-27, 1990.

(2) R.A. Rudder, J.B. Posthill, R.J. Markunas, Electronics Lett. 25, 1220 (1989).

(3) R.A. Rudder, G. C. Hudson, Y. M. LeGrice, M.J. Mantini, J.B. Posthill, R.J. Nemanich, and R.J. Markunas, Mat. Res. Soc. EA-19

(4) D.E. Rosner and J. Strakey, J. Phys. Chem. 77, 690 (1973).

(5) R.A. Rudder, G.C. Hudson, J.B. Posthill, R.E. Thomas, and R.J. Markunas, submitted to Appl. Phys. Lett.

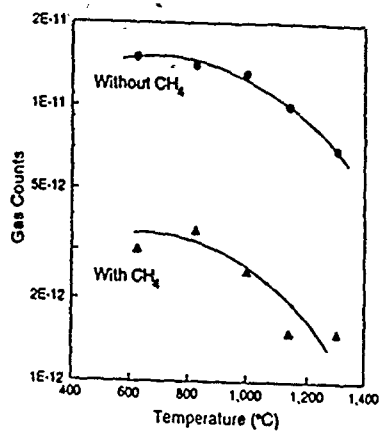

Figure 1. Observed CF_3 counts in the mass spectrometer as a function of the graphite heater temperature. Notice that the introduction of CH_4 into the graphite hot zone diminishes the CF_4 production.

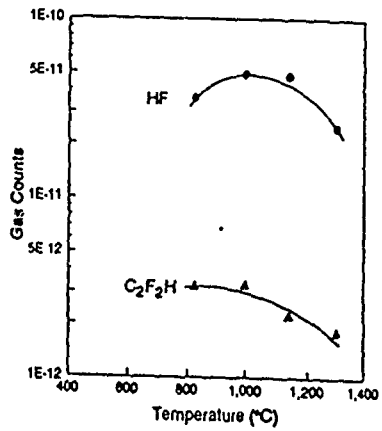

Figure 2. Dependence of by-product production on graphite heater temperature.

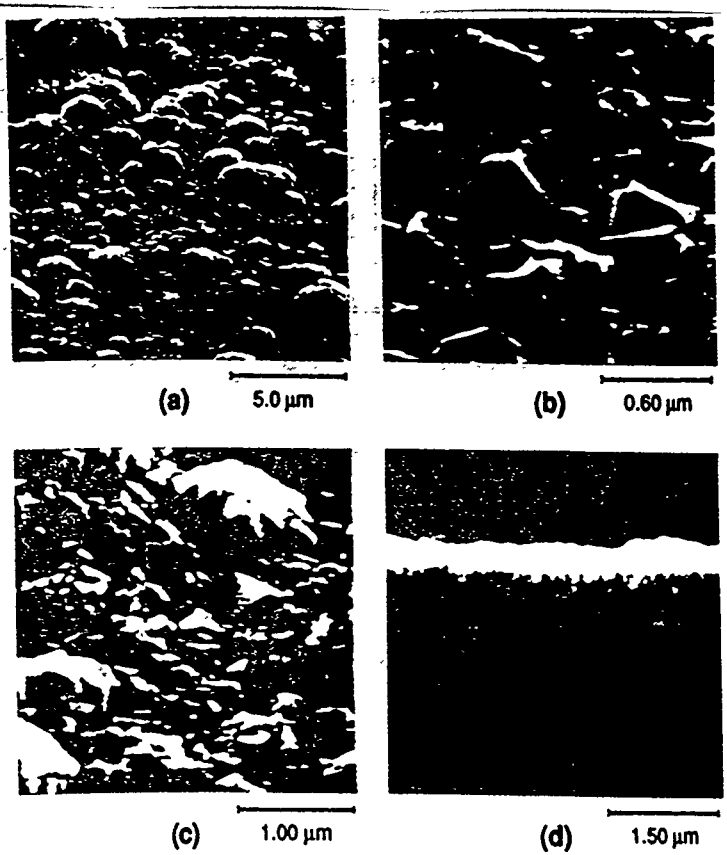

Figure 3. SEM micrographs of a polycrystalline diamond film deposited from the H_2 - CF_4 process.

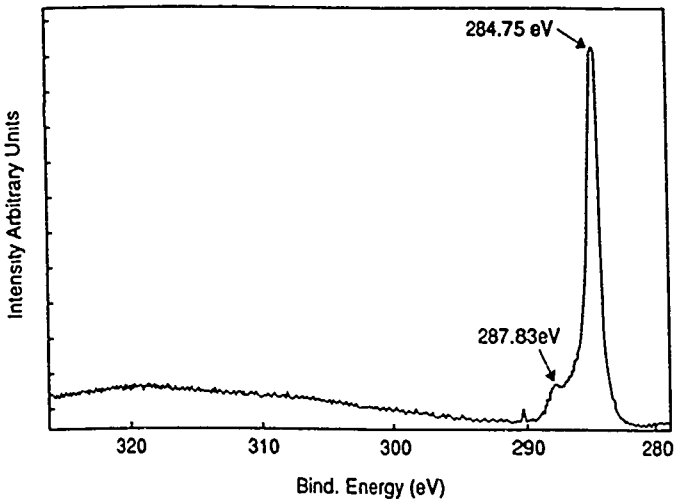

Figure 4. A high resolution x-ray photoelectron spectrum of the C 1s line.

ACETYLENE PRODUCTION IN A DIAMOND-PRODUCING LOW PRESSURE rf-PLASMA ASSISTED CHEMICAL VAPOR DEPOSITION ENVIRONMENT

R.A. Rudder, G.C. Hudson, J.B. Posthill, R.E. Thomas, and R.J Markunas
Research Triangle Institute, P.O.Box 12194, Research Triangle Park, NC 27709

R.J. Nemanich, Y.M. LeGrice, and T.P. Humphreys
Department of Physics
North Carolina State University, Raleigh, NC 27695-8202

ABSTRACT

We have examined using quadrupole mass spectroscopy the production of acetylene molecules under diamond growth conditions wherein no acetylene was introduced. There are two pathways available for the production of acetylene. One path for acetylene production is through conversion of CH_4 into C_2H_2 in the high temperature plasma region. The other path for acetylene production is through gasification of the graphite. In the pressure range from 1 - 10 Torr using a rf plasma discharge, the graphite gasification is the dominant path and the diamond deposition rate appears to correlate fairly well with the acetylene concentration in the reactor. The correlation can be understood by considering the acetylene production rate to be proportional to the atomic hydrogen flux to the graphite susceptor and, hence, to the atomic hydrogen flux to the diamond growth surface.

Introduction

Many workers are studying the importance of acetylene and methyl radicals in the vapor phase growth of diamond. Techniques such as infrared diode laser absorption spectroscopy and multiphoton ionization have been used to examine the gaseous environment of the diamond deposition(1). Other workers have used isotopic labeling to identify the parentage of carbon atoms deposited as diamond(2). In this work, we have used quadrupole mass spectroscopy to monitor acetylene production during diamond deposition in a low pressure rf-plasma chemical vapor deposition environment. We find that there are two channels for acetylene production, one via conversion of CH_4 into C_2H_2 and second via gasification of graphite into C_2H_2. By realizing that a requirement for graphite gasification is the atomic hydrogen flux to the graphite surface, mass quadrupole spectroscopy of the gasification products has been able to demonstrate that the diamond deposition rate is proportional to the atomic hydrogen flux.

Experimental Approach and Results

Diamond depositions have been accomplished in a low pressure rf plasma assisted chemical vapor deposition system using 1% CH_4 in H_2 gas at pressures from 1 - 10 Torr. Details of that reactor and the growth process have been previously reported(3). The vacuum system for diamond deposition is shown schematically in Figure 1. It consists of a stainless steel 150 mm conflat flange 6-way cross upon which the reactor tube, pumps, control orifice valve, vacuum gauges, quadrupole mass spectrometer, and load lock are appended. Samples are introduced into the reactor on a graphite carrier/susceptor through a vacuum load lock, transferred horizontally onto a heater stage. and raised vertically into the quartz reaction tube. The reaction tube consists of a double-walled 50 mm inside diameter quartz tube sealed to the stainless chamber by compression viton o-ring seals. The reactor tube is water cooled through the use of a heat exchanger which maintains the water temperature at 15 °C. A 8 mm water-cooled copper tube formed into a 3-turn helix 100 mm long provides the inductive coupling from the rf generator to the discharge. The rf power output from a power amplifier tube couples to the plasma using a LC resonant circuit with the plasma coil constituting the inductive component. The vacuum system is evacuated by a Balzers 500 l/s corrosive series turbomolecular pump. The pressure of the reactor is 1.0×10^{-7} Torr prior to introducing the reactant gasses.

Conditions for diamond growth are given in Table I over the presure range from 1 - 10 Torr. Note that the temperature of the hydrogen plasma has been calculated from the relative emission intensities of the atomic hydrogen Balmer series assuming a Boltzman distribution and collisionless lifetimes. These assumptions may be in error, but this calculation allows some internal standard for the power input to the plasma.

Table I

Pressure	Flow rate (sccm)	Estimated rf power (w)	T_{plasma} (K)
1	1.3	400	3420
3	3.8	660	3350
5	6.3	1000	3200
7	8.8	1800	3200
10	12.5	2400	3270

One notices that the pressure in this series is varied by maintaining a constant pumping speed and reducing the gas flow into the reactor. The estimated plasma temperature remains constant throughout this pressure range despite

the 6-fold increase in power input. Without this increase in power at the higher pressures, it would not be possible to maintain the atomic hydrogen emission. This increase in applied power also increases the substrate temperature. The substrate temperature varies from $\approx$650 °C at 1.0 Torr to $\approx$850 °C at 10 Torr.

Following deposition, films were analyzed using scanning electron microscopy (SEM) and Raman scattering spectroscopy. Cleaved sectional analysis in the SEM was used to ascertain diamond deposition rates at the different pressures. We assumed the deposition rate was linear in time. The silicon substrates used in this work were diamond polished prior to introduction into the reactor to provide immediate nucleation sites.

SEM micrographs show that the deposited films are polycrystalline showing well-defined faceting. The crystallite sizes vary from 0.5 - 2.5 μm. The crystallites appeared to have nucleated at point sites upon which growth proceeded 3-dimensionally into a continuous film. Raman spectra for the complete series are given in Figure 2. All samples display a 1332 cm^{-1} diamond Raman line. Samples grown at lower pressures show more non-diamond bonding. It is not clear at this point if the appearance of the non-diamond bonding components (i.e. the appearance of Raman features between 1500 and 1600 cm^{-1}) is due to a reduction in pressure or a reduction in substrate temperature. It is clear that all conditions produced diamond from the gas phase using the low pressure rf-plasma system.

The environment of the diamond growth was probed by mass spectroscopic analysis of gasses downstream from the plasma region. Samples were positioned near the rf coil on a graphite susceptor. By comparing the C_2H_2 production observed with the graphite susceptor removed from the discharge tube to the C_2H_2 production when the susceptor was positioned near the rf coil, one can distinguish CH_4 conversion to C_2H_2 in the gas phase from gasification of the graphite to C_2H_2 at the susceptor surface. (It should be noted that these experiments were performed when the plasma tube was fairly clean of carbon deposits. The graphite susceptor represents the largest source of solid carbon exposed to the plasma.) Figure 3 shows the conversion of CH_4 to C_2H_2 as a function of total pressure when the graphite susceptor is *not* present in the reactor. This figure shows a nearly constant ratio of CH_4 to C_2H_2 across the pressure series. Given that two CH_4 molecules are necessary for C_2H_2 production, we conclude that approximately 60% of the CH_4 is converted into C_2H_2. Figure 4 shows the observed C_2H_2 production when the graphite susceptor is inserted 3.0 mm below the rf coil with 1% CH_4 in H_2 discharge. There is a pronounced pressure dependence to the C_2H_2 production. At 3 Torr, there is approximately 4 times more C_2H_2 partial pressure in the reactor with the graphite susceptor present than there was with the graphite susceptor absent. More C_2H_2 is produced at 3 Torr by graphite gasification than is produced by CH_4 conversion into C_2H_2.

It is interesting to compare the diamond deposition rate with the C_2H_2 production rate. Figure 5 shows the growth rate as a function of pressure for this series. We find that the deposition rate is a maximum for a pressure of approximately 3 Torr. A comparison with Figure 4 shows that the deposition rate and the C_2H_2 production rate both show a similar dependence on reactor pressure with the highest deposition rate and the highest C_2H_2 production rate occuring at 3 Torr.

Discussions and Conclusions

This work shows an apparent correlation between the deposition rate of diamond and rate of gasification of the graphite susceptor into C_2H_2. Perhaps, the growth rate of diamond is inhibited by graphitic sites which must be removed before diamond can propagate. Hence, growth conditions which rapidly gasify graphite, remove graphitic sites from the diamond surface allowing diamond growth to propagate. Mucha et al.(4) used similar arguments to explain higher effective growth rates in microwave CVD experiments when alternating cycles of H_2 and CH_4 were introduced into the reactor. Alternatively, the C_2H_2 radical may be promoting diamond growth as Frenklach et al.(5) have suggested. Thus, higher concentrations of C_2H_2 in the gas phase may be responsible for the higher growth rate.

The work of Balooch and Olander(6) yields considerable insight into the data presented in this paper. Balooch and Olander showed that the gasification products observed when atomic hydrogen interacts with pyrolytic graphite are distinctly different depending on the temperature of the graphite. At temperatures below 550°C, the primary product was CH_4. At temperatures above 900°C, the primary product was C_2H_2. Balooch and Olander argued that in the intermediate temperature range H atoms recombined on the pyrolytic graphite surfaces without substantial graphite gasification. In the pressure series reported in this paper, the graphite susceptor is certainly above 550°C. We, as Balooch and Olander, do observe C_2H_2 as a by-product of atomic H with graphite. We are able to deposit diamond films in the intermediate temperature range where atomic hydrogen is not as efficient in dissolving graphite. It should be noted that the flux of atomic hydrogen present to a diamond CVD growth surface is orders of magnitude higher than the fluxes used by Balooch and Olander. Consequently, graphite removal from a diamond CVD growth surfaces with atomic H is undoubtedly possible.

The production of C_2H_2 from a graphite surface at elevated temperatures will be proportional to the atomic hydrogen flux. If one interprets the C_2H_2 production rate shown in Figure 4 as proportional to the atomic hydrogen flux to the graphite surface and hence to the diamond CVD growth surface, then one

concludes that the atomic hydrogen flux to the growth surface is a strong function of pressure. Hence, the correlation between diamond growth rate and acetylene production is more concisely a consequence of the differing atomic hydrogen fluxes. The higher fluxes of atomic hydrogen dissolve graphite and promote diamond bonding. These results are strong support for the work of Yarbrough(7) showing that at high atomic hydrogen concentrations diamond precipitated as the stable phase.

Acknowledgements The authors wish to thank the Strategic Defense Initiative Organization/Innovative Science and Technology Office through the Office of Naval Research (N-00014-86-C-0460) and the Office of Naval Research (N00014-90-J-1707) for the financial support of this work.

REFERENCES

(1) F.G. Celii, P.E. Pehrsson, H.-T. Wang, and J.E. Butler, Appl. Phys. Lett. 52, 2045 (1988).

(2) C. Judith Chu, Mark P. D'Evelyn, Robert H. Hauge, and John L. Margrave, J. Mat. Res. 5, 2405 (1990).

(3) R.A. Rudder, G. C. Hudson, Y. M. LeGrice, M.J. Mantini, J.B. Posthill, R.J. Nemanich, and R.J. Markunas, Mat. Res. Soc. EA-19, 89 (1989).

(4) J.A. Mucha, D.L. Flamm, and D.E. Ibbotson, J. Appl. Phys. 65, 3448 (1989).

(5) Michael Frenklach and Hai Wang, Phys. Rev. B 43, 1520 (1991).

(6) M. Balooch and D.R. Olander, J. Chem. Phys. 63. 4772 (1975).

(7) Walter A. Yarbrough, Mat. Res. Soc. Symp. Proc. 162, 75 (1990).

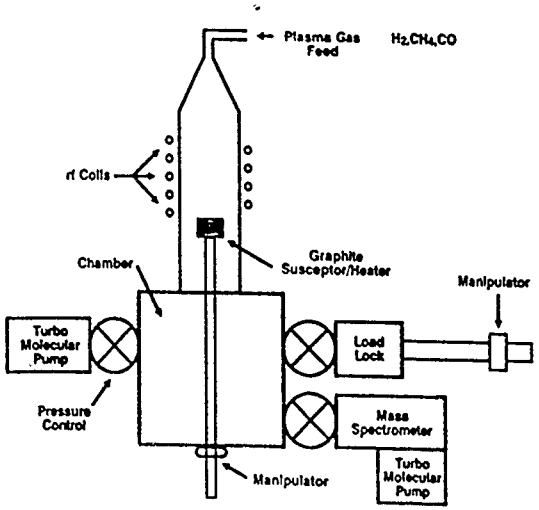

Figure 1. Schematic of low pressure rf-plasma assisted chemical vapor deposition system.

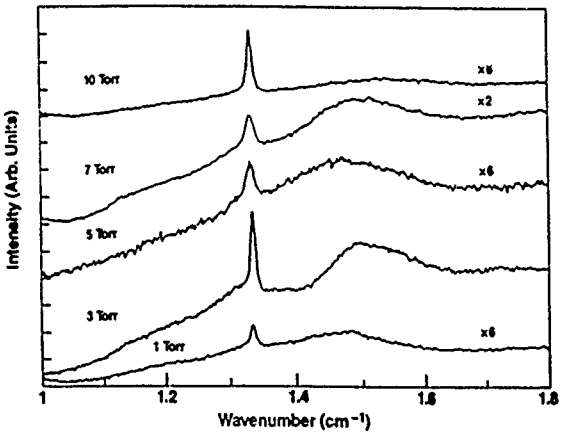

Figure 2. Raman spectra for diamond films deposited from 1 to 10 Torr using 1% CH_4 in H_2.

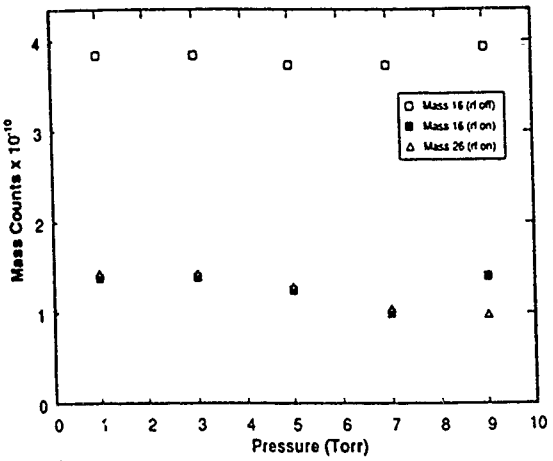

Figure 3. Conversion of CH_4 into C_2H_2 without the graphite susceptor in the reactor.

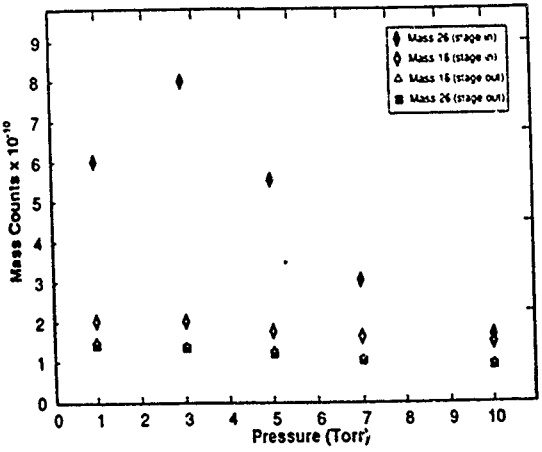

Figure 4. Production of C_2H_2 in the growth reactor as a function of pressure with the graphite susceptor in place.

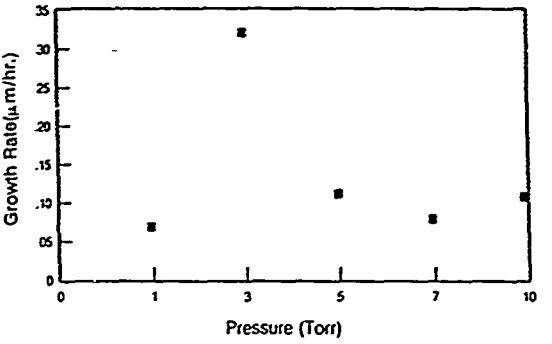

Figure 5. Diamond deposition rate as a function of pressure. Thickness values were obtained from SEM micrographs of cleaved sections.

SUBSTRATE EFFECTS AND THE GROWTH OF HOMOEPITAXIAL DIAMOND (100) LAYERS USING LOW PRESSURE rf PLASMA-ENHANCED CHEMICAL VAPOR DEPOSITION

J.B. Posthill, R.A. Rudder. G.C. Hudson, D.P. Malta.
G.G. Fountain. R.E. Thomas. and R.J. Markunas
Research Triangle Institute. Research Triangle Park. NC 27709-2194

T.P. Humphreys and R.J. Nemanich
Department of Physics
North Carolina State University, Raleigh, NC 27695-8202

D.R. Black
National Institute of Standards and Technology, Gaithersburg, MD 20899

ABSTRACT

The technological evaluation of commercially-available, single crystal diamond substrates for homoepitaxial diamond growth is presented. Surface topographies of insulating diamonds (types Ia. IIa, and Ib) are shown. and microstructural comparisons are examined with X-ray topography. Wet chemical and mechanical cleaning procedures are briefly reviewed. The effect of the starting substrate on the resultant homoepitaxial diamond film can be partially mitigated by the proper choice of substrate. appropriate cleaning protoc , and the use of a well-qualified diamond deposition technology.

Introduction

The thermal and electrical properties of diamond make it an excellent candidate for electronic applications. A number of significant problems must be overcome before the potential of diamond can be realized. While suitable heteroepitaxial substrates have not been developed yet, the fabrication of diamond transistors on natural diamond substrates allows testing and evaluation of diamond electronics [1]. One problem arising in the fabrication of diamond devices on diamond is the quality of the natural diamond substrates. Recent studies indicate that X-ray topography is a potentially valuable technique for characterizing structural defects in diamond single crystal substrates [2]. Selection of high quality diamond substrates is imperative to the growth of high mobility homoepitaxial diamond layers. In order to achieve the highest electrical quality diamond films, growth techniques may have to be developed which deposit epitaxial layers without replicating the crystalline defects commonly found in diamond single crystals.

This paper presents technological results accumulated over the last two years that pertain to the quality of commercially-available single crystal

diamond substrates, the cleaning of these substrates, and the resultant homoepitaxial diamond growth by low pressure rf plasma-enhanced chemical vapor deposition (PECVD). Both uniform coverage and selective-area diamond homoepitaxy are described.

Experimental Procedures

Natural type Ia and IIa and synthetically-produced type Ib diamond single crystals have been evaluated for their suitability for diamond homoepitaxy. Cutting and polishing to nominal (100) orientation were performed commercially by the vendors, and analysis has included scanning electron microscopy (SEM) [equipped with a field emission gun] on uncoated diamond substrates. X-ray topography [3], using near-parallel and monochromatic X-rays prepared from synchrotron radiation, has been used to evaluate the microstructure of selected type Ia, IIa, and Ib single crystal diamonds (not necessarily cut and polished to a specific orientation).

Two different chemical cleaning methods were utilized. Diamond substrates were cleaned with the RCA cleaning technique [4], which has found wide-spread use in silicon integrated circuit fabrication, or with sequential exposure to boiling CrO_3/H_2SO_4 solution (glass cleaning solution) for 15 minutes followed by boiling aqua regia for 15 minutes followed by a dip in 10:1 H_2O:HF solution and complete deionized water rinse. The efficacy of swabbing to remove particulates has also been evaluated. Cotton-tipped swabs were used in deionized water.

Homoepitaxial diamond growth was accomplished using a 13.56 MHz inductively-coupled plasma-enhanced chemical vapor deposition (PECVD) system as described in more detail elsewhere [5]. Briefly, the system is UHV-compatible and the nominal conditions used were: 1% CH_4 in H_2 or 1:2 mixture of 2% CO in H_2 and 1% CH_4 in H_2, total gas flow = 20-30 sccm (32.2-48.3 Pa-L-s^{-1}), pressure = 5.0 Torr (667 Pa), temperature = 500-800°C, and rf power $\simeq$ 1.5kW. The homoepitaxial diamond films have been characterized with SEM and Raman spectroscopy.

Results and Discussion

Diamond Substrates

Features have been observed on the surfaces of commercially-supplied diamond substrates which might inhibit high quality epitaxial growth. Figure 1 shows a series of SEM micrographs from several as-received natural Type IIa diamond (100) substrates (size: 4 × 4 × 0.25 mm). It can be seen that the surface topographies do vary from substrate to substrate, and some are clearly "better" than others. However, the fine unidirectional scratches are observed on all substrates of this size. Commercially-produced synthetic, type Ib diamonds can also have surface topographies that may influence subsequent

epitaxy (Figure 2). However, it must be borne in mind that a less than perfectly smooth surface topography only indicates that the polishing process needs optimization and does not necessarily imply that the bulk of the substrate is microstructurally defective. This has been shown by electron-beam-induced current (EBIC) imaging of natural semiconducting type IIb diamonds in the SEM, where it has been seen that the surface scratches bear no relationship to subsurface microstructural defects that are nonradiative recombination sites [6].

The extent of microstructural defects in a diamond substrate is perhaps a more crucial issue pertaining to the attainment of low-defect-density homoepitaxial diamond films for electronic evaluation. To begin to examine this issue, X-ray topographs have been taken of natural and synthetic diamond single crystals. X-ray topography has revealed differences in the internal structure of type Ia [7] and type IIa diamonds (Figure 3). Although the type Ia diamond appears to show planar defects in projection, there appear to be fewer defects and defects with a lower degree of strain and/or crystallographic misorientation than the type IIa crystals. This is qualitatively consistent with the observations that type Ia diamond crystals tend to exhibit superior axial ion channeling characteristics than type IIa crystals [8]. While these results appear to indicate a trend, variations between different natural diamond crystals may not permit these results to be generally applicable to all diamond substrates of a given type. Also shown is an X-ray topograph of a synthetically produced type Ib diamond which has defects that appear to have propagated radially from the center of the crystal.

Substrate Cleaning

Both of the chemical cleaning procedures described above have been used, and both techniques have met with successful homoepitaxial growth. Unfortunately, the success has not been uniform and unequivocal. The reason for this has been that residual particulates remain on the surface of the diamond substrate. The effect of particulates on the surface is the nucleation of sporadic regions of polycrystalline diamond material interspersed throughout the homoepitaxial film. The particulates are believed to result from the commercial polishing processes, and apparently are not removed with wet chemical cleaning. Mechanically cleaning the substrates by swabbing with cotton-tipped swabs in deionized water will remove most of the particulates. This effect is shown dramatically in Figure 4 where a diamond substrate, which had been intentionally contaminated with particulates and then chemically cleaned (particulates still remain adherent), is shown to be free of these particulates after a short time ($\sim$ 1 min.) of swabbing.

Diamond Homoepitaxy

Figure 5 shows the change in surface morphology after 1 μm of diamond deposition on a diamond substrate. Before deposition the surface shows pits

and polishing scratches present. After deposition, the surface finish is greatly improved as little surface topography is visible. This planarization is an important feature for development of electronic devices in diamond.

The effect of surface planarization during homoepitaxial growth can also be illustrated using selective homoepitaxial deposition. Epitaxial lateral overgrowth (ELO) has been demonstrated using this low pressure rf-driven PECVD technique [9]. A lithographically patterned 200 nm thick Si mask, which substantially inhibits diamond nucleation, has been used to define the diamond "seeds" for homoepitaxial diamond growth. The overgrowth was best revealed by chemically etching the Si from the diamond. Figure 6 shows SEM of a cleaved cross-section showing diamond ELO. The sample has been sputter-coated with 10 nm of Pt to prevent charging during SEM examination. Growth of homoepitaxial diamond was observed to be approximately isotropic, extending over the Si mask by 0.45 μm and above the mask by 0.50 μm. There is evidence for smooth epitaxial growth above the diamond seed windows and faceting on the overgrowth. Comparing the surface of the epitaxial layer to the surface of the substrate, the initial substrate topography has been planarized by this diamond homoepitaxial deposition process.

Both macro- and micro-Raman spectroscopy have been routinely employed to assess the crystalline quality of the homoepitaxial diamond films. Spectra were excited using the 514.5 nm line of an Ar^+ ion laser with a micro-Raman spot size at the sample surface of < 5 μm. Shown in Figure 7 are micro-Raman spectra showing the 1332 cm^{-1} diamond LO phonon line taken from the selective-area homoepitaxial film and taken off the film where scattered and isolated polycrystalline diamond crystals have grown on the Si mask. The full-width at half-maximum (FWHM) values from these spectra differ by 1.6 cm^{-1} - with the homoepitaxial film having the narrower peak. This is consistent with the fact that the Raman signal from polycrystalline diamond films have greater FWHM than from single crystal diamonds. Another homoepitaxial diamond film with uniform coverage that was grown on a (100) type IIa substrate was examined with micro-Raman spectroscopy by focusing on the surface of the homoepitaxial film. The corresponding 1332 cm^{-1} diamond LO phonon line was found to have a FWHM of 2.1 cm^{-1}. Because of the small depth of focus of the micro-Raman system, it was also possible to focus into the bulk of the type IIa substrate. In this case, the FWHM increased to 2.4 cm^{-1}. Although this technique cannot completely isolate the Raman signals from the epitaxial film and the substrate, it shows qualitatively that this homoepitaxial diamond film is of greater perfection than the substrate. This same trend has been seen for homoepitaxial diamond grown on (100) type Ia diamond substrates, but the differential between the FWHM of the epitaxial film and the type Ia substrate is less (on the order of 0.1 cm^{-1}).

Summary

From the point of view of commercial availability, type Ia diamond substrates currently appear to be microstructurally superior for homoepitaxial growth. Although there remains diamond substrate surface topography concerns, if the substrates are mechanically and chemically cleaned properly and an adequate diamond deposition technique is used. the surface can be planarized for device fabrication. The evidence accumulated thus far indicates that homoepitaxial diamond films grown with rf PECVD are superior to the starting substrates. The ability to grow homoepitaxial diamond selectively with ELO allows for the possibility of creating films that are less microstructurally defective than the starting substrate.

Acknowledgements: The authors gratefully acknowledge the support of this work by the SDIO/IST through ONR, Contract No. N00014-86-C-0460. TPH and RJN gratefully acknowledge the support of this work by SDIO/IST through ONR, Contract No. N00014-90-J-1707.

REFERENCES

1. G.G. Fountain, R.A. Rudder, D.P. Malta, S.V. Hattangady, R.G. Alley, G.C. Hudson, J.B. Posthill, R.J. Markunas, T.P. Humphreys, R.J. Nemanich, V. Venkatesan, and K. Das, this proceedings.
2. Andrew R. Lang, 2nd Intl. Conf. on the New Diamond Science and Technology, Washington, DC, September 23-27, 1990, in press.
3. B.K. Tanner, *X-ray Diffraction Topography*. Pergamon Press. Oxford (1976).
4. W. Kern and D.A. Puotinen, RCA Rev.. 31, 187 (1970).
5. R.A. Rudder. G.C. Hudson, Y.M. LeGrice, M.J. Mantini, J.B. Posthill, R.J. Nemanich. and R.J. Markunas, Mater. Res. Soc. Symp. Proc., EA-19, 89 (1989).
6. D.P. Malta, S.A. Willard, R.A. Rudder, G.C. Hudson. J.B. Posthill, R.E. Thomas, and R.J. Markunas, Proc. 49th Annual Meeting of the Electron Microscopy Society of America, (1991) in press.
7. The type Ia crystal examined in this study had a thin $\sim 0.5\mu$m epitaxial film grown selectively on it. The film was not visible, and its presence did not affect the X-ray topography images of the substrate microstructure.
8. G.S Sandu, N.R. Parikh, and M.L. Swanson. private communication of unpublished results, University of North Carolina, Chapel Hill, 1989.
9. R.A. Rudder, J.B. Posthill, G.C. Hudson, D.P. Malta, R.E. Thomas, R.J. Markunas, T.P. Humphreys, and R.J. Nemanich, 2nd Intl. Conf. on the New Diamond Science and Technology, Washington, DC, September 23-27, 1990, in press.

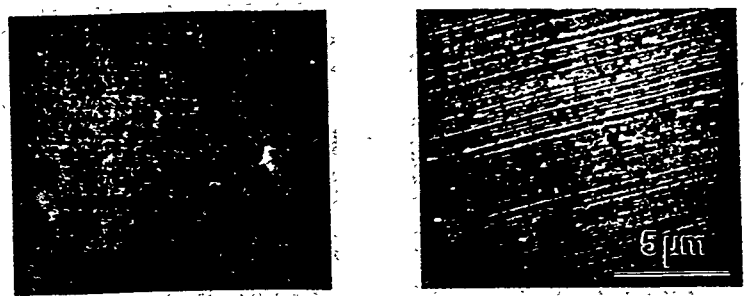

Figure 1. Surfaces of different as-received (100) type IIa diamond substrates.

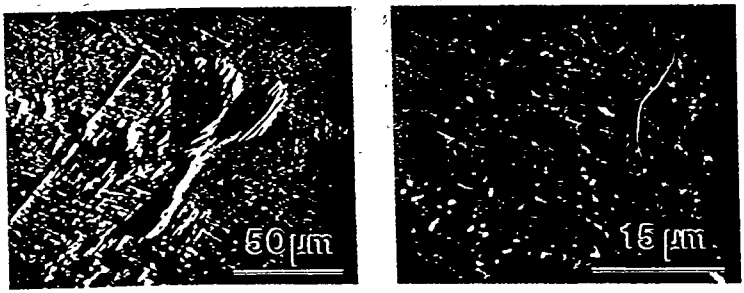

Figure 2. Surface of representative as-received (100) type Ib diamond substrate.

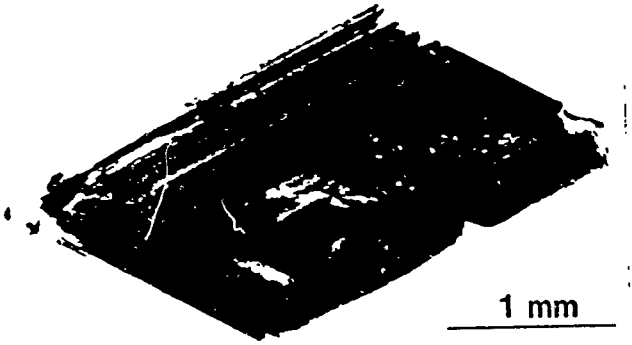

Figure 3. Representative X-ray topographs from: (A) type Ia diamond, $(0\bar{4}0)_{ST}$ [the radial defects are believed to have been created when the diamond was cleaved prior to analysis];

Figure 6. Cleaved cross-section showing ELO of diamond over a Si mask that has been chemically removed: (A) inclined view and (B) edge-on view.

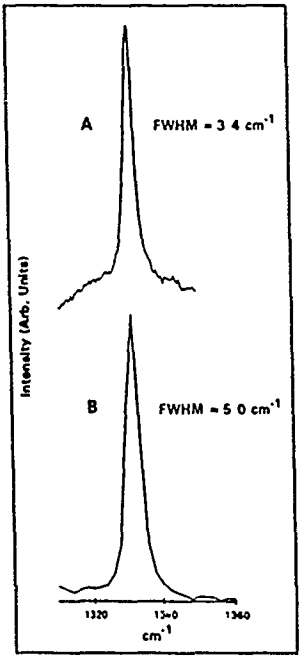

Figure 7. Micro-Raman spectra from: (A) selective-area homoepitaxial diamond (shown in Figure 6) and (B) polycrystalline diamond nucleated on mask (not shown in Figure 6 because it was etched off).

To be presented at the
179th Meeting of the Electrochemical Society
Washington, D. C. May 5 - 10, 1991

EFFECT OF THIN INTERFACIAL SiO_2 FILMS ON METAL CONTACTS TO BORON DOPED DIAMOND FILMS

V.VENKATESAN, K. DAS, D. L. DREIFUS

KOBE STEEL RESEARCH LABORATORIES, USA
ELECTRONIC MATERIALS CENTER
P. O. BOX 13608, RESEARCH TRIANGLE PARK, NC 27709

G. G. FOUNTAIN, R. A. RUDDER, J. B. POSTHILL, and
R. J. MARKUNAS

RESEARCH TRIANGLE INSTITUTE, RESEARCH TRIANGLE PARK, NC 27709-2194

ABSTRACT

The effect of thin interfacial films of SiO_2 (~20 Å) on the electrical characteristics of metal contacts fabricated on polycrystalline and homoepitaxial diamond films has been studied. These films were grown using plasma-enhanced chemical vapor deposition techniques. In order to minimize the effect of defects and / or hydrogen on the metal contact characteristics, these films were annealed at 950°C for 30 min. Metal-semiconductor contacts were formed by electron-beam evaporation of aluminum on both as-received and annealed polycrystalline films, whereas, gold metallization was used for the homoepitaxial film. Active diode dots were defined by a standard photolithographic process. It has been demonstrated that the introduction of a thin SiO_2 film at the interface between the metal and the diamond semiconductor film allows the fabrication of a rectifying contact, that is not otherwise possible for the films studied here.

INTRODUCTION

Semiconducting diamond, as a potential material for high temperature, high speed and high power device applications, has been the subject of some excellent reviews (1, 2). A number of these devices will rely on a rectifying metal / semiconductor contact for their operation. A metal / semiconductor contact also provides a suitable vehicle for electrical characterization of the device material. However, it has been observed that the formation of good rectifying contacts is not always easily accomplished on diamond films grown by chemical vapor deposition (CVD) (3). Contacts established with Al or Au on CVD films exhibit highly resistive ohmic or nominally asymmetric behavior, whereas these metals can be used almost routinely to form rectifying contacts on synthetic (4) and natural semiconducting diamond crystals (5). In the case of CVD grown homoepitaxial films, a chemical treatment in hot $CrO_3 + H_2SO_4$ solution has enabled the fabrication of Au

rectifying contacts (6). Characteristics of rectifying contacts on CVD grown films of both homoepitaxial (7) and polycrystalline diamond (8) have been improved by growing an insulating undoped diamond film on a previously deposited B doped semiconducting film.

In the present investigation, the effect of thin interfacial SiO_2 films on the electrical characteristics of metal contacts fabricated on B doped polycrystalline and homoepitaxial films has been studied. It has been demonstrated that the introduction of a thin SiO_2 film at the interface between the metal and the diamond semiconductor film allows the fabrication of a rectifying contact, that is not otherwise possible for the films studied here.

EXPERIMENTAL DETAILS

Both the polycrystalline and homoepitaxial B doped diamond films used for the study were grown using plasma-enhanced chemical vapor deposition (PECVD) techniques. The diamond films were materially characterized by scanning electron microscopy (SEM) and by Raman Spectroscopy. In addition, secondary ion mass spectroscopy (SIMS) analysis of selected samples were performed in order to determine the atomic concentration of B in the films.

As-deposited diamond films

A microwave plasma CVD reactor described in reference (9), was employed in this study for the deposition of the polycrystalline diamond films. These films were grown on low resistivity (<1 Ω cm) boron doped Si ((111) oriented) substrates using H_2 (99.5 %) and CH_4 (0.5 %) at a pressure of 35 torr. The substrates were maintained at 800°C during deposition. Moreover, these films were doped with boron using B_2H_6. Ratios of B_2H_6 to the total gas flow, of 0.002, 0.005, 0.008, 0.01, 0.05, 0.5 and 1.0 ppm were used to obtain films with a varied B concentration. In some cases O_2 (0.1 %) was also included in the gas mixture (for B_2H_6 ratios of 0.002, 0.005, 0.008 and 0.01 ppm). These films were grown for 14 hr. For the higher B_2H_6 ratios (0.05, 0.5 and 0.1 ppm) O_2 was not used and films were grown for 7 hr.

Details of the rf plasma CVD reactor utilized for the homoepitaxial film growth are given in reference (10). The homoepitaxial film was grown on a type I A insulating natural diamond crystal using 0.4 % CH_4 and 1 % CO in H_2 rf plasma. The film was also doped with B_2H_6 during growth.

Metal contacts on control samples without an SiO_2 interfacial layer were fabricated in the following way. After deposition the diamond films were cleaned using the RCA cleaning procedure (11). Approximately 2000 Å of aluminum was then electron-beam evaporated directly onto 0.002 ppm (B_2H_6 ratio) polycrystalline diamond sample to form a metal-semiconductor contact. For the homoepitaxial diamond sample a chemical treatment in hot $CrO_3 + H_2SO_4$ solution (to remove any non-sp^3 component in the diamond film) was also included and a gold metallization employed. An important point to note in the gold metallization procedure is that the electron-beam evaporation was a two step process. The deposition rate was 1Å/s for the first 100 Å of gold and then 5 Å/s for the rest of the ~ 2000Å film. This procedure markedly improved the adhesion of gold. Active diode areas, 100 μm in diameter separated from the field region by a 100 μm annular ring, were delineated by photolithography followed by Au or Al etching as the case may be. For the

photolithography process a mask pattern proposed by Ioannou et al.(12) was used. The 'infinitely' large area of the field-region ensured an adequate quasi-ohmic contact with the required current handling capability, particularly in the case of the homoepitaxial film that was deposited on an insulating natural diamond crystal.

Similar metal contact diodes were also fabricated on a 0.002 ppm (B_2H_6 ratio) polycrystalline diamond sample, which was deposited at the same time as the control sample. On this test sample ~ 20 Å thick film of SiO_2 was deposited by a remote plasma-enhanced CVD technique (13). Subsequently, this test sample was metallized with ~ 2000 Å Al. Active diode areas similar to those on the control sample were delineated by photolithography followed by Al etching. For the homoepitaxial film, following electrical measurements on the Au contacts fabricated on the control sample (i.e. without the SiO_2 interfacial film), the metal was etched in aqua regia (3HCl and 1HNO_3). This test sample was then cleaned employing the RCA cleaning procedure and a ~ 20 Å thick film of SiO_2 was deposited. Approximately 2000 Å Au was subsequently electron-beam evaporated onto the test sample. Active diode areas were defined by photolithography and Au etching. Cross-sectional diagrams of the contact structure on the diamond films, (a) without, and (b) with the the SiO_2 film are shown in Fig. 1. The control and test samples were then electrically characterized using a HP 4145 B semiconductor parameter analyzer equipped with a probe station for high temperature measurements.

Heat treated diamond films

The polycrystalline films were annealed at a temperature of 950°C for 30 min, in order to minimize the effect of defects and/or hydrogen on the electrical characteristics of metal contacts on these films. Aluminum metal contacts were then fabricated on the annealed films both with and without an SiO_2 interfacial layer, following the procedure described in the previous section. Current-Voltage (I-V) measurements were then performed on these metal-semiconductor contacts. For the contacts fabricated on annealed 0.05 ppm (B_2H_6 ratio) samples with an SiO_2 interfacial layer, I-V measurements were conducted from room-temperature upto ~ 250 °C, at increments of ~ 50 °C.

RESULTS AND DISCUSSION

As-deposited diamond films

Scanning electron microscopy of the B-doped diamond films investigated here showed clear (111) facets and five-fold multiply twinned particles. Scanning electron microscopy also indicated that the polycrystalline diamond films grown with O_2 (lower B_2H_6 ratio) had a quality superior to those grown without O_2 (higher B_2H_6 ratio). The crystal quality was investigated using laser Raman spectroscopy. The Raman peak position characteristic of diamond was located near 1333 cm^{-1}. A relatively small sp^2 peak at 1500 cm^{-1} was also observed in the Raman spectrum of the diamond films. A SIMS analysis of the as-deposited 0.05 ppm (B_2H_6 ratio) diamond film showed an atomic B concentration of ~ 1.0×10^{18} cm^{-3}.

Current-voltage characteristics of Al contacts to as-deposited polycrystalline sample (0.002 ppm diborane concentration) are shown in Figs. 2 (a) and (b). Directly deposited Al contacts (Fig. 2 (a)) on this sample without the interfacial SiO_2 film showed near-ohmic I-

V characteristics. The subsequent introduction of the SiO_2 film provided rectifying characteristics as shown in Fig. 2 (b). Directly deposited Au contacts on the as-deposited homoepitaxial film also exhibited near-ohmic I-V characteristics as shown in Fig. 3 (a). With the introduction of the thin SiO_2 film good rectification is obtained as shown in Fig. 3 (b). In the presence of the SiO_2 film, low leakage currents (<.1 nA at 5 V) in the reverse direction were observed in both the polycrystalline and the homoepitaxial film. A breakdown voltage of ~7 V was observed for both as-deposited polycrystalline and the homoepitaxial films.

Heat treated diamond films

Current-voltage characteristics on Al contacts fabricated on annealed films with the lower B_2H_6 ratios, showed a drastic reduction in current in both the forward and reverse directions. Since the magnitude of the current was approximately the same in all the films (0.002, 0.005, 0.008 and 0.01 ppm B_2H_6 ratio), a representative plot from the 0.01 ppm sample is shown in Fig. 4. This reduction in current conduction on annealing is in conformity with observations reported by Landstrass et al. (14, 15), Albin et al. (16) and Muto et al. (17). Hydrogen dissociation and/or defect annihilation could account for the increased resistivity in these annealed diamond films.

Directly deposited Al contacts on annealed, 0.05 ppm (B_2H_6 ratio) polycrystalline sample without the interfacial SiO_2 film exhibited I-V characteristic, as shown in Fig. 5 (a). The subsequent introduction of the SiO_2 film provided rectifying characteristics as shown in Fig. 5 (b). A breakdown voltage of ~ 6 V was observed for this film. A background doping concentration of ~ 5.3×10^{18} cm^{-3} in this film was obtained using an approximate 'universal' expression for the breakdown voltage given by (18):

$$V_B = 60(E_g/1.1)^{3/2}(N_B/10^{16})^{-3/4}$$

where, V_B is the breakdown voltage for a plane-parallel junction, E_g, the band-gap of the material, and N_B, the doping concentration. A band gap of 5.45 eV for diamond and the experimentally observed breakdown voltage of 6 V was used in the above calculation. Assuming that the active B concentration in this high B concentration film is not very different from the atomic B concentration (~1.0×10^{18} cm^{-3}) as determined from SIMS analysis, the calculated value of the background doping concentration seems to agree within an order of magnitude with the SIMS results. It should be noted that for high concentrations of B of the order of 10^{19} - 10^{20} cm^{-3} in diamond, a complete activation of the impurity has been reported (19). However, it has not been established whether a similar effect can be expected at a B concentration of 1.0×10^{18} cm^{-3}. It should also be pointed out that a plane-parallel junction approximation will provide an underestimation of the breakdown voltage as edge effects are expected to produce a significant lowering of the breakdown voltage for a given doping concentration. An estimation of doping concentration from the observed breakdown voltage of the structute used here, therefore, will provide an overestimation of the doping concentration. Moreover, since the dielectric strength of SiO_2 is 10^7 V/cm (Appendix I of reference (18)) the breakdown voltage of ~ 20 Å SiO_2 film is ~ 2 V. This indicates that the experimentally observed breakdown voltage of this film (~ 6 V) is likely to be the breakdown voltage of the diamond film and not that of the dielectric. The I-V characteristics of this annealed diamond film (0.05 ppm B_2H_6 ratio) with interfacial SiO_2 measured at temperatures ranging from room temperature (RT) to 248

°C in ~ 50 °C increments, are shown in Fig. 6. It is seen that as the temperature is increased the reverse leakage current increases and the reverse breakdown voltage decreases. Nevertheless, a fairly good rectification behavior can be observed upto ~ 100 °C.

Conclusions

It has been demonstrated that the introduction of a thin SiO_2 film at the interface between the metal and the diamond semiconductor film allows the fabrication of a rectifying contact, that is not otherwise possible for the films studied here. This improvement in characteristics is probably due to a modification in the barrier height and field distribution and/or to passivation of the surface. Further work in this area is in progress to fully understand the reason for such behavior.

Acknowledgements

The authors are grateful to Dr. K. Kobashi, ERL, Kobe Steel, Ltd. Kobe, Japan, for providing the polycrystalline diamond films used in this study and to C. P. Tully, Kobe EMC for his assistance in prepation of the manuscript. GGF, RAR, JBP, and RJM gratefully acknowledge support from SDIO/IST through ONR (Contract No. N00014-86-C-0460).

References

1. A.T. Collins, Semicond. Sci. Technol. 4, 605 (1989).
2. G.Sh. Gildenblat, S.A. Grot, A. Badzian, to be published, Proc. IEEE.
3. V. Venkatesan, and K. Das, unpublished work, (1990).
4. G.H. Glover, Solid St. Elect. 16, 973 (1973).
5. E.C. Lightowlers and A.T. Collins, J. Phys. D : Appl. Phys. 9, 73 (1976).
6. S.A. Grot, G.Sh. Gildenblat, C.W. Hatfield, C.R. Wronski, A.R. Badzian, T. Badzian, R. Messier, IEEE Electron Dev. Lett. 11, 100 (1990).
7. H. Shiomi, Y. Nishibayashi and N. Fujimuro, presented at the 2nd Intl. Conf. New Diamond Sc. Tech., Washington, D.C., Sept 23-27 (1990).
8. K. Miyata, D.L. Dreifus, K. Das, J.T. Glass and K. Kobashi, to be presented at the Electrochem. Soc. Meeting, Washington, D.C., May 6-10 (1991).
9. 14. K. Kobashi, K. Nishimura, Y. Kawate, and T. Horiuchi, Phys. Rev. B 38, 4067 (1988).
10. R.A. Rudder, G.C. Hudson, Y.M. LeGrice, M.J. Mantini, J.B. Posthill, R.J. Nemanich, and R.J. Markunas, Mat Res. Soc. EA-19, 89 (1989).
11. W. Kern, and D. A. Puotinen, RCA Rev. 31, 187 (1970).
12. D. E. Ioannou, N. A. Papanicolaou, and P. E. Nordquist, Jr., IEEE Trans Electron Devices, ED-34, 1694(1987).
13. G.G. Fountain, R.A. Rudder, S.V. Hattangady, R.J. Markunas, and P.S. Lindorme, J. Appl. Phys. 63 (9), 4744 (1988).
14. M.I. Landstrass and K.V. Ravi, Appl. Phys. Lett. 55, 975 (1989).
15. M.I. Landstrass and K.V. Ravi, Appl. Phys. Lett. 55, 1391 (1989).
16. S. Albin and L. Watkins, IEEE Electron Dev. Lett. 11, 159 (1990).
17. Y. Muto, T.Sugino, J. Shirafuji and K. Kobashi, submitted for publication: Appl. Phys. Lett. (1990).

18. S.M. Sze, 'Physics of Semiconduction Devices', Wiley-Inter-science publication, New York, 1981.
19. K. Nishimura, K. Das and J.T. Glass, J. Appl. Phys. 69, 3142 (1991).

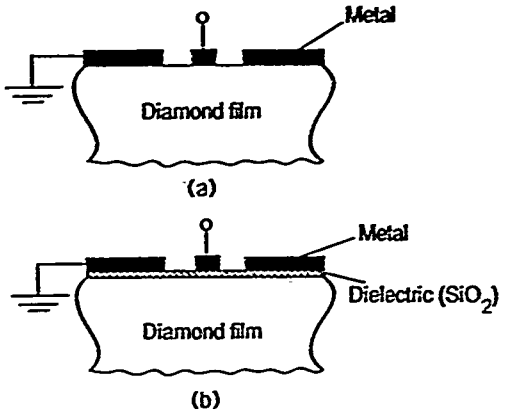

Figure 1: Cross-sectioal diagram of contact structure on diamond film, (a) without dielectric layer and (b) with dielectric layer.

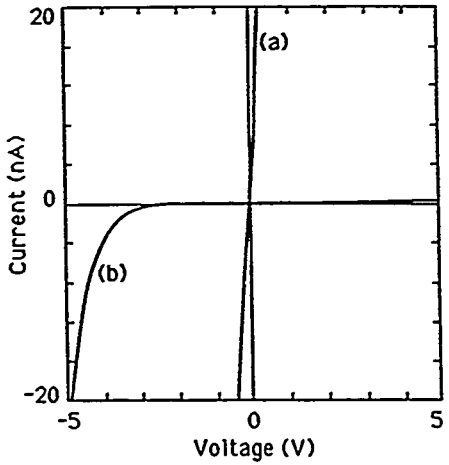

Figure 2: Current-voltage characteristics of Al contacts on polycrystalline diamond film (0.002 ppm), (a) direct metalization and (b) with interfacial SiO_2.

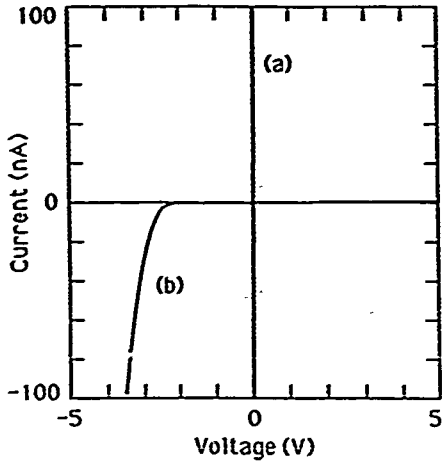

Figure 3: Current-voltage characteristics of Au contacts on homoepitaxial diamond film, (a) direct metalization and (b) with interfacial SiO_2.

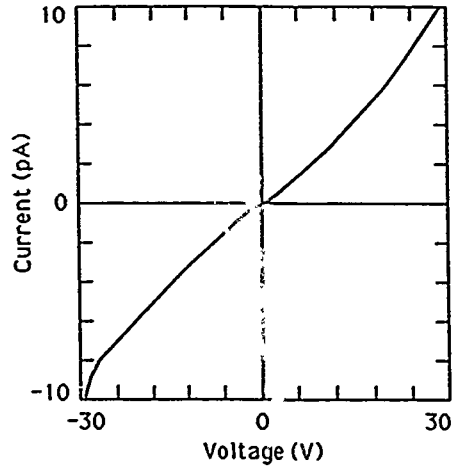

Figure 4. Current-voltage characteristic of Al contacts on annealed diamond film (0.01 ppm).

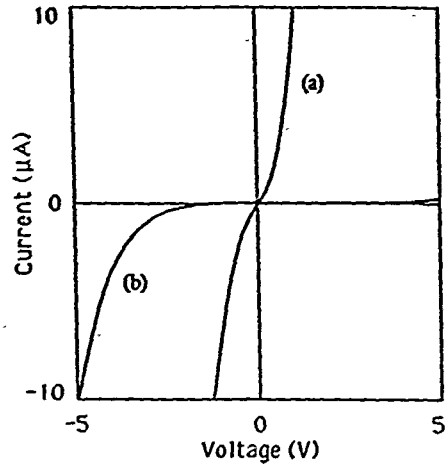

Figure 5: Current-voltage characteristic of Al contacts on annealed diamond film (0.05 ppm), (a) direct metalization and (b) with interfacial SiO_2.

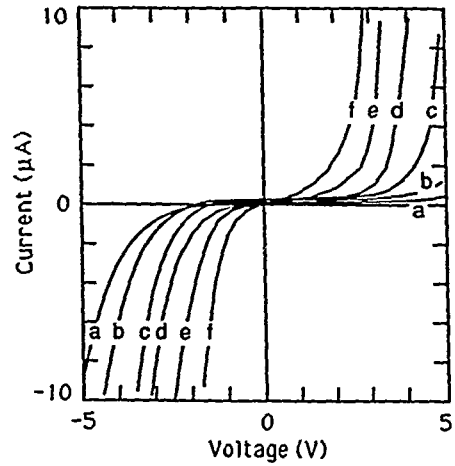

Figure 6: Current-voltage characteristic of Al contacts on annealed diamond film (0.05 ppm) with interfacial SiO_2 at (a) RT, (b) 50°C, (c) 99°C, (d) 149°C, (e) 198°C, and (f) 248°C.

IGFET FABRICATION ON HOMOEPITAXIAL DIAMOND USING IN SITU BORON AND LITHIUM DOPING

J.G. Fountain, R.A. Rudder, D.P. Malta, S.V. Hattangady, R.G. Alley, G.C. Hudson, J.B. Posthill, and R.J. Markunas
Research Triangle Institute, Research Triangle Park, NC 27709

T.P. Humphreys and R.J. Nemanich
North Carolina State University
Raleigh, NC 27695-8202

V. Venkatesan and K. Das
Kobe Steel Research Laboratories
Electronic Materials Center
Research Triangle Park, NC 27709

ABSTRACT

The use of boron and lithium as dopant impurities in diamond has been investigated using diborane and lithium fluoride as in situ dopant sources. The lithium was investigated as a possible n-type dopant. The diamond material, grown by rf plasma discharge at low pressure, was characterized electrically and microstructurally. The boron was found to be p-type, as expected, with an activation energy of 0.24 eV. The lithium doped material was also found to be p-type with a similar activation energy. SIMS data indicates that the lithium doped samples also contain significant concentrations of boron, enough to account for the electrically active species. However the mobility of the carriers in the lithium/boron doped material seem to be somewhat higher. Schottky barrier diodes were formed on the lithium/boron doped material which showed good rectifying behavior. The minority carrier diffusion length in the material was estimated from EBIC measurements to be ~ 0.5 μm. The lithium appears to be electrically inactive in this material, although it may improve the electrical characteristics of the material. IGFET devices were fabricated in the boron doped and lithium boron doped materials using a selective deposition fabrication scheme. The boron doped device exhibited a transconductance of 38 μS/mm.

Introduction

The extremely selective nature of the plasma activated diamond deposition processes provides a very useful and flexible vehicle for device fabrication sequences. Other workers have already reported diamond insulated gate field effect transistor (IGFET) fabrication using selective diamond deposition with a sputtered quartz insulator [1]. The doping of active layers for diamond devices is a crucial topic and is currently under study by several groups [2,3,4]. Boron has been established as a p-type

dopant for diamond. Boron doping has been accomplished using solid boron etched in situ and using diborane as a gaseous source. Although there have been specific reports of the formation of n-type diamond [5], this is still an area that requires further development. Li has been proposed as a potential n-type dopant for diamond based on theoretical modelling [6]. We have undertaken a preliminary study to investigate the suitability of using LiF as a solid source to dope diamond growing in a plasma-enhanced chemical vapor deposition (PECVD) environment. In this paper, we report fabrication of a diamond IGFET structure using selective diamond deposition with boron and lithium doping in conjunction with a remote plasma enhanced chemical vapor deposition (RPECVD) of a SiO_2 insulating dielectric layer.

Doping Studies

The system used for the growth of homoepitaxial diamond consists of a 13.56 MHz inductively-coupled PECVD system. A gas mixture of 98.5% H_2, 1.0% CO and 0.5% CH_4 flowed through a 62.5 mm quartz tube at a rate of 30 sccm at 5.0 Torr. The sample is positioned near the rf coil on a graphite susceptor and is held at $\sim 800^\circ$C during growth. Type Ia and IIa natural (100) diamond crystals were used in these studies. Boron and lithium were investigated as in situ dopants.

Boron doping was accomplished by introducing diborane diluted in H_2 into the reactor during diamond deposition. The diborane source was diluted in hydrogen to 1000 ppm. The diborane was leaked into the chamber with a flow rate of less than 0.5 sccm. Calculations bases on the partial pressure of diborane indicate that the incorporation efficiency is on the order of unity.

Lithium doping was accomplished via introduction of a solid source of LiF on the graphite susceptor during the deposition, or via introduction of the solid source to "dose" the reactor prior to loading the substrate for diamond growth. It was found that under diamond growth conditions, the LiF is dissolved by the atomic hydrogen in the reactor. Lithium emissions were observed in the reactor once the sources began to volatilize. Diamond deposition, with a Li source present in the reactor, resulted in high incorporation of Li into the samples ($> 10^{20}$ cm^{-3}) Consequently, growths were performed with no source of Li in the reactor other than the Li residing on the chamber fixtures following "reactor dosing". Typically, a solid source would be introduced into the reactor, a discharge initiated, whereby emissions of Li were detected, the solid source removed, and the reactor deconditioned by a hydrogen discharge to reduce the Li concentration in the reactor prior to epitaxial growth.

Electrical and Physical Analysis of Doped Diamond Films

The doped diamond samples were characterized by Van der Pauw Hall measurement for carrier density and mobility. The measurement was carried out as a function of temperature to attain activation energies of the dopant species.

The boron doped samples were determined to be p-type as expected with a carrier density in the $10^{17}cm^{-3}$ range. Two levels were seen in the plot of carrier density vs. temperature as shown in Figure 1. One had a low activation energy of 0.0062 eV, and the other had an activation energy of 0.24 eV. The origin of the low activation energy level is unknown at this point. The 0.24 eV level is more characteristic of boron activation in diamond [3]. Hall mobilities measured were on the order of 45 $cm^2/Vsec$. It is likely that the boron is compensated by some other level in the diamond, possibly a damage or crystalline defect related level.

Lithium samples were also characterized by Hall measurements. Data from a heavily lithium doped sample is shown in Figure 2. Data from a more lightly doped sample is shown in Figure 3. Both samples exhibit p-type behavior, which was unexpected. The activation energies of the acceptor levels in the samples seemed surprisingly close to the level measured for the boron doping. The lightly doped sample did however exhibit the higher mobility than the boron doped sample.

SIMS analysis of the heavily lithium-doped sample showed both Li and B in the film. The amount of Li was $\sim 10^{21}\,cm^{-3}$; the amount of B was $\sim 10^{18}\,cm^{-3}$. The source of the boron is at this point undetermined; however, it is likely to be a deposition system component. It is very probable that the p-type behavior is from the boron in the film and not the lithium. The lithium does, however, seem to have a beneficial effect on the electrical properties of the film.

Au Schottky diode structures were fabricated on a heavily lithium-doped sample that had received a 30 minute hydrogen plasma treatment (1500 watts of RF power into the plasma), at 5 Torr, at approximately 700°C. These diodes showed good rectification behavior with a turn-on voltage of 2.5 V and a breakdown voltage of 6 to 8 V. The reverse leakage current is on the order of 12.5 $\mu A/cm^2$. Au contacts which had been deposited on material doped with boron alone (which had received a similar hydrogen plasma treatment) exhibited ohmic behavior.

The Au Schottky contact was used to perform electron-beam induced current (EBIC) measurements. EBIC was used to estimate the minority-carrier diffusion lengths. A thin Au Schottky contact was used for charge collection, and the induced current was measured as a function of distance, in plan-view, from the contact. For primary beam energies from 10keV - 20 keV, the minority-carrier diffusion length was measured to be 0.5μm. This compares with measured minority-carrier diffusion lengths of $\sim 3\mu m$ in natural type IIb diamond (B-doped) [7].

Diamond IGFET Fabrication and Testing

Transistor structures were fabricated on a Type IA natural diamond (100) substrate from Drucker-Harris. The diamond substrate was cleaned using a conventional RCA wet chemical clean [8]. Polysilicon layers as well as SiO_2-polysilicon composite

layers were used as masking materials. During diamond deposition the top layer of the silicon is carbonized making it impervious to the hydrogen etching environment. It was found that SiO_2 masks were removed by the hydrogen environment if no oxygen was used in the process. The composite structure assures that the carbonized silicon layer can be removed from the wafer. The mask was patterned using standard lithographic techniques and wet etching to open holes for deposition of the conducting p-type diamond areas. Following diamond deposition, the silicon mask was etch removed. The sample was then coated with a 250 Å RPECVD SiO_2 gate dielectric. This process has been used to deposit low temperature, gate-quality dielectrics on Si and other semiconductors [9,10]. Titanium gate electrodes were formed using liftoff. Source-drain contact openings were patterned and openings etched in the oxide using buffer HF solution. Titanium contacts were formed using liftoff. The contacts were ohmic as deposited. The gate length and width of the transistors was 8μm and 50μm, respectively.

Two types of working IGFET structures were fabricated, one using boron doping alone and one using the lithium doping. In both cases a major limitation on the device fabrication process was control of the dopant concentration.

The boron doped diamond IGFET source drain I-V characteristics are shown in Figure 4. The device showed transistor action characteristic of a p-channel, depletion mode device. The device cannot be pinched off with the available gate voltage. The leakage current is most likely due to defects in the material or surface leakage. The maximum transconductance of the device is 38 μS/mm at 8 V drain to source. The transconductance of the device is slightly larger for the 1 to 2 V gate step than for the 0 to 1 V gate step. This increase in transconductance with increasing depletion is indicative of a relatively high density of surface states at or near the diamond/SiO_2 interface. The geometry of the FET is such that the source to gate resistance is on the order of $2 \times 10^5\ \Omega$. This resistance would decrease the transconductance of the device by a factor of about 2.

The diamond material used for the transistor channel had a resistivity of 12 Ω-cm. The specific contact resistance of the titanium contacts on this material were measured using a transmission line model test structure. The specific contact resistance is 0.09 Ω-cm^2. Titanium contacts were also fabricated on heavily boron doped material with a resistivity of 0.08 Ω-cm. These contacts exhibited a specific contact resistance of $1.4 \times 10^{-4}\ \Omega$-cm^2. Such layers could be used for contact layers to reduce parasitic resistances in the source and drain using an additional selective diamond deposition step.

The lithium/boron doped diamond IGFET source drain I-V characteristics are shown in Figure 5. This device exhibited much better saturation behavior than the boron doped device. This device has a more lightly doped channel than the boron doped device as evidenced by the lower saturation current. This device showed both depletion and enhancement behavior. However it is not clear whether this enhanced current is due to accumulation of a conducting layer at the surface or just un-depleting

of the channel. It is likely that, since the doping level is approximately 2 orders of magnitude lower in this device than the first device, the channel is nearly fully depleted at 0.0 V gate bias. The device has a substantial leakage current. Comparison of this leakage current level with the leakage between isolated devices indicated that the current is principally substrate current.

Conclusions

In situ boron and lithium doping of diamond has been carried out using a diborane gas source and a lithium fluoride solid source in a low pressure rf diamond deposition process. The boron was found to be p-type with an activation energy of 0.24 eV. The lithium was judged to be electrically inactive in the material evaluated here. The activation energy of the conductivity along with SIMS data on impurity levels indicated that the conduction is probably due to unintentionally incorporated boron in the film. The lithium appeared to have some beneficial effects on the electrical properties of the the doped diamond films. This effect requires further study. Working IGFET devices were fabricated using the boron doped material and the lithium/unintentional boron doped material. A maximum transconductance of 38 μS/mm was measured for the boron doped device. Improvements in device performance could be achieved through reducing the source drain parasitic resistances and by improving the diamond/SiO_2 interfacial characteristics.

Acknowledgements The authors wish to thank the Strategic Defense Initative Organization/Innovative Science and Technology Office through the Office of Naval Research (N-00014-86-C-0460) for the financial support of this work. TPH and RJN gratefully acknowledge the support of this work by the ONR, Contract No N00014-90-J-1707.

REFERENCES

1. S.A. Grot, C.W. Hatfield. G. Sh. Gildenblat, A.R. Badzian, and T. Badzian, presented at the Second International Conference on the New Diamond SCience and Technology (ICNDST-2), Washington, DC(USA), September 23-27, 1990

2. Naoji Fujimori, Kideaki Nakahata, and Takahiro Imai, Jap. J. Appl. Phys. 29, 824 (1990).

3. B.V. Derjaguin, B.V. Spitsyn, A.E. Goridetsky, A P. Fakharov, L.L. Bouilov, and A.E. Sleksenko, J. Cryst Growth, 31, 44 (1975).

4. G.Sh. Gildenblat, S A. Grot, C.W. Hatfield, C.R. Wronski, A.R. Budzian, T. Badzian, and R. Messien. Mat. Res. Soc Symp. Proc 162, 297 (1990).

5. Ken Okano, Hideo Kiyota, Tatsuya Iwasaki, Tateki Kurosu, Masamori Iida and Terutaro Nakamura, presented at ICNDST-2, Washington, DC(USA), September 23-27, 1990.

6. J. Bernholc, S. Kajihara, and A. Antonelli, presented at ICNDST-2, Washington, DC(USA), September 23-27, 1990.

7. D.P. Malta, S A Willard, J.B Posthill, and R.J. Markunas, unpublished results, Research Triangle Institute, 1989.

8. R.A Rudder, G.C Hudson, Y M. LeGrice, M.J. Mantini, J.B. Posthill, R J. Nemanich, and R J. Markunas, Mat Res Soc. EA-19, 89 (1989)

9. G.G. Fountain, R A. Rudder, S.V Hattangady, R J Markunas, P.S Lindorm, J. Appl Phys, 63, 4744 (1988).

10. D.J. Vitkavage, G G Fountain, R A. Rudder, S.V. Hattangady, R.J Markunas, Appl. Phys Lett, 53, 692 (1988).

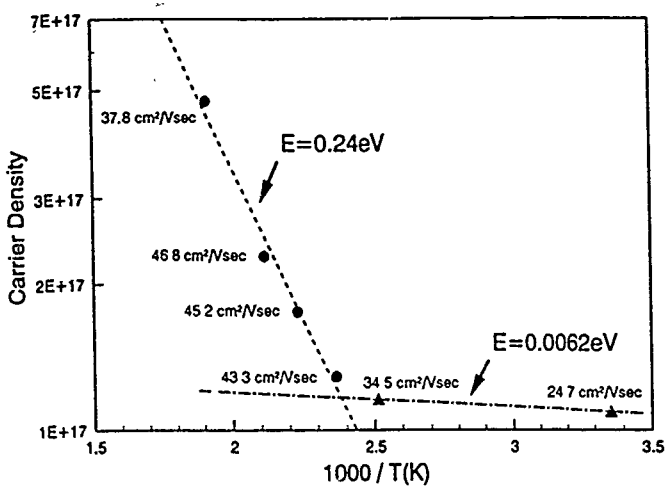

Figure 1 Carrier concentration vs reciprocal temperature for a boron-doped homoepitaxial film. The material is p-type Hall mobilities are listed.

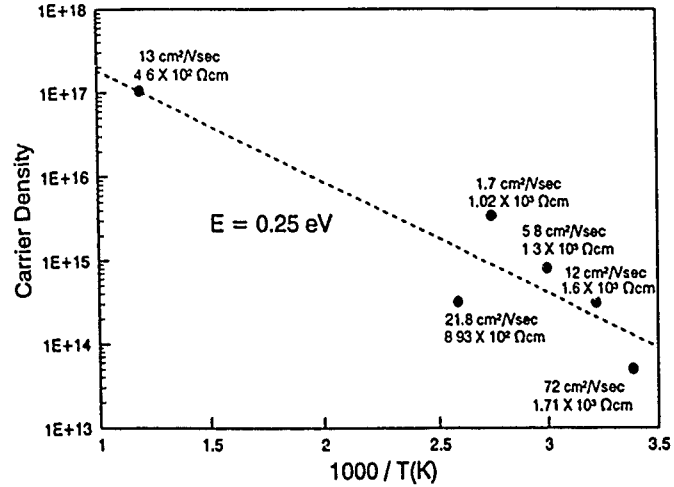

Figure 2 Carrier concentration vs. reciprocal temperature for a heavily Li doped homoepitaxial film. The material is p-type, probably due to boron contamination. Hall mobilities are listed.